4. SITE 148

The Shipboard Scientific Party[1]

Position:
13°25.12'N
63°43.25'W.

Water Depth: 1232 meters.

Penetration: 272 meters.

Recovery: 181.8 meters (66%).

ABSTRACT

Site 148 is located on the crest of a ridge on the western margin of the Aves Ridge about 30 miles northwest of Site 30, drilled on Leg 4. The section includes 250 meters of calcareous clay of Early Pliocene to Late Pleistocene age and a basal 22-meter-thick layer of volcanic sands and clays. The lower unit contains reworked fossils that give a questionable Paleocene age. No basalt was encountered. An apparent unconformity that may reflect submarine or subaerial weathering separates the two units.

Three periods recognized are a period of relatively deep water adjacent to an emergent volcanic island (volcanic sands and clays), possibly a period in shallow water or emergent, and a final deeper stage of pelagic sedimentation (calcareous clay).

Volcanic ash layers in the mid-Pleistocene mark the initiation of intense volcanic activity in the Lesser Antilles previously inferred on geomorphic grounds.

BACKGROUND

The Aves Ridge, a third arc, is an elongate structural high lying parallel to and west of the Lesser Antilles. It bears to the Lesser Antilles a relationship which is apparently analogous to that of several Pacific submerged ridges and their accompanying arcs (Marianas, Tonga Islands, etc.). The nature of their relationship to the island arcs is not clearly understood, but in the Tonga-Kermadec system (Karig, 1970) and in the Philippine Basin (Karig and Glassley, 1970), its origin is attributed to crustal generation or spreading, a concept supported by data from investigators working in other island arcs, such as Barker's (1970) magnetic data in the Scotia Sea. Others postulate that the Aves Ridge is an ancient island arc that became

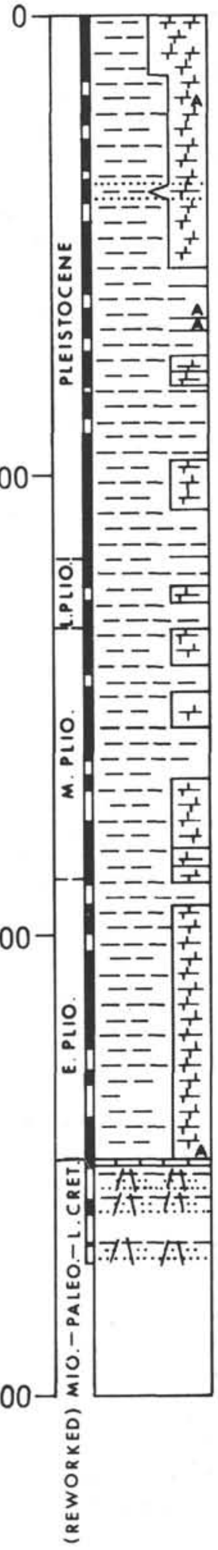

---

[1] N. Terence Edgar, Scripps Institution of Oceanography; John B. Saunders, Texaco Trinidad Inc.; Thomas W. Donnelly, State University of New York at Binghamton; Nahum Schneidermann, University of Illinois, Urbana; Florentin Maurasse, Lamont-Doherty Geological Observatory, Palisades, N. Y.; Hans M. Bolli, Eidgenossische Technische Hochschule, Zurich, Switzerland; William W. Hay, Rosenstiel Institute of Marine & Atmospheric Sciences, Miami, Fla.; William R. Riedel, Scripps Institution of Oceanography; Isabella Premoli Silva, University of Milan; Robert E. Boyce, Scripps Institution of Oceanography; Warren Prell, Lamont-Doherty Geological Observatory, Palisades, N. Y.

dormant when the center of activity shifted to the site of the present Lesser Antilles (Malfait and Dinkleman, 1972). Another concept is that the Aves Ridge resulted from the thickening of the crust of the Venezuelan Basin as a result of the Caribbean-Atlantic plate interaction (Edgar et al., 1971).

The upper crustal structure of the Aves Ridge is similar to that found in the Venezuelan Basin (Officer et al., 1957; Ewing, J. et al., 1957; Officer et al., 1959; Edgar et al., 1971). The deepest crustal and mantle velocities were not recorded. The highest velocity recorded is 6.2 to 6.3 km/sec and the layer represented is overlain by thick layers of 3.2 to 4.8 km/sec material, the latter probably made up of volcanic and intrusive rock.

Dredge hauls (Fox et al., 1971) from the Aves Ridge have yielded granodiorite, diabase, basalt, limestone, and chert. Of particular interest is the recovery of granodiorite from the extreme southern end of the ridge not far from the island of La Blanquilla, which is underlain by Cretaceous granitic rocks. Fox et al. have suggested that the entire Aves Ridge and Venezulan Basin may be underlain by granitic rocks based on their correlation with Caribbean crustal seismic velocities of 6.2 km/sec, which is well within the velocity range for a granite.

Figure 1 is a contour map of the southern part of the Aves Ridge showing (a) the ship track of Woods Hole's R/V *Chain* from which the drilling site was selected, (b) the track of *Glomar Challenger,* and (c) the locations of Site 30 (Leg 4) and Site 148. The *Chain* reflection record (Figure 2) shows that the sediments on the Aves Ridge are confined by two small ridges on the margins of the broad, smooth crest. The basement reflector on the western small ridge lies at about 0.25 second reflection time below the sea floor. The sediment over the deepest reflector (basement?) also thins over a broad rise in the central part of the ridge but the presence of strong reflectors made this a less desirable drilling location. The small ridge on the western margin was therefore selected for drilling. Figure 3 shows the reflection record made by *Glomar Challenger* during a short survey over the area and Figure 4 shows the corresponding track.

During Leg 4 (Bader, Gerard et al., 1970), Site 30 was drilled on the southern part of the Aves Ridge at 12°52.92'N, 63°23.00'W (Figures 1 and 5). The hole was drilled to a depth of 430 meters and terminated in Middle Miocene sediments. The basic lithology recovered was gray green calcareous and noncalcareous silty clays. Volcanic ash is found only in the Miocene sediments with glauconite, mollusc shell fragments, indistinct crossbedding, and mudballs, suggesting the presence of currents during deposition.

OBJECTIVES

1. Determine the age and nature of the deepest reflector at 0.25 seconds reflection time. Although the possibility was admittedly slim, it was hoped we could recover information relating to the possible granitic nature of the crust below the Aves Swell.

2. Obtain, through continuous coring of the upper section, a record of biostratigraphy and volcanic activity in the Lesser Antilles. The time of inception of the volcanic activity associated with the major volcanic centers of the Lesser Antilles was previously based on geomorphic reasoning.

3. Recover undisturbed sediments in a volcanic regime well above the depth of calcium carbonate compensation for pore water investigation.

OPERATIONS

The site was approached on 2 January 1971 in high seas and a strong wind. A survey (Figure 4) of the area was conducted for several hours to ensure that the optimal location was selected to achieve our objectives. Final position was near the crest of a small ridge trending along the western margins of the Aves Ridge (Figure 3).

The first core was taken using a piston inserted in the core barrel to minimize drilling disturbance in the soft uppermost ooze. The next three cores of slightly smaller diameter, were taken with a core barrel that extended beyond the bit. Subsequent cores taken with the standard barrel were notably more disturbed. Core recovery was fairly good throughout the hole (66%). At 250 meters, the coring rate slowed to about one meter per hour in hard volcanic sands and clays. The hole was terminated on 3 January at 272 meters because of the slow drilling rate.

LITHOLOGY

The sediments at Site 148 fall into two distinct lithologic groups: an upper pelagic sequence of marls and clays with a variable content of volcanic ash and a lower sequence of indurated coarse volcanic sands.

The upper sediment sequence varies from a greenish gray marl, with as much as 50 percent carbonate, to a dark greenish calcareous clay, with about 10 to 20 percent carbonate. The average carbonate content is slightly higher in the upper seven cores (0-63 m) and is expressed in lighter colors and a subtle color layering. Volcanic ash beds a few centimeters thick are found in the same upper cores, although drilling disturbance has commonly disrupted these severely. In the lower part of Unit I (63-249 m), the clay is uniformly dark with very rare recognizable ash layers.

The sediment throughout is pyritic and glauconitic, and scattered, very small siderite rhombs are found below 100 meters. Volcanic constituents are widely scattered through the entire upper sequence. Although relatively few distinct ash layers were seen, many smear slides were rich in broken crystals of plagioclase, with common clinopyroxene, orthopyroxene, and hornblende. Glass is rare and red hornblende, biotite, and apatite are extremely rare. This debris apparently represents the products of explosive eruptions in the Lesser Antilles.

Fossils found in this sequence are well preserved and include a rich assemblage of planktonic foraminifera with echinoid spines and molluscan remains. Radiolaria occur sparsely in the uppermost cores.

The lower sequence, Unit II (249-272 m), of volcanic sands and clays lies unconformably beneath the pelagic sequence. An unconformity, marked by a chocolate-colored, phosphatic iron oxide clay, separates the two units. The lower sequence consists of coarse grains of porphyritic andesite, plagioclase, quartz, green hornblende, glass (both fresh and divitrified), glauconite pellets, red

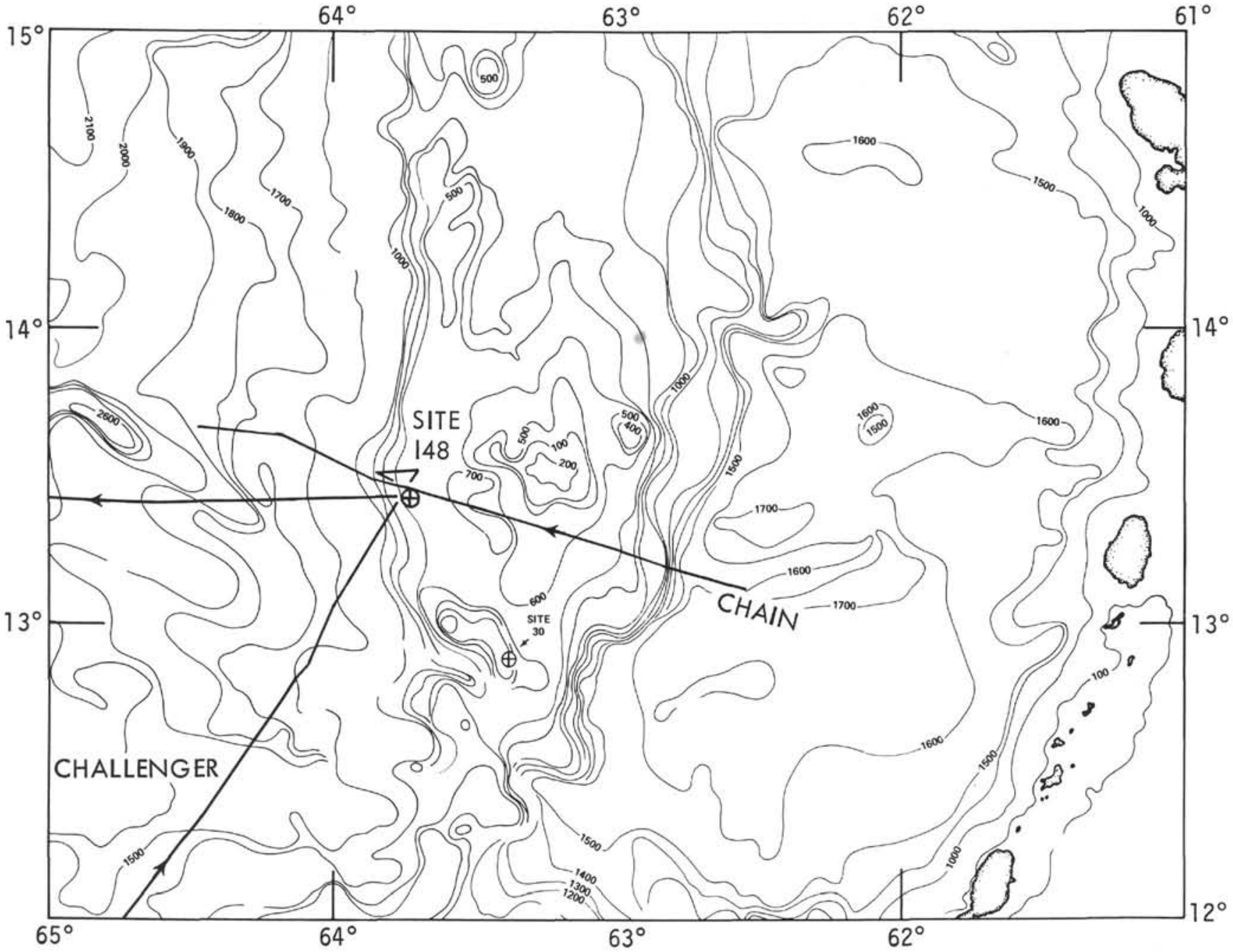

Figure 1. *Contour chart of the southern end of the Aves Ridge showing the track of R/V* Chain *and* Glomar Challenger, *and the locations of Sites 30 and 148. Topography from U.S. Navy Hydrographic office chart BC-0703N.*

hornblende, zircon, apatite, and indeterminate, possibly metamorphic, minerals. Beds are highly indurated, but extreme disturbance during drilling prevents any textural or fabric analysis of these sands.

PHYSICAL PROPERTIES

Wet-bulk Density, Water Content, and Porosity

Wet-bulk density and porosity were measured aboard *Glomar Challanger* by the Gamma Ray Attenuation Porosity Evaluator (GRAPE) and by individual sample volume-weight measurements (sample data are the enclosed dots in hole summaries). Water content was determined by weight-weight relationships. In general, the precision of the data is about ±5 percent. The methods, equipment, assumptions, error, correction factors, and interpretation precautions are discussed in the Appendix.

Cores 2, 3, and 4, in the upper part of Hole 148, were collected with a small-diameter punch core (2.25 inches internal diameter) rather than the normal 2.60-inch (internal diameter) core. Correction of the GRAPE data from the smaller diameter to be equivalent to a 2.60-inch core was calculated by the following formula.

$$\begin{aligned} \textit{Corrected Density} &= A + A\,\frac{(2.60\text{-}2.25)}{2.25} \\ &= 1.155A \end{aligned}$$

where A is the apparent GRAPE density.

At Site 148, Pleistocene to Paleocene clay and marl from the sediment surface to 270 meters below the sediment surface had wet-bulk densities from 1.38 g/cc (74% porosity) to 2.00 g/cc (40%), which, with minor variation, regularly increased with increasing depth and age. Densities between 0 and 30 meters below the sea floor were 1.38 g/cc (74%) to 1.5 g/cc (62%) while from 36 meters to 275 meters depth, densities were 1.55 g/cc (62%) to 2.00 g/cc (40%).

There does not appear to be any obvious correlation of density with major sediment types such as marl versus clay. Minor amounts of volcanic sand, however, had typical densities as high as 1.94 g/cc (40% porosity). Occasional

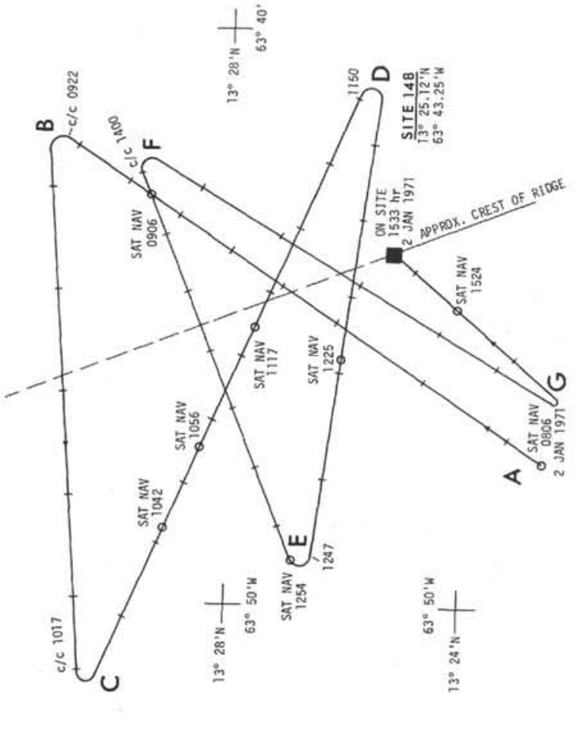

Figure 4. *Track of* Glomar Challenger *corresponding to reflection record shown in Figure 3. Chart shows locations of Site 148.*

pyrite concretions within the sediment are observed as high density (low porosity) GRAPE spikes in Cores 11, 19, 23, 24, 25, and 27, but these spikes do not represent the density of pyrite alone.

Water content varied from 52 to 31 percent and, in general, increased with increasing depth and age, with minor variations. Percentages decreased from 52 to 40 percent between the sediment surface and 36 meters, and, between 36 and 200 meters, decreased to 21 percent.

Sound Velocity

The Hamilton Frame Velocimeter was not on board when Site 148 was drilled. Measurements on soft sediment that had to some extent dried by the time the velocimeter had arrived on board would not be valid.

Natural Gamma Radiation

Natural gamma emissions were counted for a 1.25-minute period at 7.62 cm (3 in) intervals along the core with a counting precision of about ±100 counts. Methods, equipment, diameter corrections, and sediment disturbance are discussed in the Appendix.

Cores 2, 3, and 4 were recovered in the extended core barrel which has a 2.25-inch internal diameter (I.D.) compared to the normal 2.60-inch I.D. core. The emission counts measured from Cores 2, 3, and 4 were corrected to be equivalent to a 2.60-inch I.D. core. The volume difference per unit length between the cylinders, relative to the smaller cylinder, is 33.7 percent; therefore, the natural gamma counts of the 2.25-inch I.D. cores were increased accordingly.

In general, natural gamma radiation at Site 148 is inversely related to the sediment porosity, but the gamma

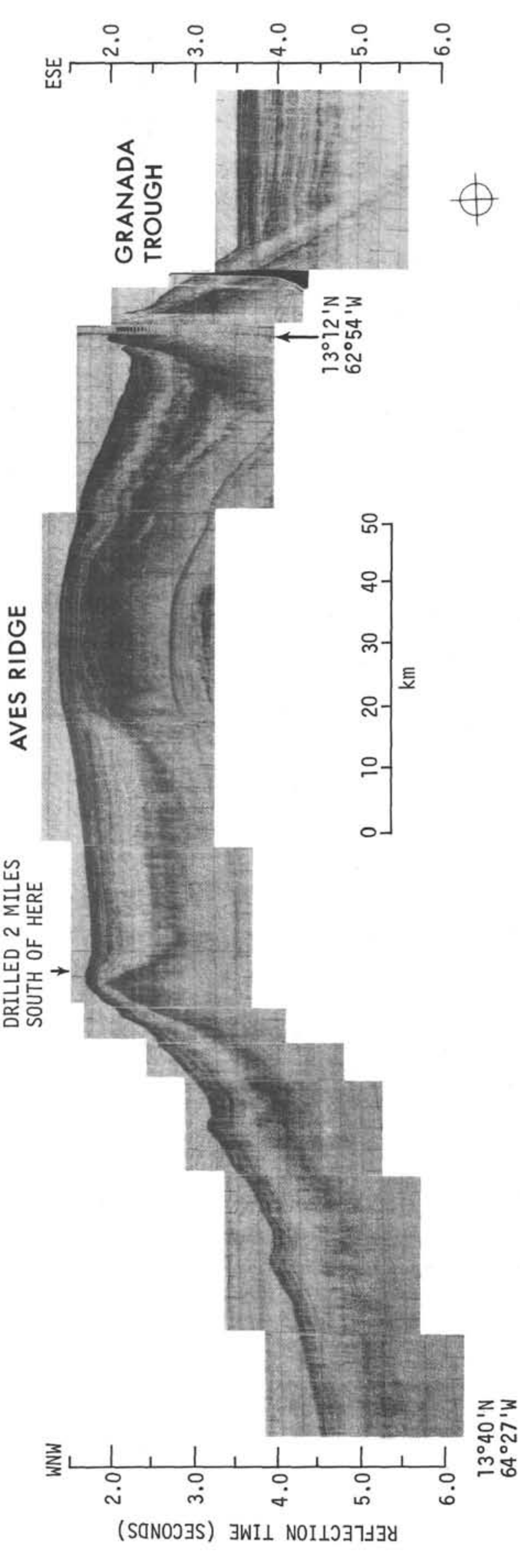

Figure 2. *Reflection record made by Woods Hole Oceanographic Institution R/V* Chain *over the Aves Ridge (from Bunce et al., 1970).*

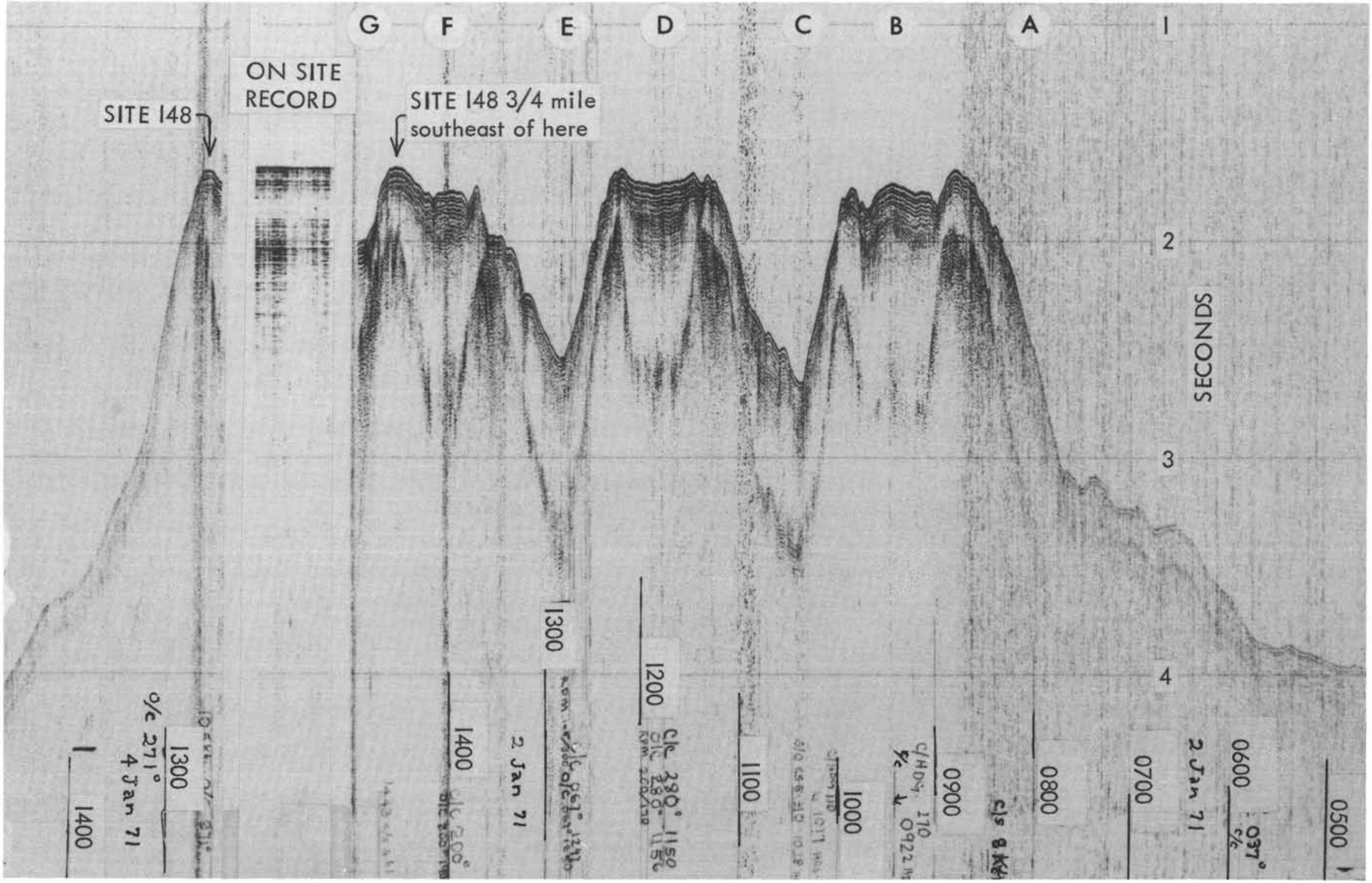

Figure 3. *Reflection record made by* Glomar Challenger *during survey. Note small patch of record made while on site which clearly establishes depth of prominent subbottom reflectors. Record to the left of on-site record was made during departure from the site. The vessel passed within 180 meters of the hole (beacon) on departure.*

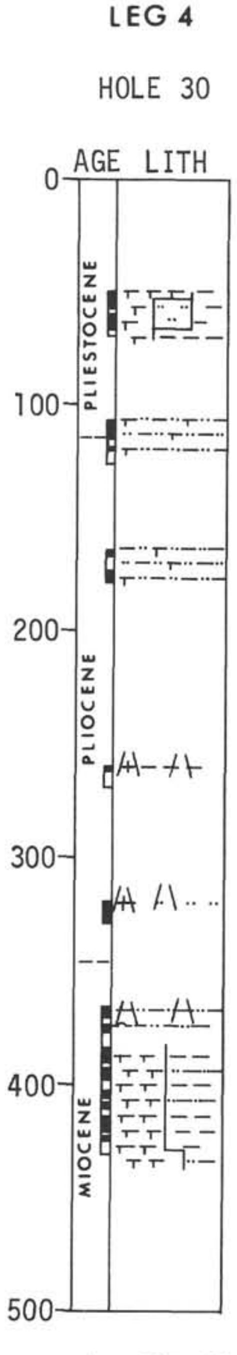

Figure 5. *Columnar section of Site 30 drilled on Leg 4. Site 30 is located about 70 km to the southeast of Site 148.*

data are not corrected to a standard porosity, or for varying porosity. A few gamma variations would decrease significantly if porosity corrections were made to a standard porosity. However, corrections would have to be made on the assumption that the core is homogeneous and the solids emit the gamma rays. (See Chapter 13 for discussions of porosity corrections).

The Pleistocene marl and clay (0 to 60 m depth) emitted counts from 700 to 1900, while Pleistocene clay (60 to 110 m) emitted counts from 500 to 2400. In general, the Pliocene-Miocene (in part Pleistocene) (110 to 260 m) clay emitted the highest counts of 1100 to 2800 with 1700 to 2700 being typical. Paleocene volcanic sand and clay (260 to 270 m) emitted relatively low gamma counts of 200 to 1600 counts per 1.25 minute period.

An ash and glauconite layer, which exists at the bottom of Core 27 (250 m depth) in the Miocene foraminifera nannofossil marl, emitted the highest single gamma count (4300) and appears as a "high spike" on the gamma plots.

Penetrometer

Needle penetration tests were performed at Site 148 with a 1-mm-diameter needle. The methods, equipment, and sediment disturbances are discussed in the Appendix.

Pleistocene to Pliocene marl and clay from 10 to 220 meters below the sea floor had needle penetrations ranging from 12 mm to less than 1 mm. These values irregularly decrease with increasing depth and age. In general, penetrations decrease from 12 mm to 5 mm between 10 and 120 meters below the sea floor, with a variation from 3 to 17 mm. From 120 meters to 220 meters depth, penetrations decrease from 5 mm to 2 mm, with a range of 1 to 7 mm, while below 140 meters depth, the typical variation decreases to 2 to 3 mm.

This very general change in slope of the penetration values versus depth, which occurs at 120 meters depth, roughly correlates with the Pleistocene-Pliocene boundary and a lithology change from clay to calcareous clay; the first occurrence of dolomite rhombs is at 105 meters depth. However, this change does not appear to be related only to differing lithologies, suggesting that depth, age and composition are the significant factors governing needle penetration.

BIOSTRATIGRAPHY

The upper lithic unit recognized at Site 148, calcareous clay about 250 meters thick (Cores 1-27), contains abundant planktonic foraminifera and calcareous nannofossils but lacks radiolaria.

Since the extinction level of *Globorotalia tumida flexuosa* lies above the samples from Core 1, neither the *Globorotalia fimbriata* Subzone nor the *Globigerina bermudezi* Subzone of the *Globorotalia truncatulinoides truncatulinoides* Zone were represented in material recovered at this site. The three lower subzones of the *Globorotalia truncatulinoides truncatulinoides* Zone are present: the *Globigerina calida calida* Subzone from the top of Core 1 to a level between the lower parts of Sections 2 and 4 of Core 3, the *Globorotalia hessi* Subzone from the middle of Core 3 to a level between the middle of Sections 3 and 6 of Core 11, and the *Globorotalia crassaformis viola* Subzone to a level between Cores 13 and 14.

Globorotalia inflata, a colder water form and always sinistrally coiled, is fairly frequent in most samples, except in Cores 6 through 8. Dextral coiled *Pulleniatina obliquiloculata obliquiloculata* and *Sphaeroidinella dehiscens* are present in most samples.

Calcareous nannofossils in this interval are well preserved and the assemblages diverse. All of the sediments recovered in Core 1 apparently belong to the *Emiliania huxleyi* Zone. The assemblage is diverse and well preserved. A number of species not found at Site 147 occur here. The lowest occurrence of *E. huxleyi* lies in the lower part of Core 2, about the middle part of Section 4.

The lower part of Core 2, all of Cores 3 through 11, and the top of Core 12 belong to the *Gephyrocapsa oceanica* Zone. The assemblages are generally rich, diverse, and well preserved. The *G. oceanica* Zone (defined as the interval between the lowest occurrence of *G. oceanica* and the lowest occurrence of *E. huxleyi*) can often be subdivided by recognizing the highest occurrence surface of *Pseudoemiliania lacunosa.* At this site, the highest specimens of *P. lacunosa* were found in samples between Sections 1 and 3 of Core 3.

The lower parts of Core 12 (base of Section 1 through Section 5), all of Core 13, and the upper parts of Core 14 (Section 1 and the top of Section 2) belong to the *Gephyrocapsa caribbeanica* Zone, which is defined as the interval between the highest occurrence of *Discoaster brouweri* and the lowest occurrence of *Gephyrocapsa oceanica*. If the terminology of Gartner (1969) is employed, the *Pseudoemiliania* Zone extends from the middle of Section 4 of Core 4 to the top of Section 2 of Core 14 and the *Gephyrocapsa* Zone is restricted to the base of Core 2, through Core 3, to the middle of Section 4 of Core 4.

If the Pliocene-Pleistocene boundary is defined as the lowest occurrence of *Globorotalia truncatulinoides truncatulinoides,* it lies at a depth of about 118 meters, between Cores 13 and 14. If it is defined as the highest occurrence of *Discoaster brouweri,* the boundary would be placed slightly lower, in Section 4 of Core 15, at a depth of about 132 meters.

The *Globorotalia truncatulinoides* cf. *tosaensis* Zone extends from the top of Core 14 to the base of Core 15. This interval lies between the extinction level of *Globorotalia miocenica* and the first appearance of keeled, though evolutionary still early, *Globorotalia truncatulinoides truncatulinoides.* Forms resembling *Gr. truncatulinoides* cf. *tosaensis* are very rare to absent in the examined samples. The *Gr. tumida* and *Gr. menardii* groups also occur only very erratically and rarely. Fairly frequent throughout this zone are specimens of the *Gr. crassaeformis* group, in particular *Gr. crassaeformis viola.*

Pulleniatina obliquiloculata obliquiloculata coils dextrally in the lower part of the zone, changes to sinistral coiling in Core 14, Section 4, and becomes dextral again in Core 14 Section 2.

Discoaster brouweri increases in abundance rapidly downward through the lower part of Core 14 and in Cores 15 and 16. In the same sections, deterioration of the calcareous nannofossil assemblages occurs, diversity decreases, and some samples contain but a few specimens. This interval, to the level of highest occurrence of *Discoaster pentaradiatus* between samples from Sections 2 and 3 of Core 16, belongs to the *D. brouweri* Zone as redefined by Martini and Worsley (1970).

Sample 15-6(127-129 cm), contains only *Gr. exilis* but no *Gr. miocenica.* The core catcher immediately below contains both species. This slightly higher range of *Gr. exilis* was also observed in Site 31. Below this level, both species are present consistently, *Gr. miocenica* usually being more frequent. The *Globorotalia miocenica* Zone (Middle Pliocene) is thus represented by Cores 16 through 20 to near the base of Section 3 of Core 21. The boundary between the upper *Globorotalia exilis* Subzone and the lower *Globigerinoides trilobus fistulosus* Subzone is marked by the highest occurrence of the latter species which lies between samples from Sections 1 and 3 of Core 18. Lower strata of this unit, to the base of Core 27, belong to the *Globorotalia margaritae* Zone (early Pliocene). Again, the two subunits, the upper *Globorotalia margaritae evoluta* and the lower *Globorotalia margaritae margaritae* Subzones, are recognizable. The evolutionary appearance of *Globorotalia margaritae evoluta* which defines the boundary between them lies between Cores 25 and 26.

The upper part of the zone is characterized by large-sized *Globorotalia margaritae,* apparently a late evolutionary stage of the species. This same form was also observed in the upper part of the zone at Sites 29 through 31 and is also known from the same stratigraphic position in the Mediterranean (Leg 13). The normal-sized *Gr. margaritae* is frequent in Core 27, where the zone lies on a sequence consisting predominantly of volcanic ash. It is likely that the basal part of the *G. margaritae* Zone is missing.

The following coiling changes were observed within Core 27:

1) *Pulleniatina obliquiloculata primalis* changes from sinistral coiling in Section 6 to dextral coiling in Section 5. The species was not seen in upper part of the *Gr. margaritae* Zone. An identical coiling change at the same stratigraphic level was noted in well Cubagua-1 on the island of that name situated between Margarita Island and the north coast of Venezuela. There, the change takes place between 1029 feet and 958 feet and the species disappears shortly after, still within the *G. margaritae* Zone, as at Site 148. While the species does not reappear in Cubagua-1, which started drilling within the Pliocene, it remains absent in Site 148 throughout the *G. miocenica* Zone only to reappear in the late Pliocene *G. truncatulinoides* cf. *tosaensis* Zone as *P. obliquiloculata obliquiloculata* and continues from there to Recent. The coiling change of *P. obliquiloculata primalis* within the *Gr. margaritae* Zone serves as a good correlation level between Cubagua-1 and Site 148, which are about 300 km apart. This level apparently coincides with Datum VII of Hays et al., (1969) of approximately 3.7 m.y. Noteworthy also is the temporary disappearance of the genus in both sections shortly after the coiling change, an indication that this may be a fairly widespread event, at least in the eastern Caribbean.

2) Forms of the *Globorotalia menardii* complex, and others intermediate between *Gr. tumida flexuosa* and *Gr. multicamerata,* change from sinistral coiling in the lower part of Section 6 to dextral coiling in higher samples. This is slightly earlier than the above-mentioned *Pulleniatina* coiling change. At the same level, an identical coiling change also takes place in the *Gr. dutertrei* complex. A comparable change of *Gr. menardii* s.l. and the *Gr. dutertrei* group was also noted in Cubagua-1, again slightly earlier than the *Pulleniatina* coiling change. A similar coiling change from sinistral to dextral of *Gr. tumida flexuosa* in the basal part of the *Gr. margaritae* Zone of well

Bodjonegoro-1 in Java might be an indication that this particular coiling change in the *tumida/menardii* complex is of more than only local significane. It again appears to correspond closely with Datum VII of Hays et al. (1969) of approximately 3.7 m.y.

While *Sphaeroidinellopsis subdehiscens* is present throughout the lower part of the *Gr. margaritae* Zone, *Sphaeroidinella dehiscens* has its lowest occurrence in Section 3 of Core 24.

Using calcareous nannofossils, the *Discoaster pentaradiatus* Zone includes strata from the base of Core 16 through Cores 17, 18, and 19. The highest occurrence of *Discoaster surculus* is difficult to fix because preservation of asteroliths below Core 16 is generally poor. Specimens with affinities to *D. surculus,* but with narrow arms, are present in Core 19, but the highest typical specimens of this distinctive species were noted in Core 20. Cores 20 through 26 and the first three sections of Core 27 are referred to the *D. surculus* Zone. Asteroliths are scarce in these sediments and the coccolith floras appear to contain unusually few species. Calcareous nannofossils are generally scarce, with coccoliths common at only a few levels. Assemblages become progressively richer toward the base of Core 27. The highest occurrence of *Sphenolithus abies* lies between samples from Sections 1 and 2 of Core 27 and the base of Core 26 in an unrecovered interval. If the terminology of Boudreaux and Hay (1969) were used, most of Core 27 would belong to the *Sphenolithus abies* Zone. The highest occurrence of *Reticulofenestra pseudoumbilica* is in the uppermost part of Section 4 of Core 27; the lower part of the core can be assigned to the *R. pseudoumbilica* Zone. The lowest occurrence of *P. lacunosa* was not reached above the volcanics so that the sediments of the lower three sections of Core 27 belong to the uppermost part of the *R. pseudoumbilica* Zone.

Rare radiolarians, moderately to poorly preserved (somewhat dissolved), occur in Cores 1 through 4 (from 0 to 36 m below the sea floor). None occur in Cores 5 through 27.

Beneath the clays with pelagic fossils lies a series of volcanic sands and clays extending from 250-272 meters (Cores 28-31). The poor foraminiferal fauna of these beds in Core 28 is heterogeneous and consists primarily of Early Miocene and Paleocene species. Species of Early Miocene aspect include *Globigerinoides primordius, Globoquadrina altispira,* and *Globigerinoides bisphericus. Globorotalia angulata* and *Bathysiphon* specimens, some of which are very large, are indicative of the Paleocene. Similar faunas are known from the lower Scotland Formation of Barbados (Saunders, 1968). Foraminifera are very scarce in Cores 29 through 31. Observed were *Globorotalia angulata, Globigerina* sp., *Bulimina* sp., and *Bathysiphon* sp. (partly large sizes as in Core 28), indicative of Paleocene but probably reworked in younger beds as are those in Core 28. Sample 29-1 (90-95 cm) contains fragments of carbonized wood. All samples of Cores 28 through 31 contain radiolaria.

The volcanic sediments contained in Core 28 through 31 also include a few fine-grained layers with mixed calcareous nannofossils of Late Cretaceous (particularly Campanian-Maestrichtian) and older Tertiary age. A few moderately preserved radiolarians (somewhat dissolved and infilled) occur, together with a few diatoms; they appear to be of Paleocene age, but the assemblages show no evidence of being reworked.

CONCLUSIONS

The pelagic sediments at Site 148 represent a high accumulation rate for carbonate-poor sediments; rates vary from about 35 to 55 m/m.y. The nonbiogenic mineralogy of the upper sequence (described in detail in Chapter 14) shows high concentrations of mica and quartz, variable kaolin, and low chlorite and montmorillonite. Although plagioclase is a pervasive volcanic constituent, the quartz-plagioclase ratio is high (average around 8/1). The volcanic islands of the Lesser Antilles are dominantly andesitic and plagioclase is far more abundant in the islands than quartz. Further, the islands are not an important source for mica minerals. The nonbiogenic component of the sediment at Site 148 is most probably from South America. The Amazon River, according to Jacobs and Ewing (1969), is high in mica and kaolin and would have constituted one source with additional sediment contributed by the Orinoco River.

The wide distribution of pyrite and scattered siderite reflects a generally reducing environment within the sediment. Apparently, trapped organic matter did not oxidize completely before burial and reacted with pore water sulfate ions to produce sulfide.

The record of volcanic activity recorded in the upper sediment sequence is of great interest in reconstructing the history of Lesser Antilles volcanism. An estimate was made of the frequency of major eruptions during the Pleistocene and Pliocene by recording the number of ash layers or smear slides with major amounts of ash and adjusting for hypothetical complete recovery of the cored interval. The "inferred major eruptions" per core varies considerably through the sequence. Six periods with at least some major eruptive activity were recognized:

1) Cores 3 through 5 (late Pleistocene) yield twenty-six inferred major eruptions (about 1 per 20,000 years).

2) Cores 7 and 8 (middle Pleistocene) yield thirteen inferred major eruptions.

3) Cores 10 and 12 (early Pleistocene) show two inferred major eruptions.

4) Core 17 (late Pliocene) yields three inferred major eruptions.

5) Core 20 (late Pliocene) yields one inferred major eruption.

6) Core 27 (middle Pliocene) yields four inferred major eruptions.

The abrupt increase in eruptive activity during the middle Pleistocene (seen also in the first appearance of orthopyroxene and a marked increase in clinopyroxene) evidently corresponds to the initiation of the current two-pyroxene andesite eruptive cycle, which has been estimated to have been in the middle Pleistocene on the basis of geomorphic reasoning (Robson and Tomblin, 1966).

This analysis is in basic agreement with the interpretation of Site 30 data presented by the Leg 4 scientists (Benson et al., 1970). They noted that there is an increase in sediment accumulation rate at Site 30 (about 30 miles southeast of Site 148) from the Miocene (4 mm/10^3 y) through the Pliocene (40 mm/20^3y) and Pleistocene (100 mm/10^3 y) which they attribute to a period of Lesser Antillean volcanic activity that started in the Pliocene and increased in the Pleistocene. However, as pointed out above, the high quartz-to-feldspar ratio and the presence of mica indicate that Lesser Antilles volcanics are not the sole source of noncarbonate minerals and may not be a major contributor.

The unconformity between the upper and lower sequence marks an abrupt change in sedimentary regime and also implies a possible vertical movement. The lower volcanic sands represent accumulation around an emergent (?) igneous-metamorphic island. No continental provenance is suggested by the constituents, and the abundance of porphyritic andesite, plagioclase, and hornblende suggests that the source was a calc-alkaline volcanic center within an oceanic island arc. The phosphatic iron-oxide layer at the unconformity implies a period of sedimentary isolation and submarine or subaerial weathering prior to the accumulation of pelagic sediments. Two possible geologic origins are hypothesized. The first hypothesis calls for a period in relatively deep water adjacent to an emergent volcanic island, a period of nondeposition or erosion caused by high-velocity bottom currents, and a final period of pelagic sediment accumulation. The second hypothesis begins with a period in relatively deep water adjacent to an emergent volcanic island, followed by a shallow-water or emergent period, and a final deeper stage during which pelagic sediments accumulated. At present, there is insufficient information to favor either hypothesis.

The single strong reflector noted on the profiler records at about 0.25 to 0.30 sec reflection time probably corresponds to the change in lithology at 250 meters. It is difficult to be certain with the vagueness of the reflector near the peak where the hole was drilled. The "on-site record" is particular vague, as is commonly the case with records made while on station.

REFERENCES

Bader, R. G., Gerard, R. D. et al., 1970. Initial Reports of the Deep Sea Drilling Project, Volume IV. Washington (U.S. Government Printing Office).

Barker, P. F., 1970. Plate tectonics of the Scotia Sea region. Nature. 228, 1293.

Benson, W. M., Gerard, R. D., and Hay, W. W., 1970. Summary and conclusions. *In* Bader, R. G., Gerard, R. D. et al., 1970. Initial Reports of the Deep Sea Drilling Project, Volume IV. Washington (U.S. Government Printing Office). 659.

Boudreaux, J. E. and Hay, W. W., 1969. Calcareous nannoplankton and biostratigraphy of the late Pliocene-Pleistocene-Recent sediments in the Submarex cores. Rev. Esp. Micropal., **1** (3).

Bunce, E. T., Phillips, J. D., Chase, R. L., and Bowin, C. O., 1970. The Lesser Antilles Arc and the eastern margin of the Caribbean Sea. *In* Maxwell, A. E. The Sea, vol. 4. 359.

Edgar, N. T., Ewing, J. I., and Hennion, J., 1971. Seismic refraction and reflection in the Caribbean Sea. Bull. Am. Assoc. Petrol. Geologists. **55**, 833.

Ewing, J. I., Officer, C. B., Johnson, H. R., and Edwards, R. S., 1957. Geophysical investigations in the eastern Caribbean: Trinidad shelf, Tobago Trough, Barbados Ridge, Atlantic Ocean. Bull. Geol. Soc. Am. **68**, 897.

Fox, P. J., Schreiber, E., and Heezen, B. C., 1971. The geology of the Caribbean crust: Tertiary sediments, granitic and basic rocks from the Aves Ridge. Tectonophysics. **12**, 89.

Gartner, S., Jr., 1969. Correlation of Neogene planktonic foraminifer and calcareous nannofossil zones. Trans. Gulf Coast Assoc. Geol. Socs. **19**, 585.

Hays, J. D., Saito, T., Opdyke, N. D., and Burckle, L. H., 1969. Pliocene-Pleistocene sediments of the equatorial Pacific: Their paleomagnetic, biostratigraphic, and climatic record. Bull. Geol. Soc. Am. **80**, 1481.

Jacobs, M. B. and Ewing, M., 1969. Mineral source and transport of the Gulf of Mexico and Caribbean Sea. Science. **163**, 805.

Karig, D. E., 1970. Ridges and basins of the Tonga-Kermodec Island Arc System. J. Geophys. Res. **75**, 239.

Karig, D. E. and Glassley, W. E., 1970. Dacite and related sediment from the west Marianna Ridge, Philippine Sea. Bull. Geol. Soc. Am. **81**, 2143.

Malfait, B. T. and Dinkelman, M. G., 1972. Circum-Caribbean tectonic and igneous activity and the evolution of the Caribbean plate. Bull. Geol. Soc. Am. 83, 251.

Martini, E. and Worsley, T., 1970. Standard Neogene calcareous nannoplankton zonation. Nature. **225**, 289.

Officer, C. B., Ewing, J. I., Edwards and Johnson, H. R., 1957. Geophysical investigations in the eastern Caribbean: Venezuelan Basin, Antilles Island Arc, and Puerto Rico Trench. Bull. Geol. Soc. Am. **68**, 359.

Officer, C. B., Ewing, J. I., Hennion, J. F., Harkrider, D. G., and Miller, D. E., 1959. Geophysical investigations in the eastern Caribbean: summary of 1955 and 1956 cruises. *In* Ahrens, L. H., Press, F., Rankama, K. and Runcorn, S. K. (Eds.), Physics and Chemistry of the Earth. New York (Pergamon Press). 17.

Robson, G. R. and Tomblin, J. F., 1966. Catalogue of the active volcanoes of the world including solfatara fields. Part XX. West Indies. Intern. Assoc. Volcanology. Rome. 56.

Saunders, J. B., 1968. Field trip guide to Barbados. Trans. IV Caribbean Geological Conference. 663.

SITE 148

LITHOLOGY

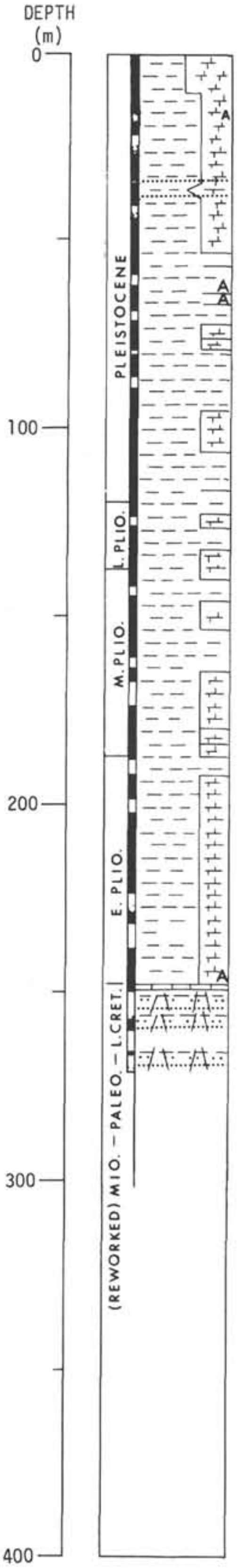

UNITS		SUBUNITS OR DESCRIPTION	
UNIT I (0 to 249.27 m) NANNO FORAM MARL, NANNO FORAM RICH CLAY, and CLAY		Subunit a. (0 to 56 m) NANNO FORAM MARL and NANNO FORAM RICH CLAY, pale yellow brown (surface) and greenish gray. Intermittent Foram rich layers, some size graded (coarser on bottom). Clear ash layers at 241.27 m.	
		Subunit b. (56.60 to 193.90 m) FORAM NANNO RICH CLAY and CLAY, interbedded greenish gray. Intermittent beds rich in forams. A=Thin brown ash layers. Occurrences of pyrite.	
		Subunit c. (193.90 to 249.27 m) FORAM NANNO RICH CLAY, greenish gray, compaction increasing with depth. At bottom pale orange FORAM LIMESTONE.	
UNIT II (249.27 to 272 m T.D.) VOLCANIC SANDS and CLAY		VOLCANIC CLAY and coarse to fine SAND, dusky yellow to olive brown. SILTY CLAY and VOLCANIC SAND, olive black, some with graded bedding.	

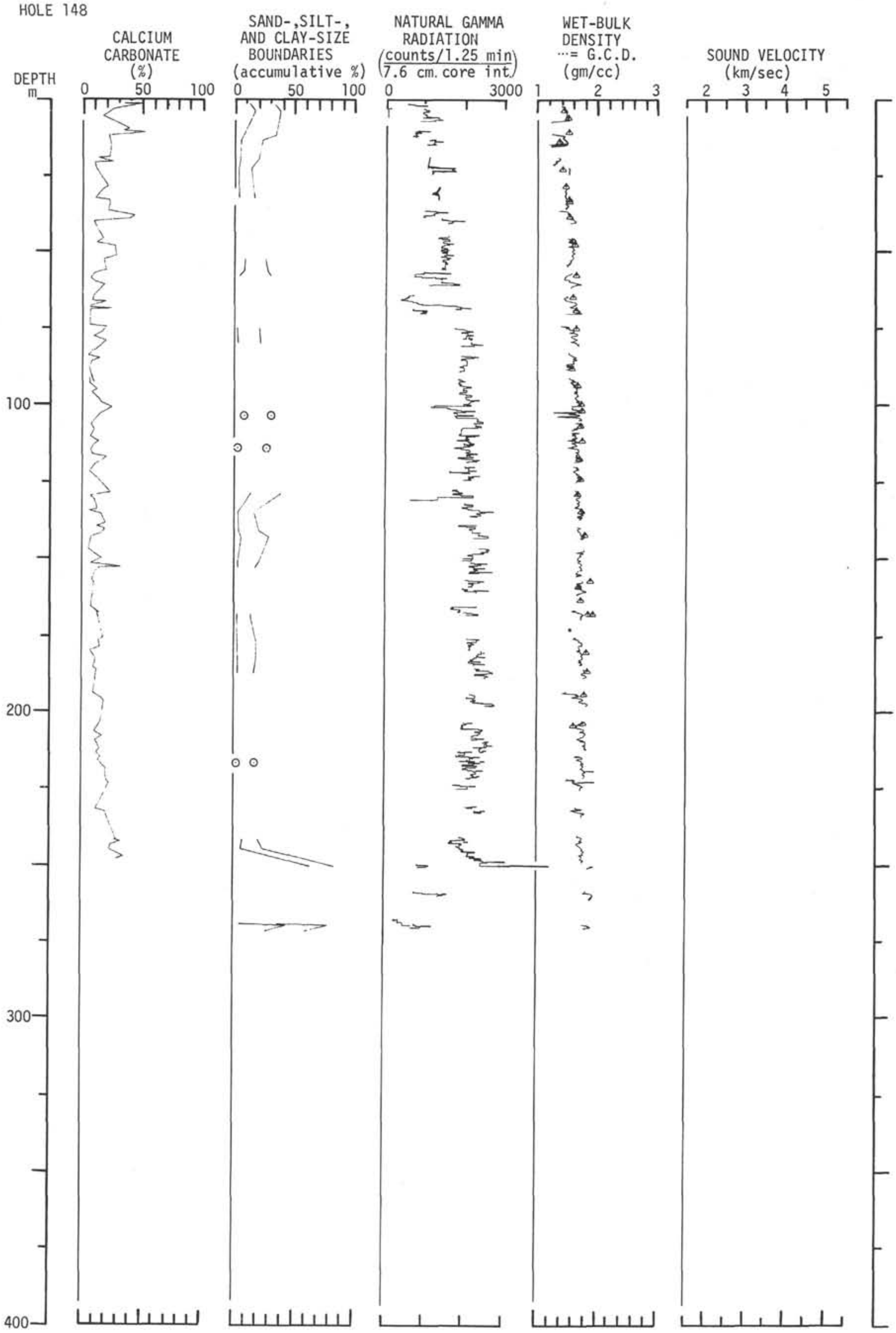
HOLE 148
DEPTH m
CALCIUM CARBONATE (%)
0
50
100
SAND-,SILT-, AND CLAY-SIZE BOUNDARIES (accumulative %)
0
50
100
NATURAL GAMMA RADIATION (counts/1.25 min / 7.6 cm. core int.)
0
3000
WET-BULK DENSITY
···= G.C.D.
(gm/cc)
1
2
3
SOUND VELOCITY (km/sec)
2
3
4
5
100
200
300
400

SITE 148 HOLE CORE 1 CORED INTERVAL (m) 0-9

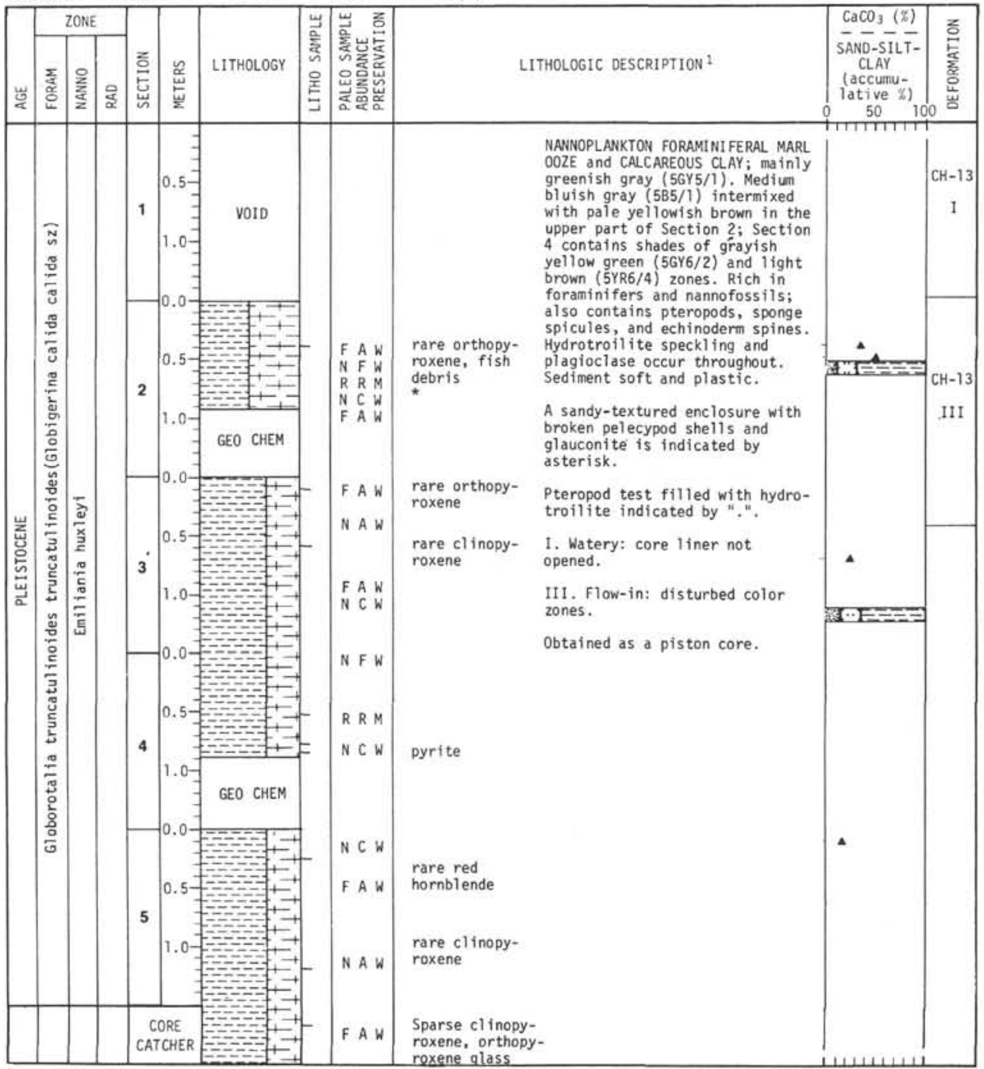

NANNOPLANKTON FORAMINIFERAL MARL OOZE and CALCAREOUS CLAY; mainly greenish gray (5GY5/1). Medium bluish gray (5B5/1) intermixed with pale yellowish brown in the upper part of Section 2; Section 4 contains shades of grayish yellow green (5GY6/2) and light brown (5YR6/4) zones. Rich in foraminifers and nannofossils; also contains pteropods, sponge spicules, and echinoderm spines. Hydrotroilite speckling and plagioclase occur throughout. Sediment soft and plastic.

A sandy-textured enclosure with broken pelecypod shells and glauconite is indicated by asterisk.

Pteropod test filled with hydrotroilite indicated by ".".

I. Watery: core liner not opened.

III. Flow-in: disturbed color zones.

Obtained as a piston core.

---

¹For explanation of symbols, see Chapter 1

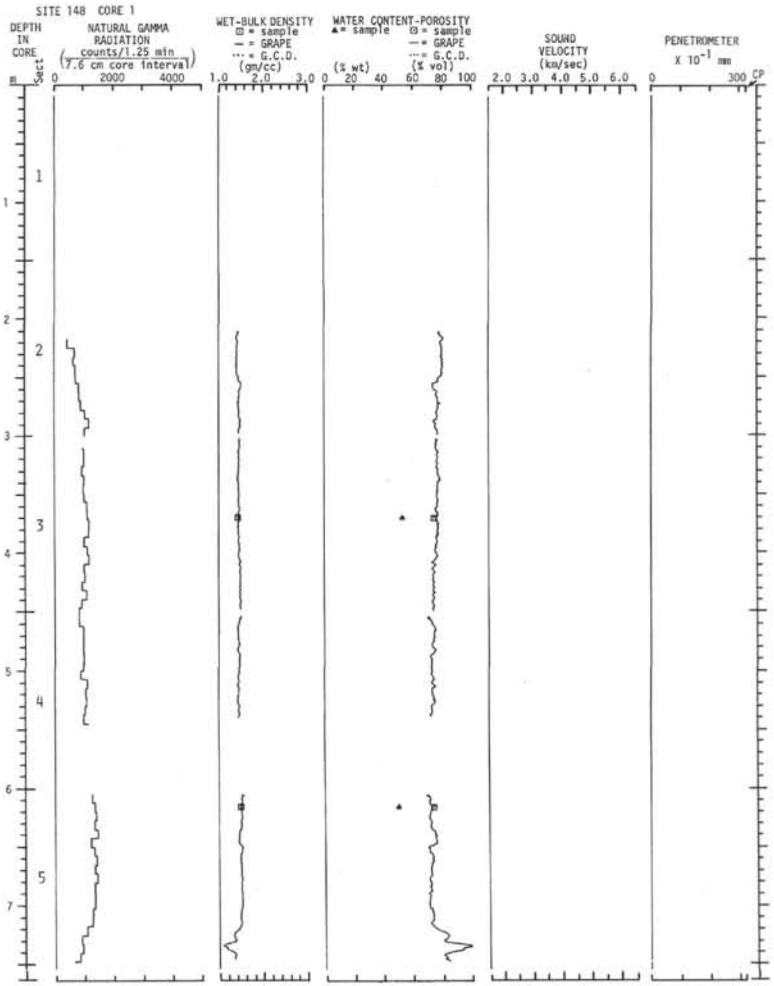

The "0" of the natural gamma data is equal to the atmospheric background count (gamma count when equipment was empty) of 1329. This background was subtracted from the data.

SITE 148 HOLE CORE 2 CORED INTERVAL (m) 9-18

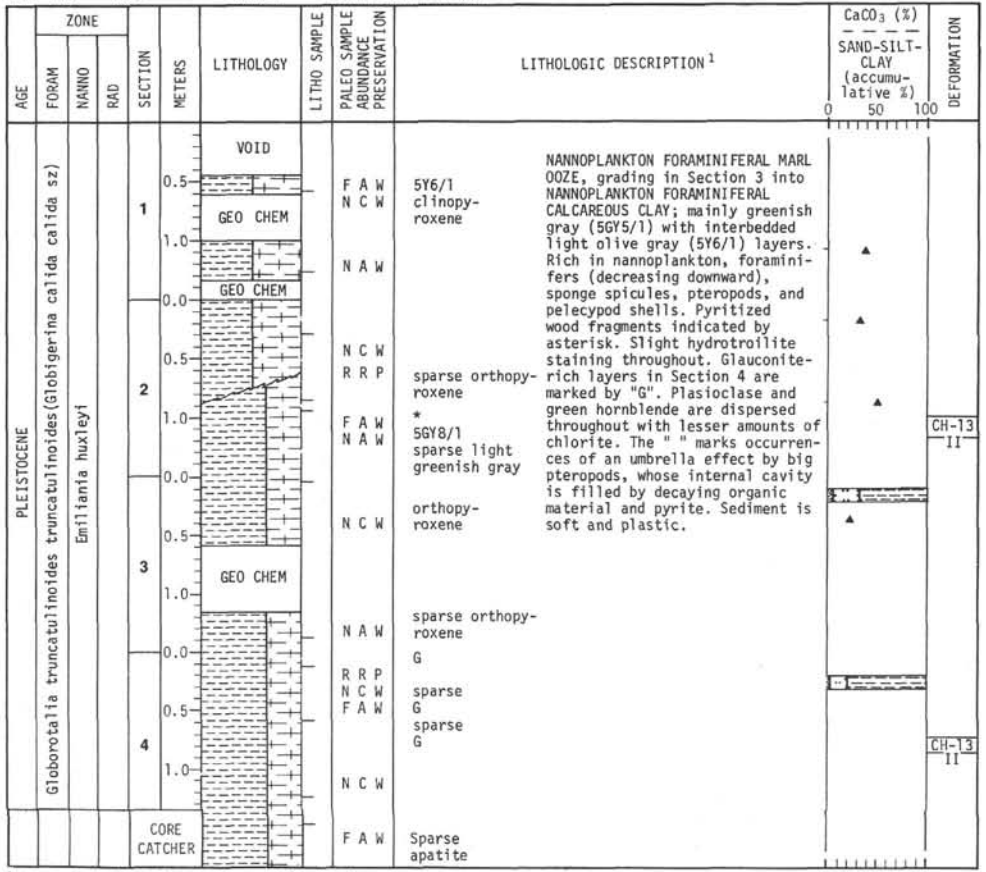

NANNOPLANKTON FORAMINIFERAL MARL OOZE, grading in Section 3 into NANNOPLANKTON FORAMINIFERAL CALCAREOUS CLAY; mainly greenish gray (5GY5/1) with interbedded light olive gray (5Y6/1) layers. Rich in nannoplankton, foraminifers (decreasing downward), sponge spicules, pteropods, and pelecypod shells. Pyritized wood fragments indicated by asterisk. Slight hydrotroilite staining throughout. Glauconite-rich layers in Section 4 are marked by "G". Plasioclase and green hornblende are dispersed throughout with lesser amounts of chlorite. The " " marks occurrences of an umbrella effect by big pteropods, whose internal cavity is filled by decaying organic material and pyrite. Sediment is soft and plastic.

¹For explanation of symbols, see Chapter 1

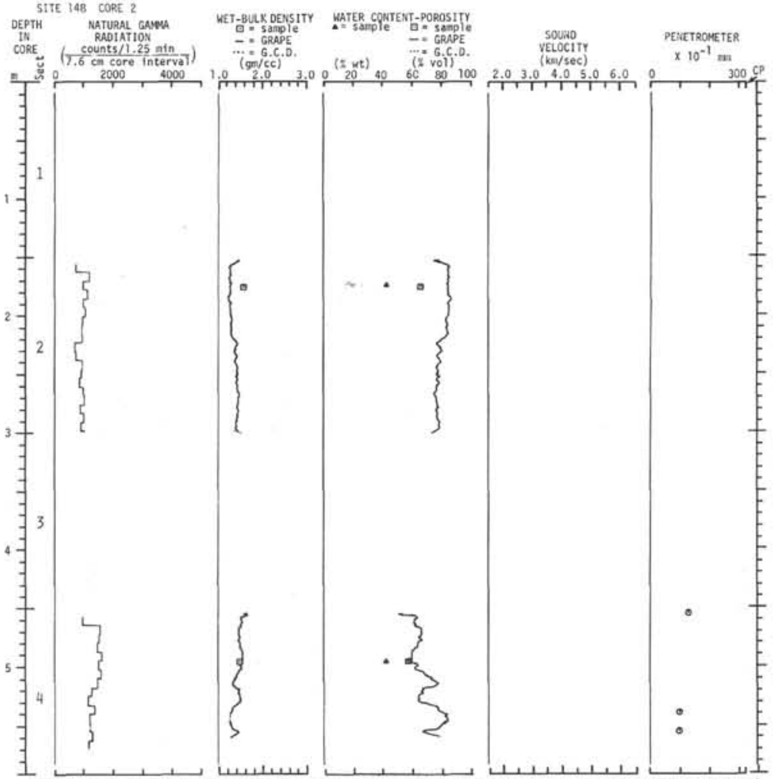

The "0" of the natural gamma data is equal to the atmospheric background count (gamma count when equipment was empty) of 1288. This background was subtracted from the data.

SITE 148 HOLE CORE 3 CORED INTERVAL (m) 18-27

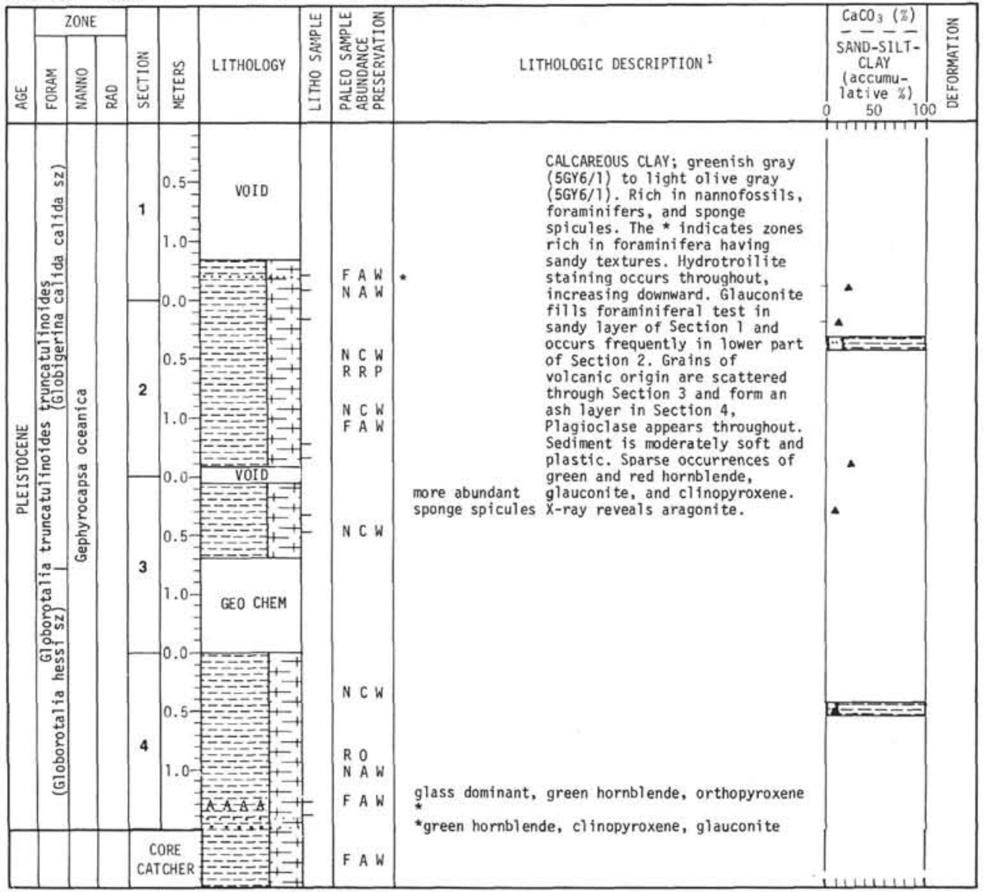

CALCAREOUS CLAY; greenish gray (5GY6/1) to light olive gray (5GY6/1). Rich in nannofossils, foraminifers, and sponge spicules. The * indicates zones rich in foraminifera having sandy textures. Hydrotroilite staining occurs throughout, increasing downward. Glauconite fills foraminiferal test in sandy layer of Section 1 and occurs frequently in lower part of Section 2. Grains of volcanic origin are scattered through Section 3 and form an ash layer in Section 4, Plagioclase appears throughout. Sediment is moderately soft and plastic. Sparse occurrences of green and red hornblende, glauconite, and clinopyroxene. X-ray reveals aragonite.

more abundant sponge spicules

glass dominant, green hornblende, orthopyroxene

*

*green hornblende, clinopyroxene, glauconite

---

¹For explanation of symbols, see Chapter 1

SITE 148 CORE 3

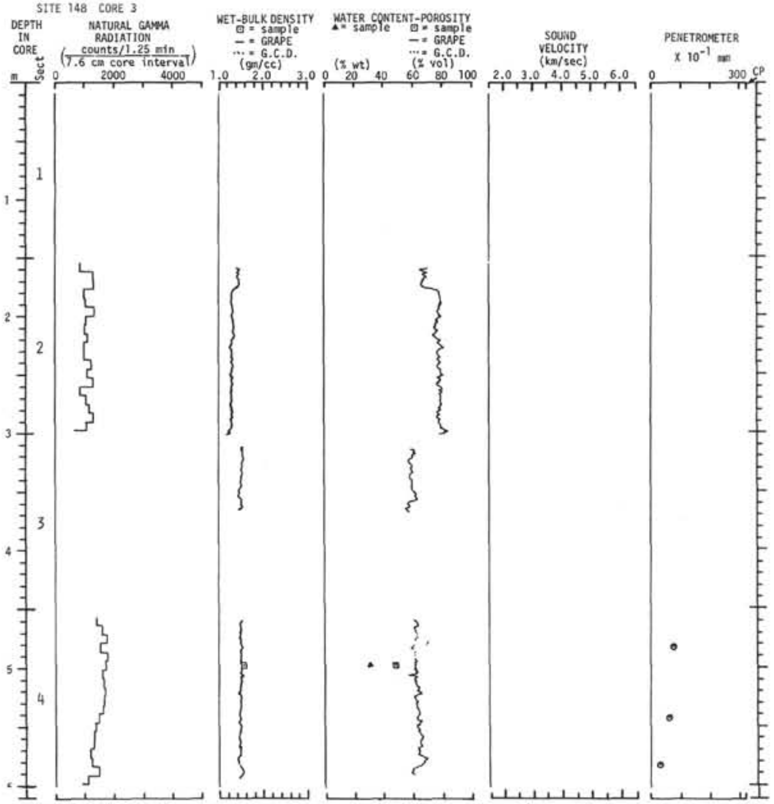

The "0" of the natural gamma data is equal to the atmospheric background count (gamma count when equipment was empty) of 1288. This background was subtracted from the data.

SITE 148 HOLE CORE 4 CORED INTERVAL (m) 27-36

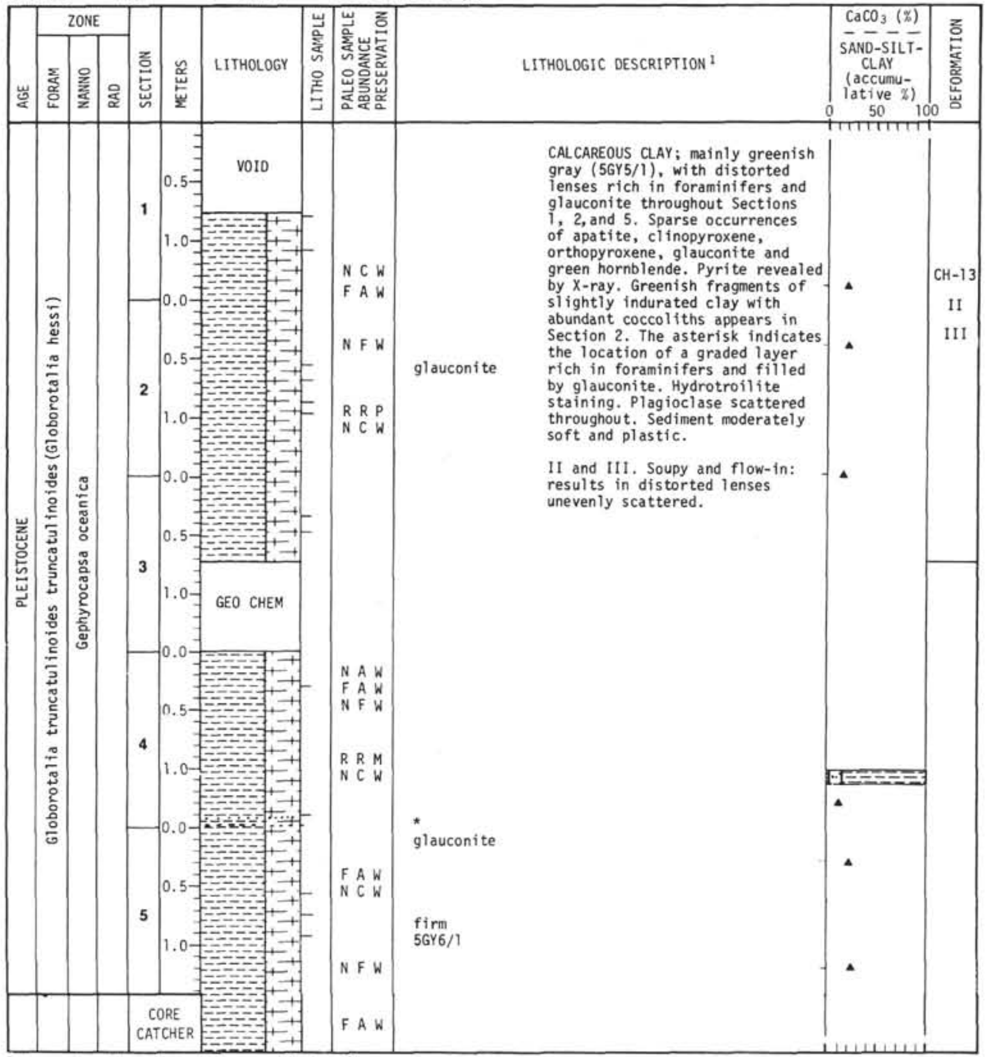

CALCAREOUS CLAY; mainly greenish gray (5GY5/1), with distorted lenses rich in foraminifers and glauconite throughout Sections 1, 2, and 5. Sparse occurrences of apatite, clinopyroxene, orthopyroxene, glauconite and green hornblende. Pyrite revealed by X-ray. Greenish fragments of slightly indurated clay with abundant coccoliths appears in Section 2. The asterisk indicates the location of a graded layer rich in foraminifers and filled by glauconite. Hydrotroilite staining. Plagioclase scattered throughout. Sediment moderately soft and plastic.

II and III. Soupy and flow-in: results in distorted lenses unevenly scattered.

¹For explanation of symbols, see Chapter 1

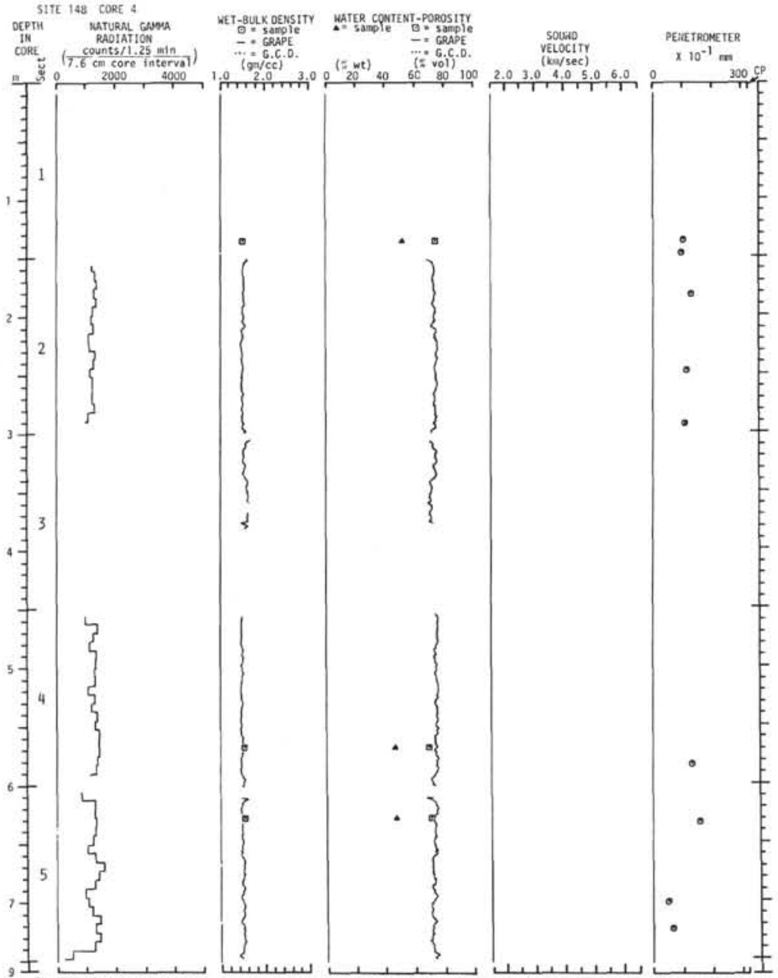

The "0" of the natural gamma data is equal to the atmospheric background count (gamma count when equipment was empty) of 1288. This background was subtracted from the data.

SITE 148 HOLE CORE 5 CORED INTERVAL (m) 36-45

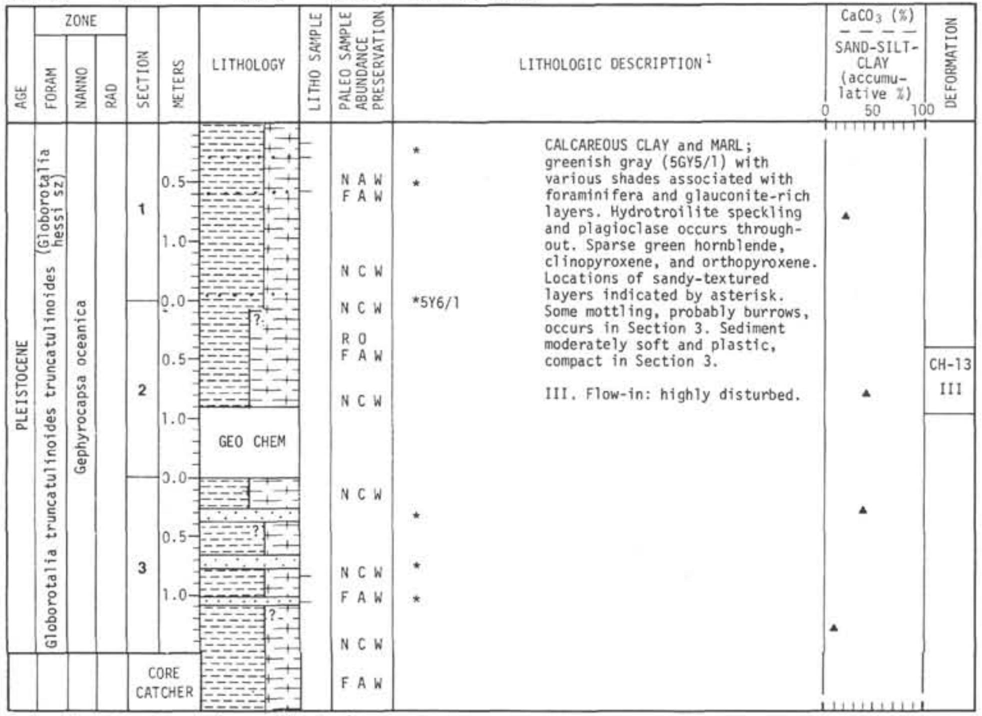

CALCAREOUS CLAY and MARL; greenish gray (5GY5/1) with various shades associated with foraminifera and glauconite-rich layers. Hydrotroilite speckling and plagioclase occurs throughout. Sparse green hornblende, clinopyroxene, and orthopyroxene. Locations of sandy-textured layers indicated by asterisk. Some mottling, probably burrows, occurs in Section 3. Sediment moderately soft and plastic, compact in Section 3.

III. Flow-in: highly disturbed.

[1]For explanation of symbols, see Chapter 1

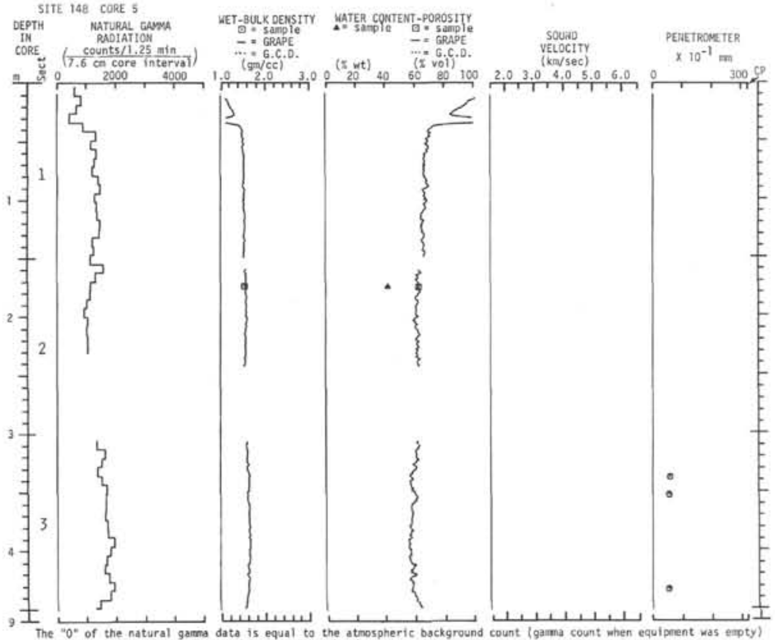

The "0" of the natural gamma data is equal to the atmospheric background count (gamma count when equipment was empty) of 1288. This background was subtracted from the data.

SITE 148 HOLE CORE 6 CORED INTERVAL (m) 45-55

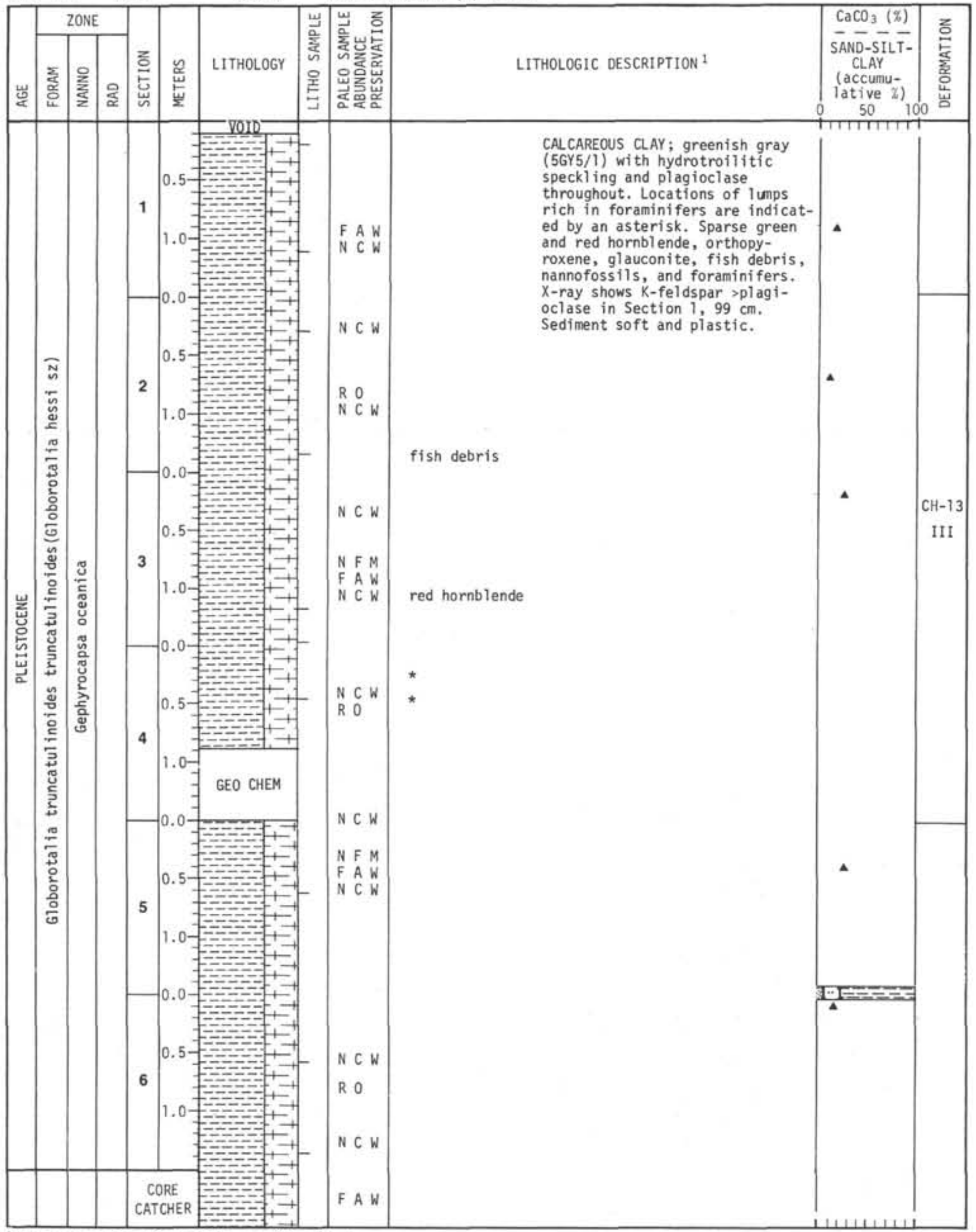

CALCAREOUS CLAY; greenish gray (5GY5/1) with hydrotroilitic speckling and plagioclase throughout. Locations of lumps rich in foraminifers are indicated by an asterisk. Sparse green and red hornblende, orthopyroxene, glauconite, fish debris, nannofossils, and foraminifers. X-ray shows K-feldspar >plagioclase in Section 1, 99 cm. Sediment soft and plastic.

¹For explanation of symbols, see Chapter 1

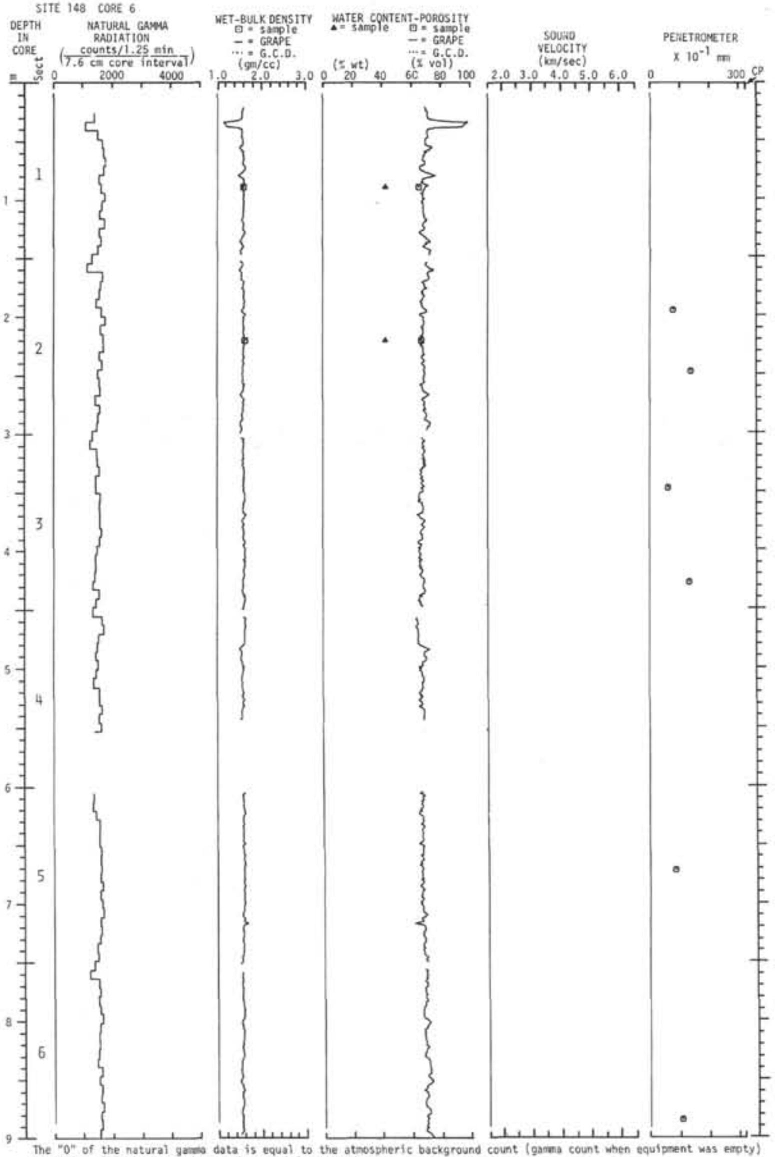

The "0" of the natural gamma data is equal to the atmospheric background count (gamma count when equipment was empty) of 1291. This background was subtracted from the data.

SITE 148 HOLE CORE 7 CORED INTERVAL (m) 55-64

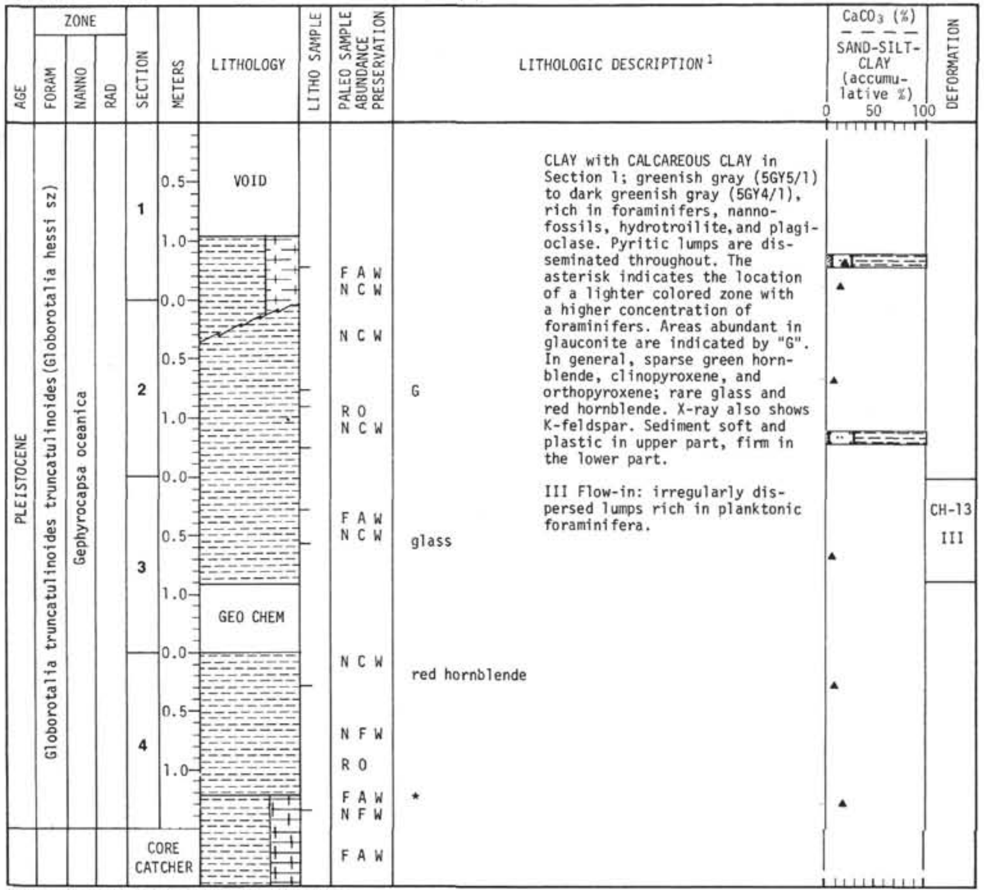

CLAY with CALCAREOUS CLAY in Section 1; greenish gray (5GY5/1) to dark greenish gray (5GY4/1), rich in foraminifers, nannofossils, hydrotroilite, and plagioclase. Pyritic lumps are disseminated throughout. The asterisk indicates the location of a lighter colored zone with a higher concentration of foraminifers. Areas abundant in glauconite are indicated by "G". In general, sparse green hornblende, clinopyroxene, and orthopyroxene; rare glass and red hornblende. X-ray also shows K-feldspar. Sediment soft and plastic in upper part, firm in the lower part.

III Flow-in: irregularly dispersed lumps rich in planktonic foraminifera.

¹For explanation of symbols, see Chapter 1

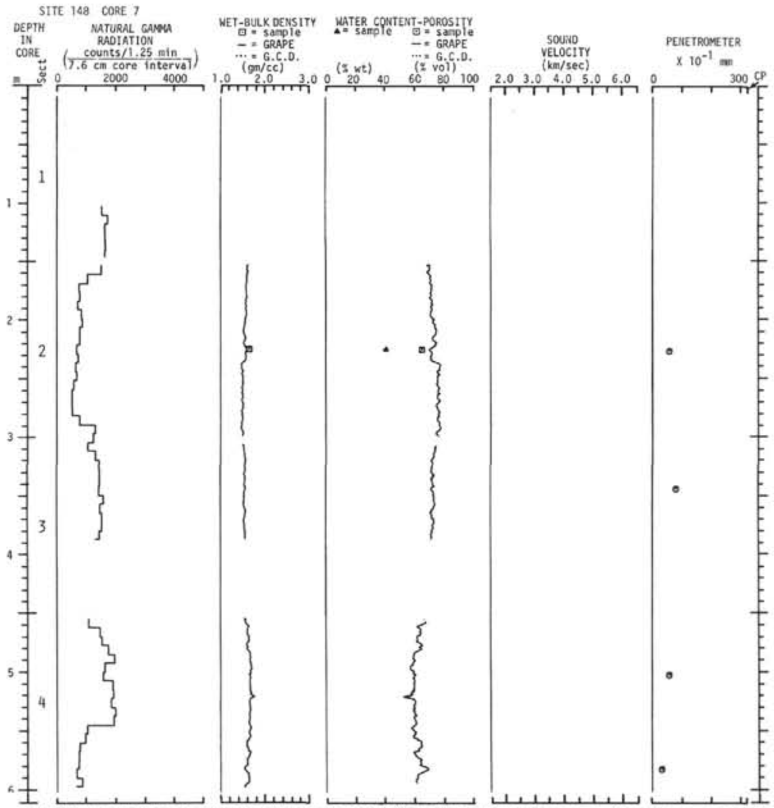

The "0" of the natural gamma data is equal to the atmospheric background count (gamma count when equipment was empty) of 1294. This background was subtracted from the data.

SITE 148 HOLE CORE 8 CORED INTERVAL (m) 64-73

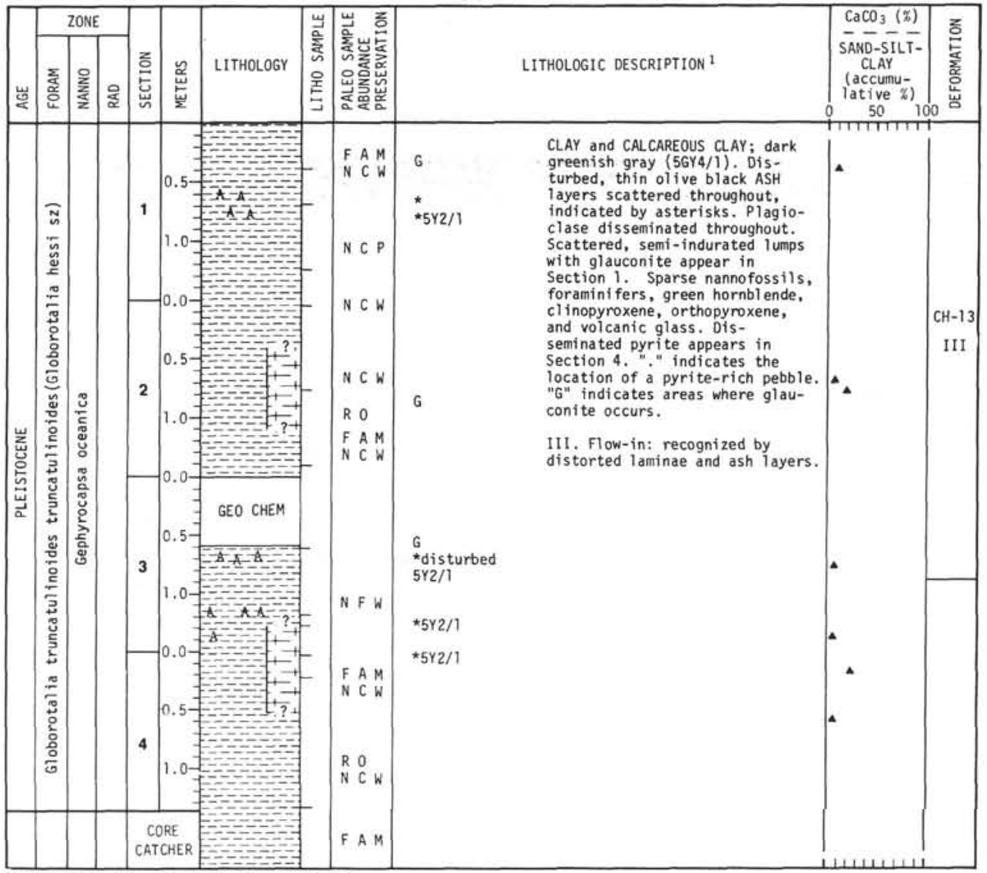

CLAY and CALCAREOUS CLAY; dark greenish gray (5GY4/1). Disturbed, thin olive black ASH layers scattered throughout, indicated by asterisks. Plagioclase disseminated throughout. Scattered, semi-indurated lumps with glauconite appear in Section 1. Sparse nannofossils, foraminifers, green hornblende, clinopyroxene, orthopyroxene, and volcanic glass. Disseminated pyrite appears in Section 4. "." indicates the location of a pyrite-rich pebble. "G" indicates areas where glauconite occurs.

III. Flow-in: recognized by distorted laminae and ash layers.

[1] For explanation of symbols, see Chapter 1

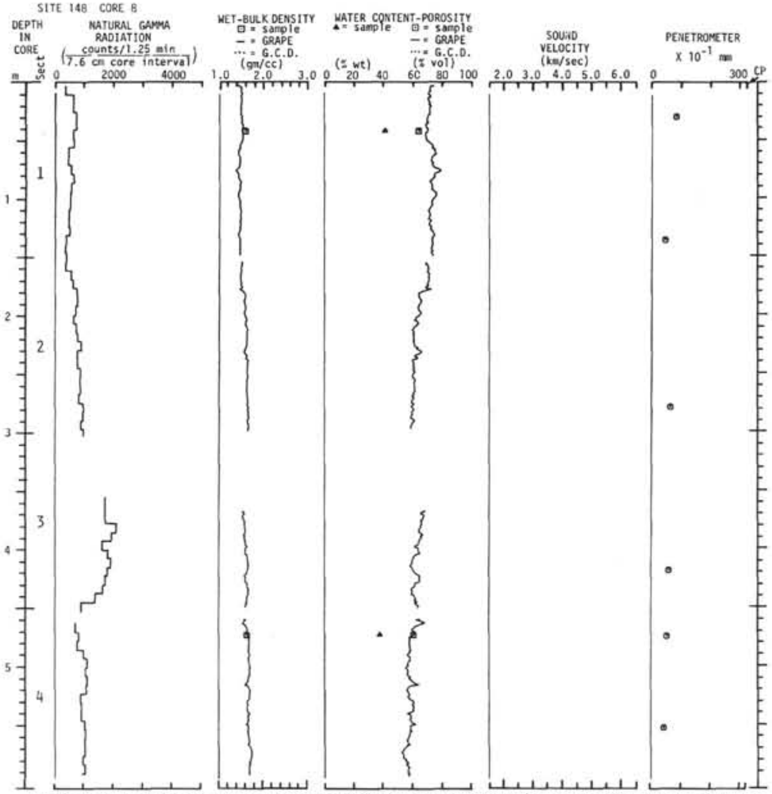

The "0" of the natural gamma data is equal to the atmospheric background count (gamma count when equipment was empty) of 1294. This background was subtracted from the data.

SITE 148 HOLE CORE 9 CORED INTERVAL (m) 73-82

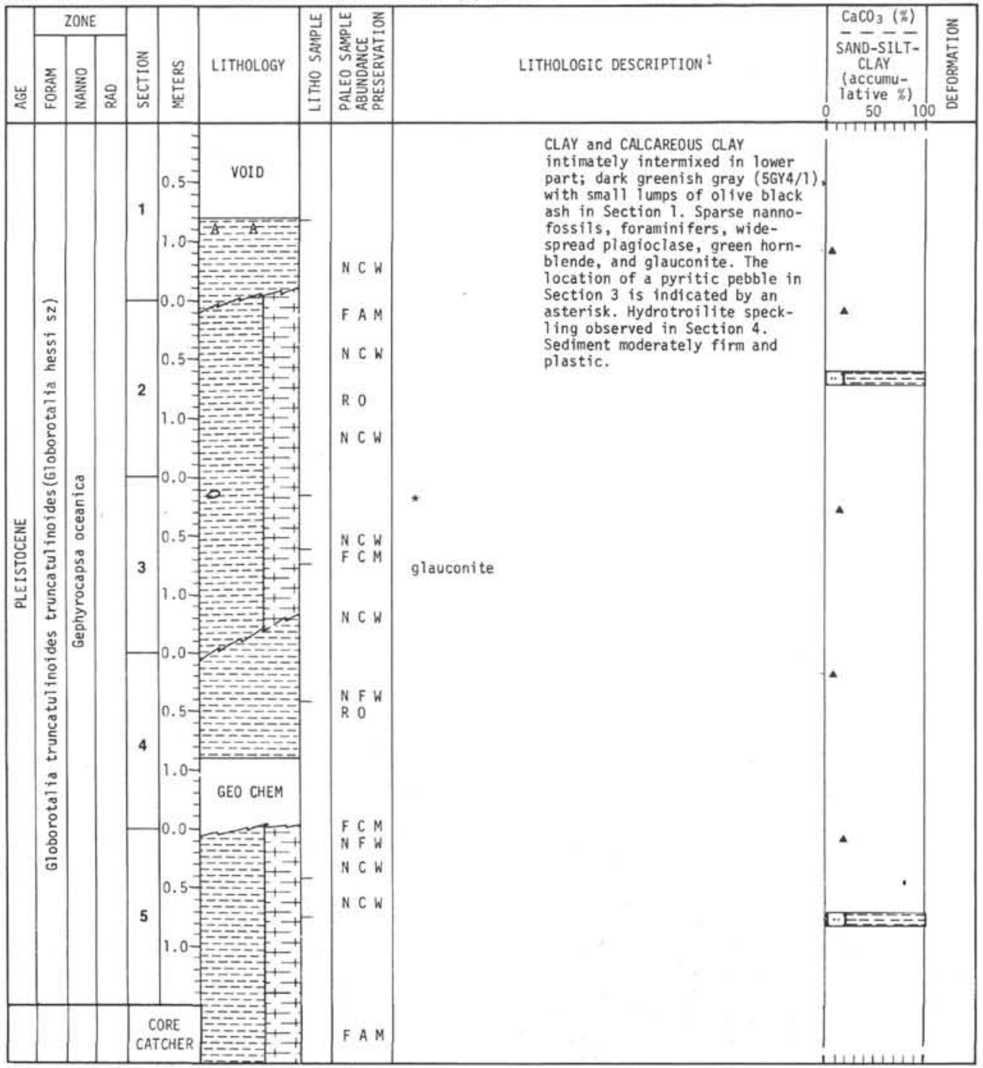

CLAY and CALCAREOUS CLAY intimately intermixed in lower part; dark greenish gray (5GY4/1), with small lumps of olive black ash in Section 1. Sparse nannofossils, foraminifers, widespread plagioclase, green hornblende, and glauconite. The location of a pyritic pebble in Section 3 is indicated by an asterisk. Hydrotroilite speckling observed in Section 4. Sediment moderately firm and plastic.

[1] For explanation of symbols, see Chapter 1

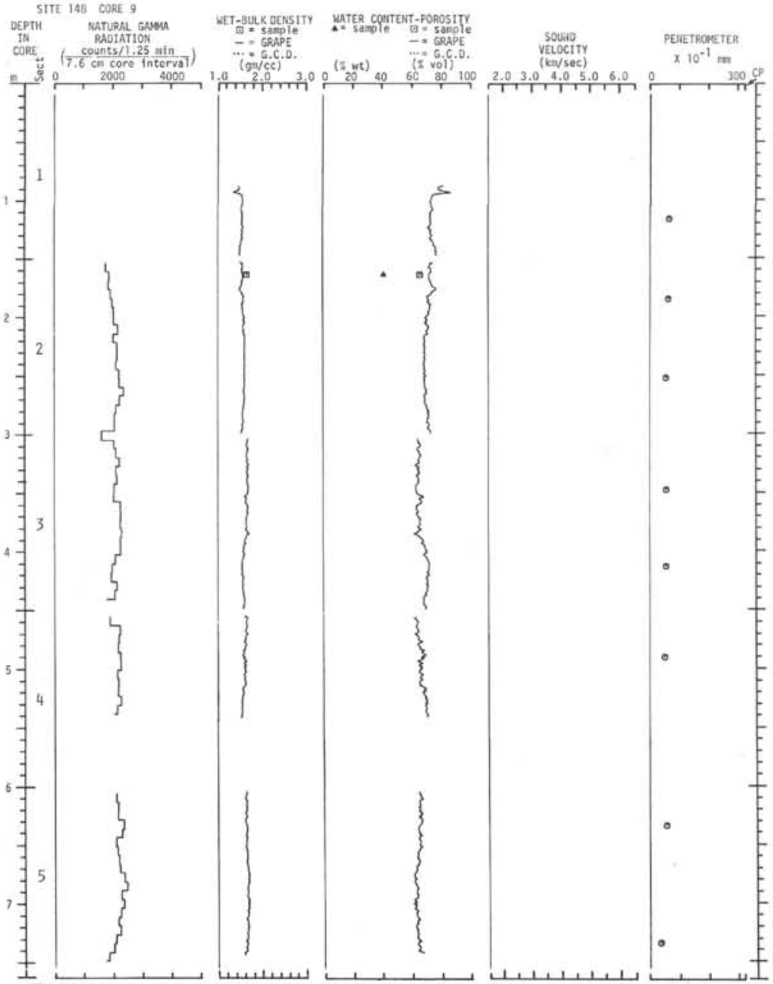

The "0" of the natural gamma data is equal to the atmospheric background count (gamma count when equipment was empty) of 1302. This background was subtracted from the data.

SITE 148 HOLE CORE 10 CORED INTERVAL (m) 82-91

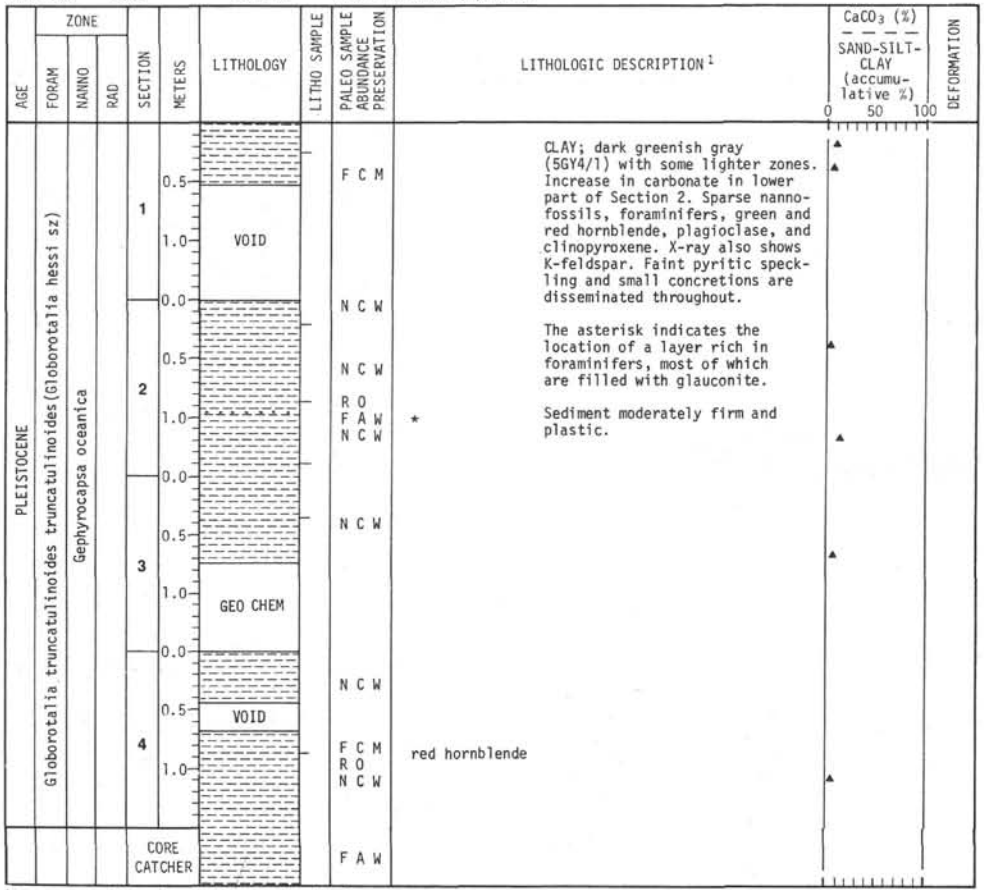

CLAY; dark greenish gray (5GY4/1) with some lighter zones. Increase in carbonate in lower part of Section 2. Sparse nannofossils, foraminifers, green and red hornblende, plagioclase, and clinopyroxene. X-ray also shows K-feldspar. Faint pyritic speckling and small concretions are disseminated throughout.

The asterisk indicates the location of a layer rich in foraminifers, most of which are filled with glauconite.

Sediment moderately firm and plastic.

¹For explanation of symbols, see Chapter 1

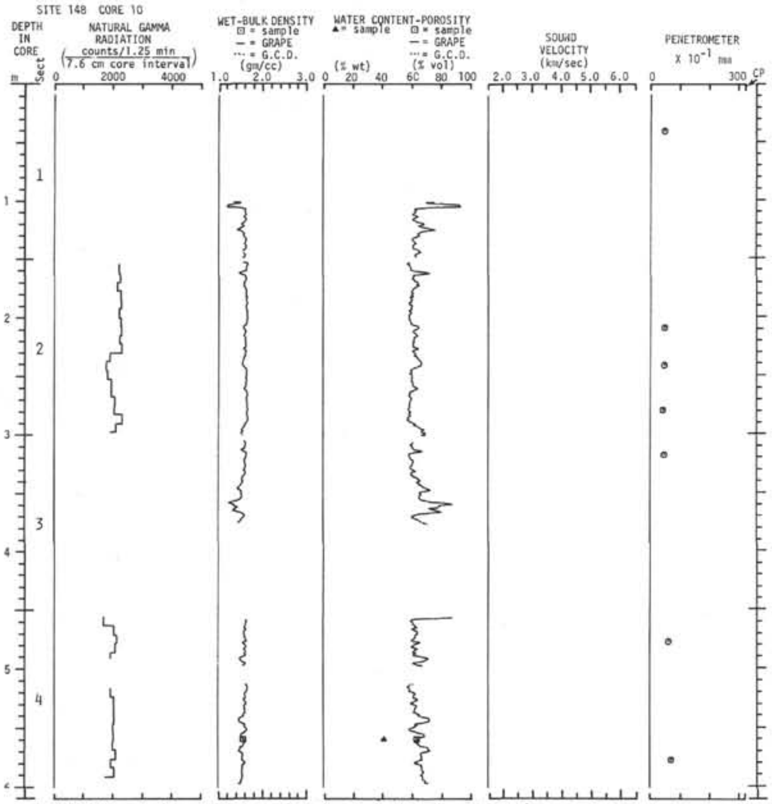

The "0" of the natural gamma data is equal to the atmospheric background count (gamma count when equipment was empty) of 1302. This background was subtracted from the data.

SITE 148 HOLE CORE 11 CORED INTERVAL (m) 91-100

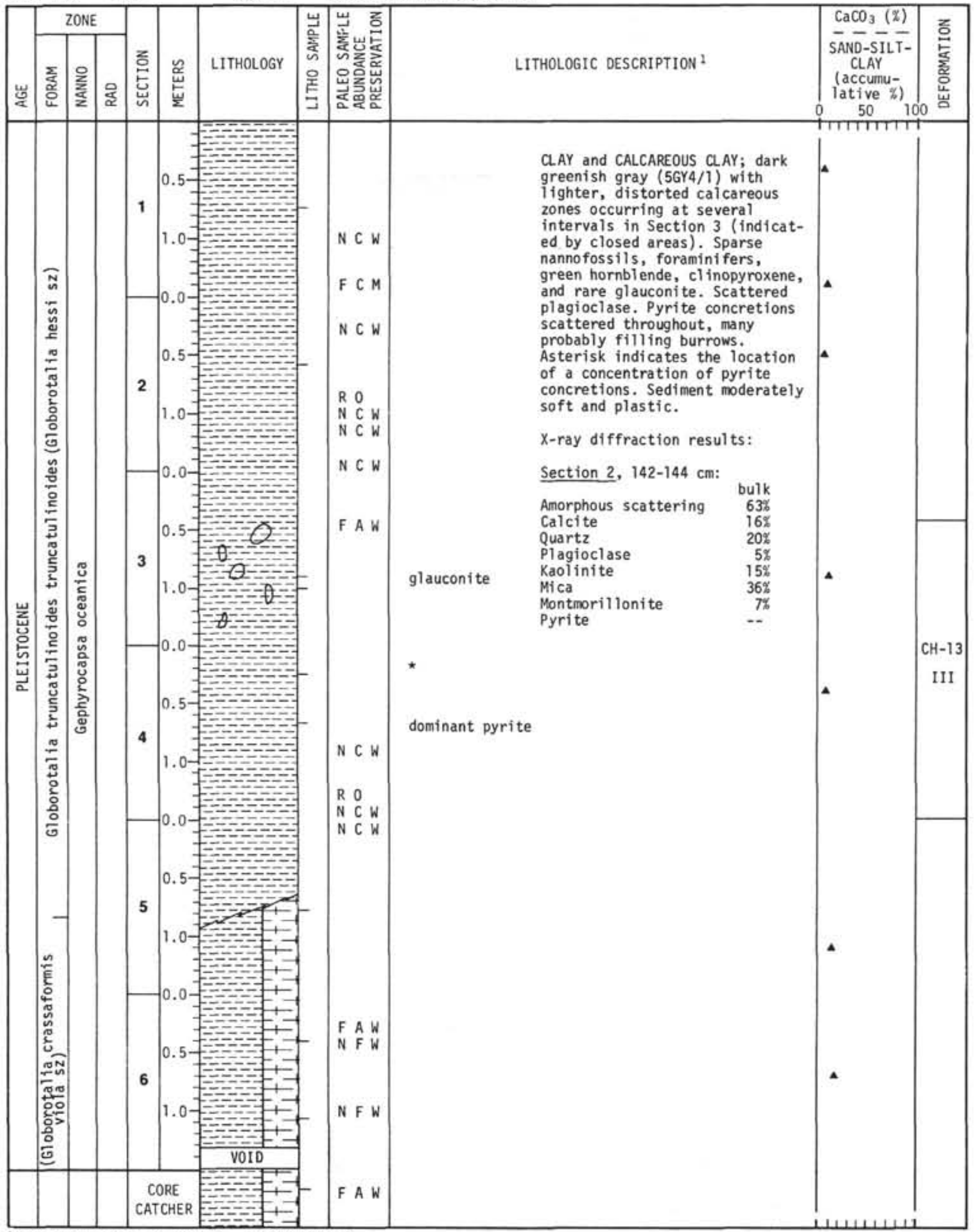

CLAY and CALCAREOUS CLAY; dark greenish gray (5GY4/1) with lighter, distorted calcareous zones occurring at several intervals in Section 3 (indicated by closed areas). Sparse nannofossils, foraminifers, green hornblende, clinopyroxene, and rare glauconite. Scattered plagioclase. Pyrite concretions scattered throughout, many probably filling burrows. Asterisk indicates the location of a concentration of pyrite concretions. Sediment moderately soft and plastic.

X-ray diffraction results:

<u>Section 2</u>, 142-144 cm:

	bulk
Amorphous scattering	63%
Calcite	16%
Quartz	20%
Plagioclase	5%
Kaolinite	15%
Mica	36%
Montmorillonite	7%
Pyrite	--

---

¹For explanation of symbols, see Chapter 1

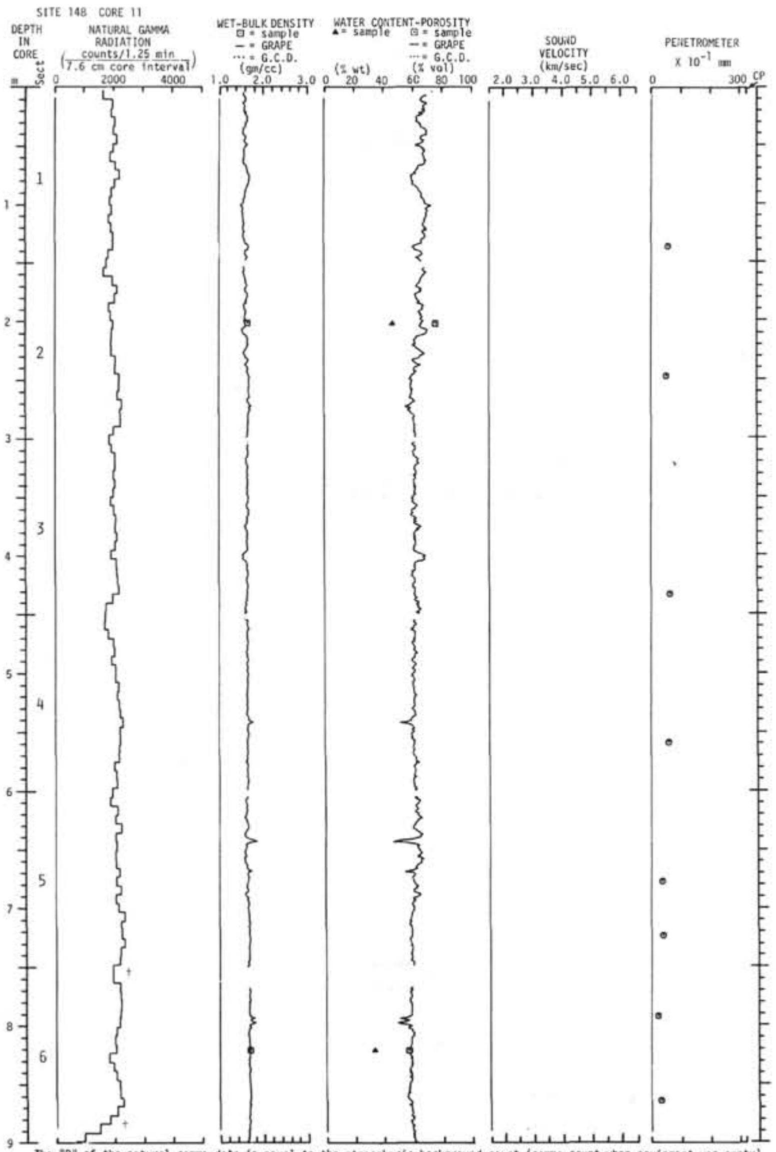

The "0" of the natural gamma data is equal to the atmospheric background count (gamma count when equipment was empty) of 1302. This background was subtracted from the data.

SITE 148 HOLE CORE 12 CORED INTERVAL (m) 100-109

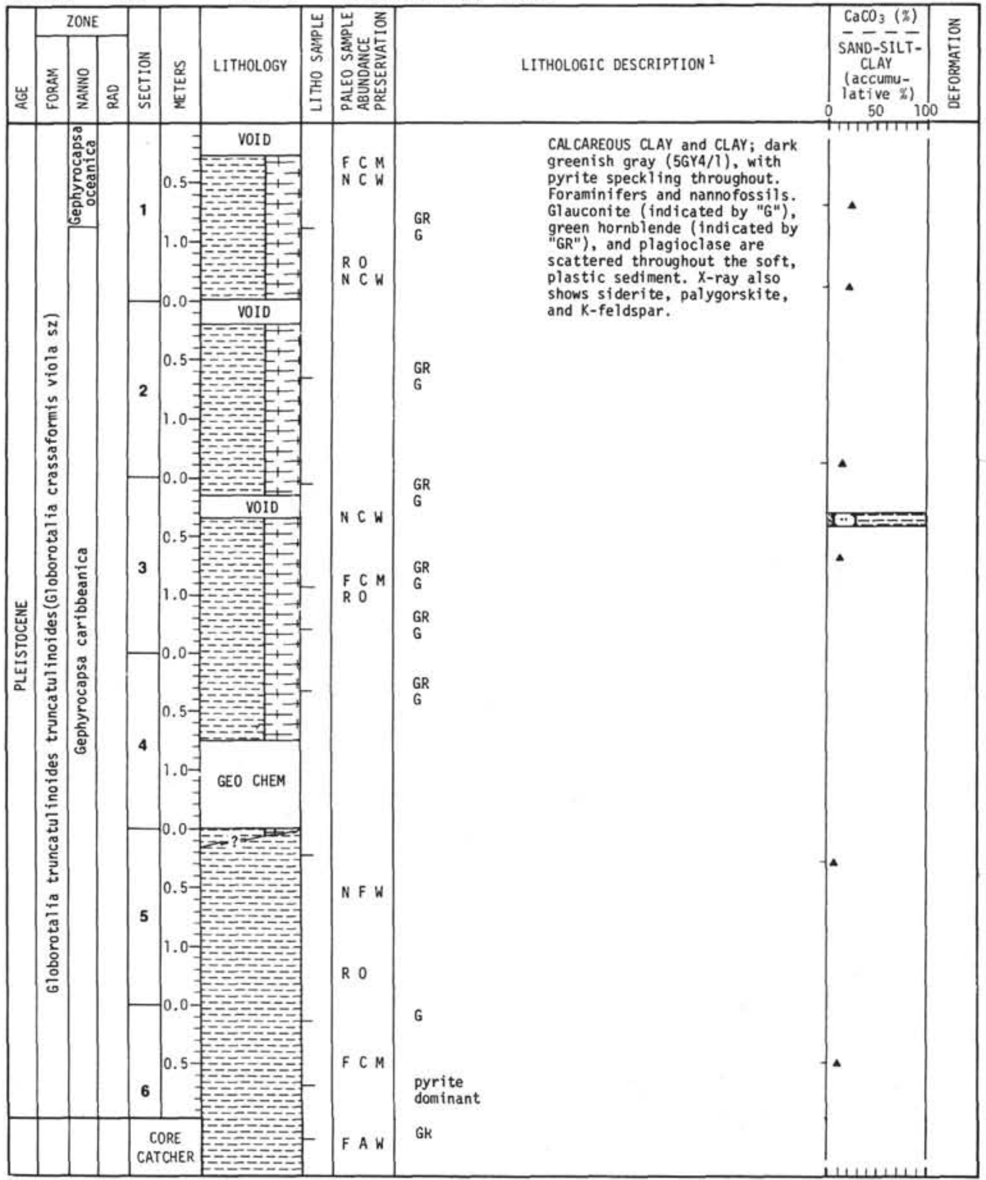

CALCAREOUS CLAY and CLAY; dark greenish gray (5GY4/1), with pyrite speckling throughout. Foraminifers and nannofossils. Glauconite (indicated by "G"), green hornblende (indicated by "GR"), and plagioclase are scattered throughout the soft, plastic sediment. X-ray also shows siderite, palygorskite, and K-feldspar.

¹For explanation of symbols, see Chapter 1

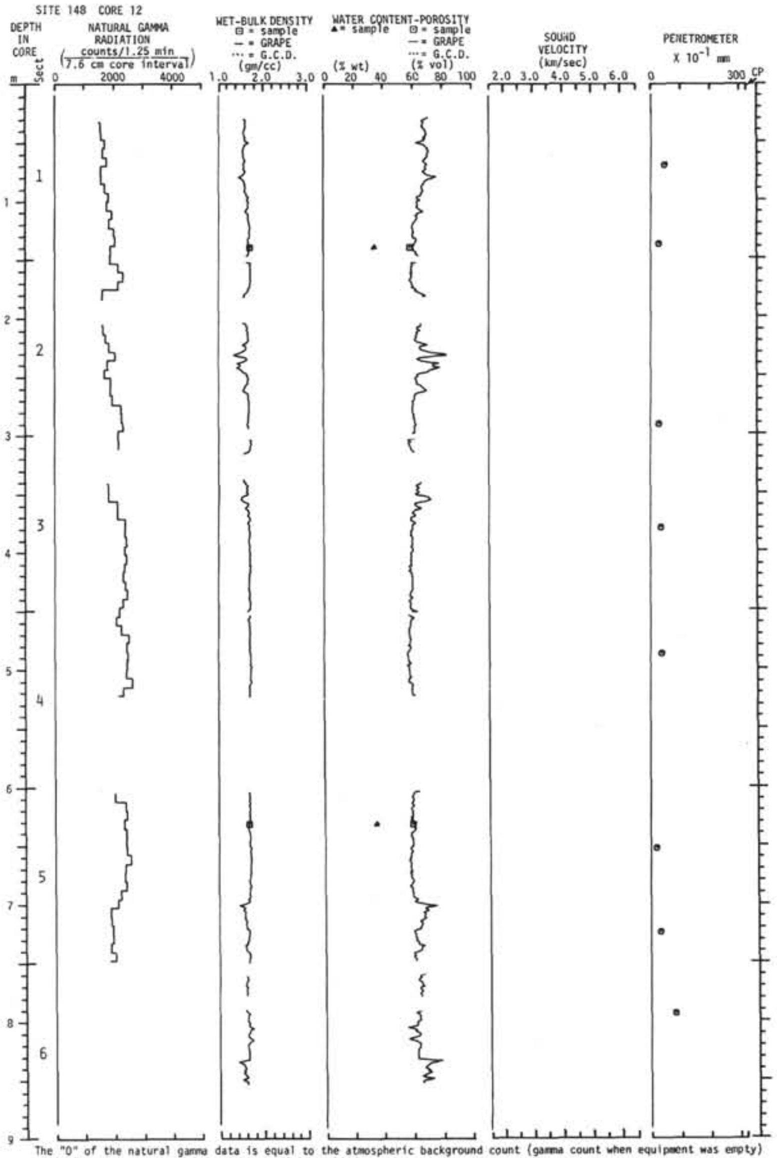

The "0" of the natural gamma data is equal to the atmospheric background count (gamma count when equipment was empty) of 1362. This background was subtracted from the data.

SITE 148 HOLE CORE 13 CORED INTERVAL (m)

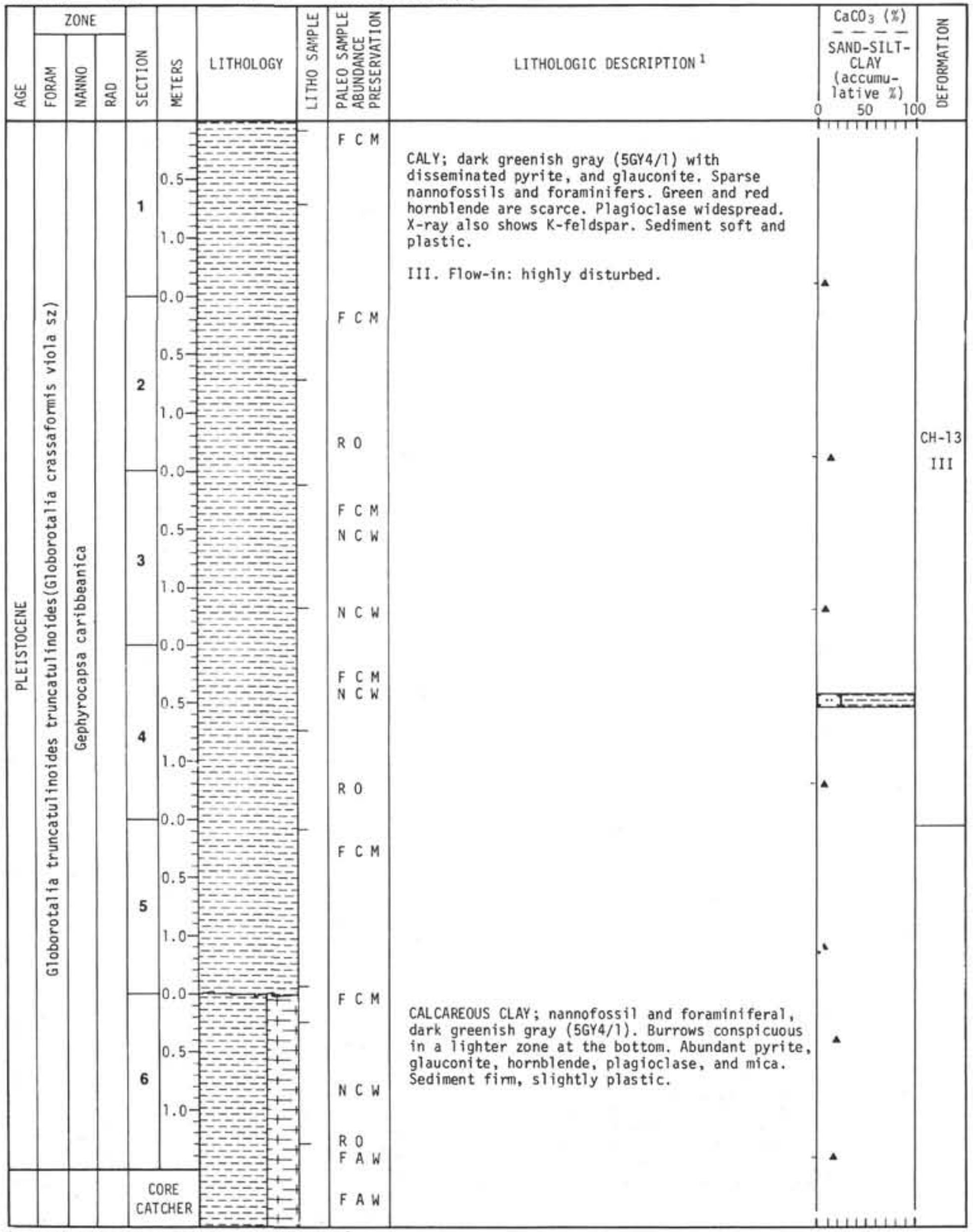

CALY; dark greenish gray (5GY4/1) with disseminated pyrite, and glauconite. Sparse nannofossils and foraminifers. Green and red hornblende are scarce. Plagioclase widespread. X-ray also shows K-feldspar. Sediment soft and plastic.

III. Flow-in: highly disturbed.

CALCAREOUS CLAY; nannofossil and foraminiferal, dark greenish gray (5GY4/1). Burrows conspicuous in a lighter zone at the bottom. Abundant pyrite, glauconite, hornblende, plagioclase, and mica. Sediment firm, slightly plastic.

¹For explanation of symbols, see Chapter 1

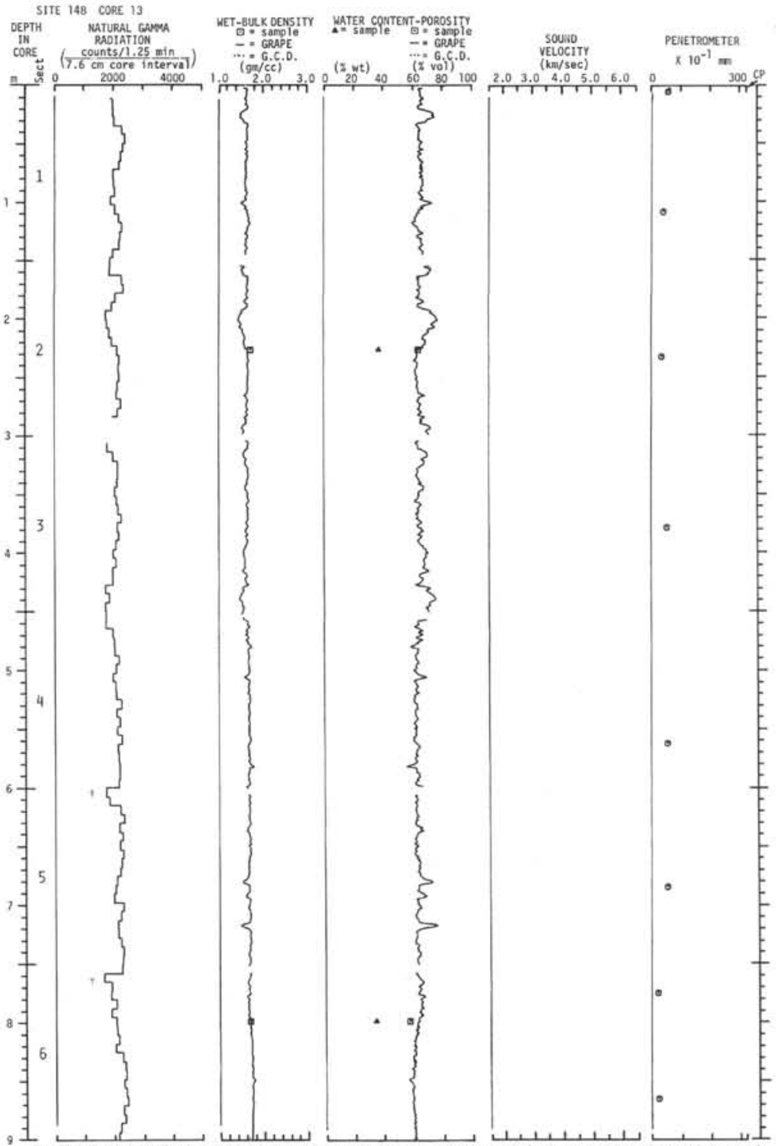

The "0" of the natural gamma data is equal to the atmospheric background count (gamma count when equipment was empty) of 1366. This background was subtracted from the data.

SITE 148 HOLE CORE 14 CORED INTERVAL (m) 118-127

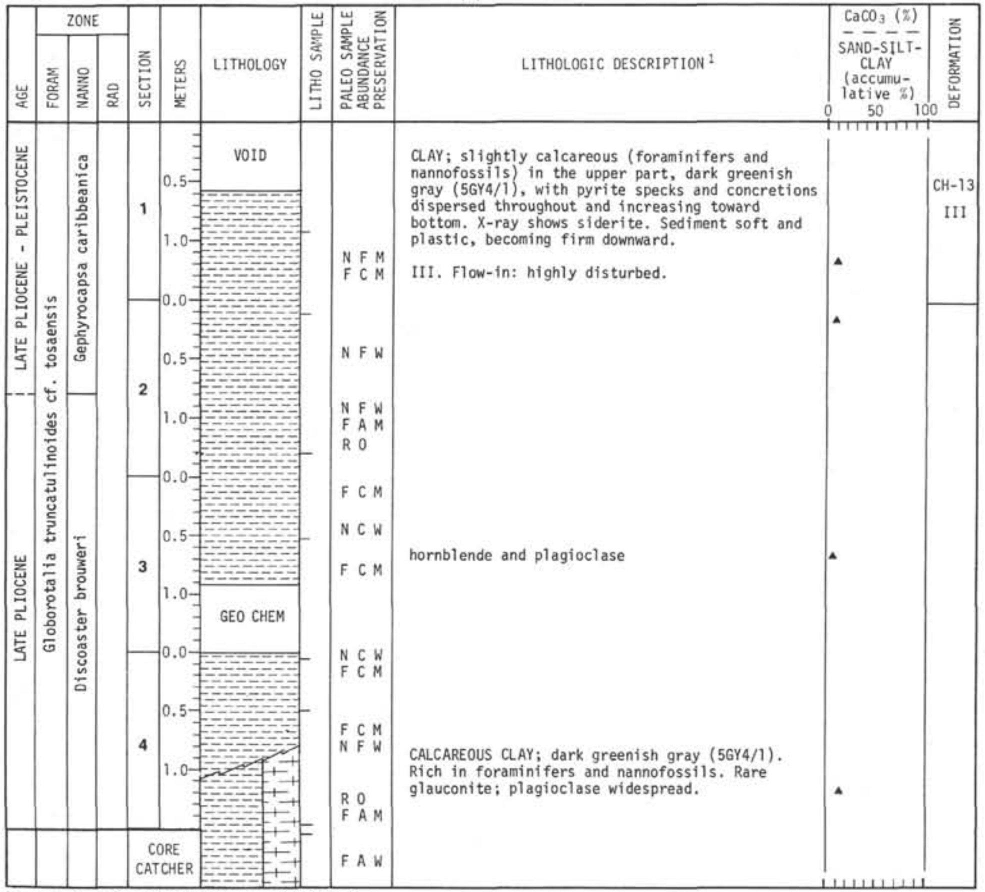

CLAY; slightly calcareous (foraminifers and nannofossils) in the upper part, dark greenish gray (5GY4/1), with pyrite specks and concretions dispersed throughout and increasing toward bottom. X-ray shows siderite. Sediment soft and plastic, becoming firm downward.

III. Flow-in: highly disturbed.

hornblende and plagioclase

CALCAREOUS CLAY; dark greenish gray (5GY4/1). Rich in foraminifers and nannofossils. Rare glauconite; plagioclase widespread.

¹For explanation of symbols, see Chapter 1

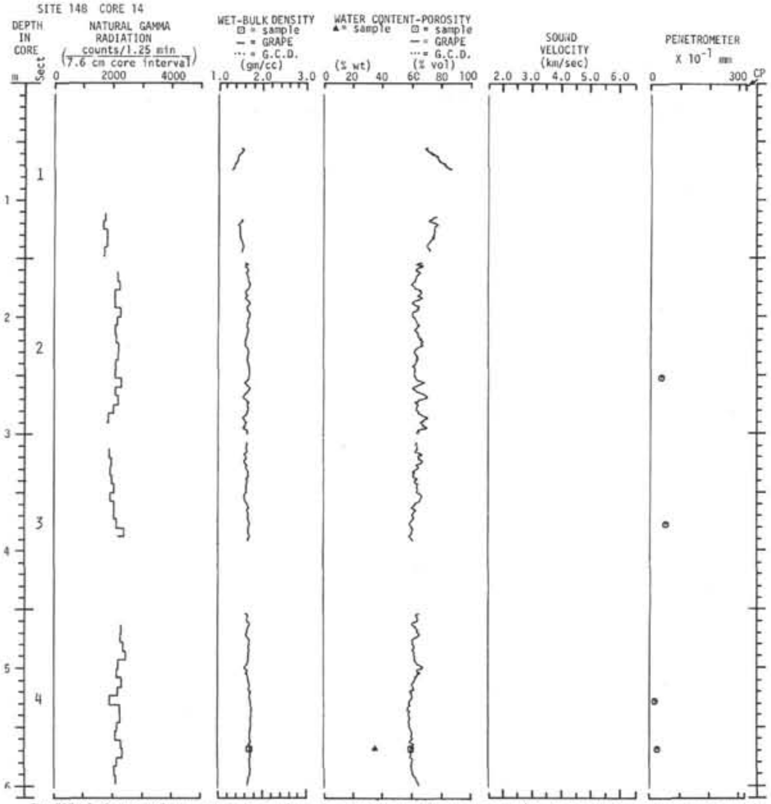

The "0" of the natural gamma data is equal to the atmospheric background count (gamma count when equipment was empty) of 1347 This background was subtracted from the data.

SITE 148 HOLE CORE 15 CORED INTERVAL (m) 127-137

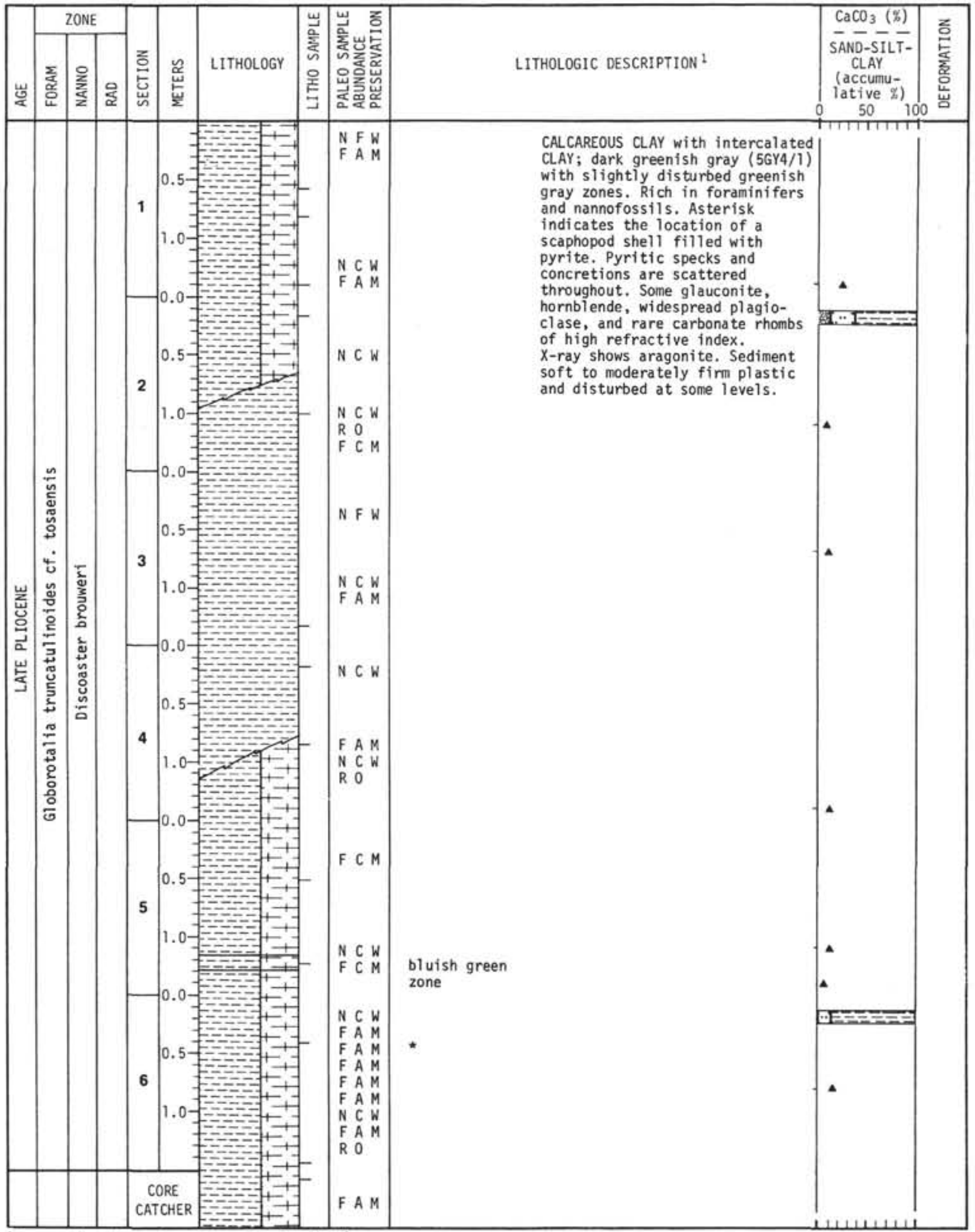

CALCAREOUS CLAY with intercalated CLAY; dark greenish gray (5GY4/1) with slightly disturbed greenish gray zones. Rich in foraminifers and nannofossils. Asterisk indicates the location of a scaphopod shell filled with pyrite. Pyritic specks and concretions are scattered throughout. Some glauconite, hornblende, widespread plagioclase, and rare carbonate rhombs of high refractive index. X-ray shows aragonite. Sediment soft to moderately firm plastic and disturbed at some levels.

¹For explanation of symbols, see Chapter 1

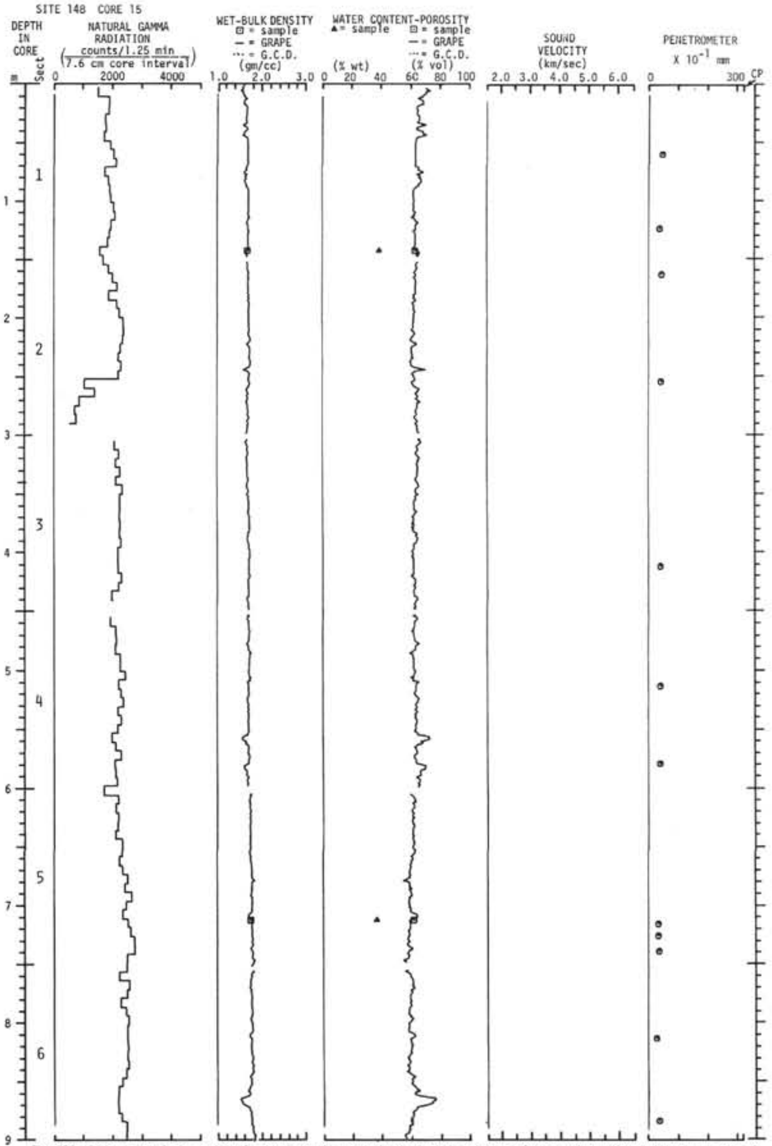

The "0" of the natural gamma data is equal to the atmospheric background count (gamma count when equipment was empty) of 1375. This background was subtracted from the data.

SITE 148 HOLE CORE 16 CORED INTERVAL (m) 137-146

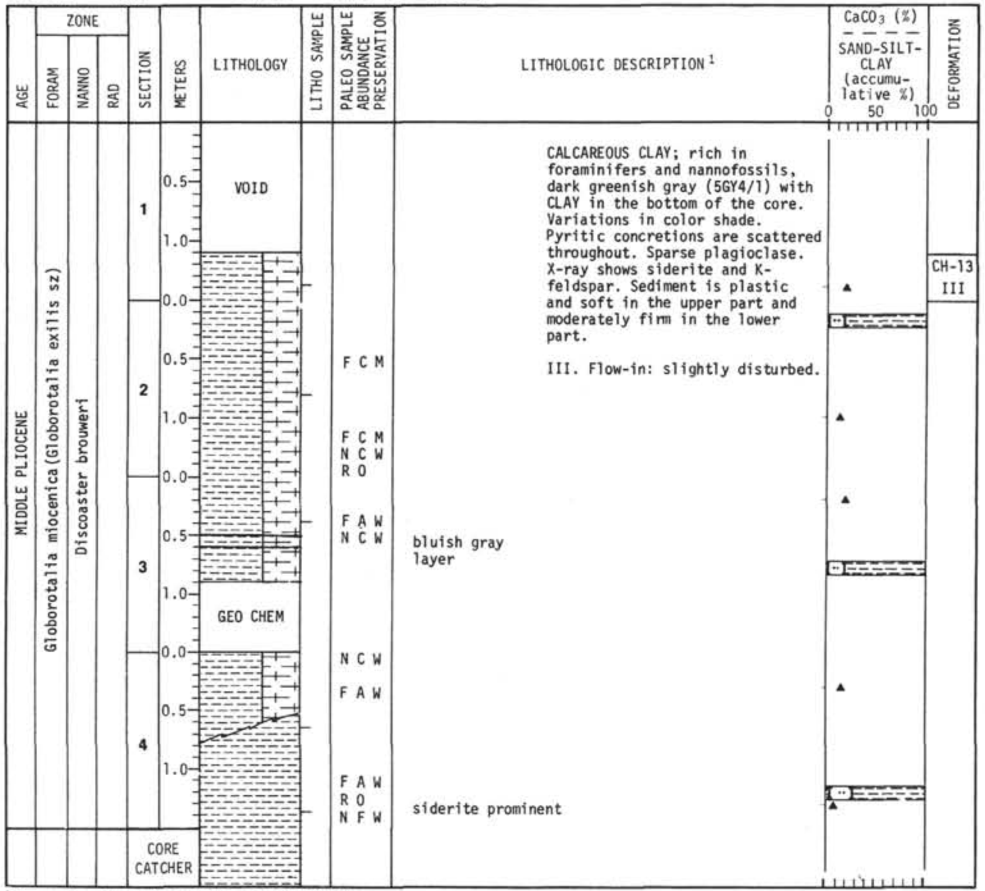

CALCAREOUS CLAY; rich in foraminifers and nannofossils, dark greenish gray (5GY4/1) with CLAY in the bottom of the core. Variations in color shade. Pyritic concretions are scattered throughout. Sparse plagioclase. X-ray shows siderite and K-feldspar. Sediment is plastic and soft in the upper part and moderately firm in the lower part.

III. Flow-in: slightly disturbed.

bluish gray layer

siderite prominent

---

[1] For explanation of symbols, see Chapter 1

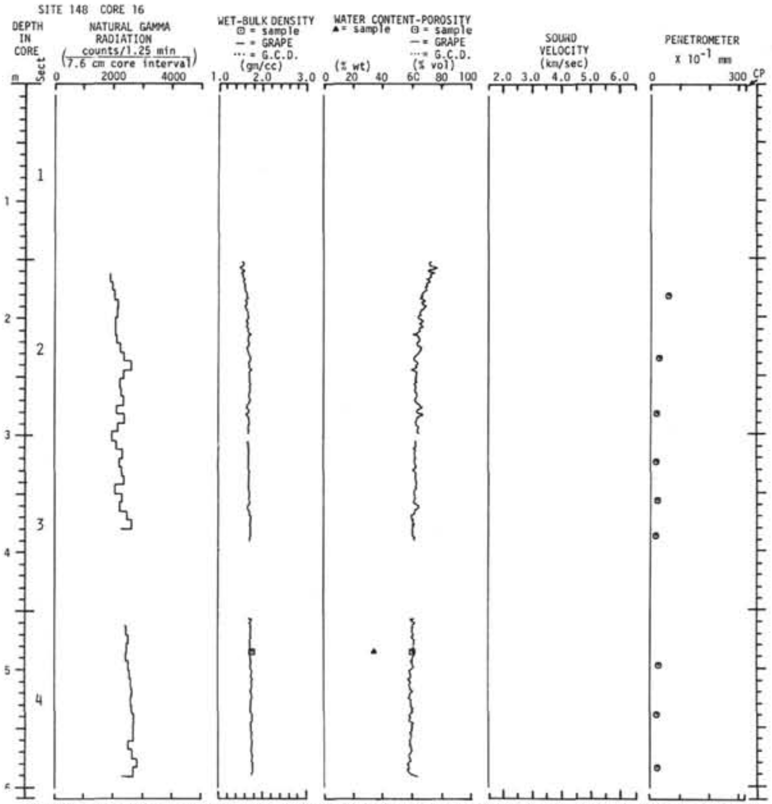

The "0" of the natural gamma data is equal to the atmospheric background count (gamma count when equipment was empty) of 1373. This background was subtracted from the data.

SITE 148 HOLE CORE 17 CORED INTERVAL (m) 146-156

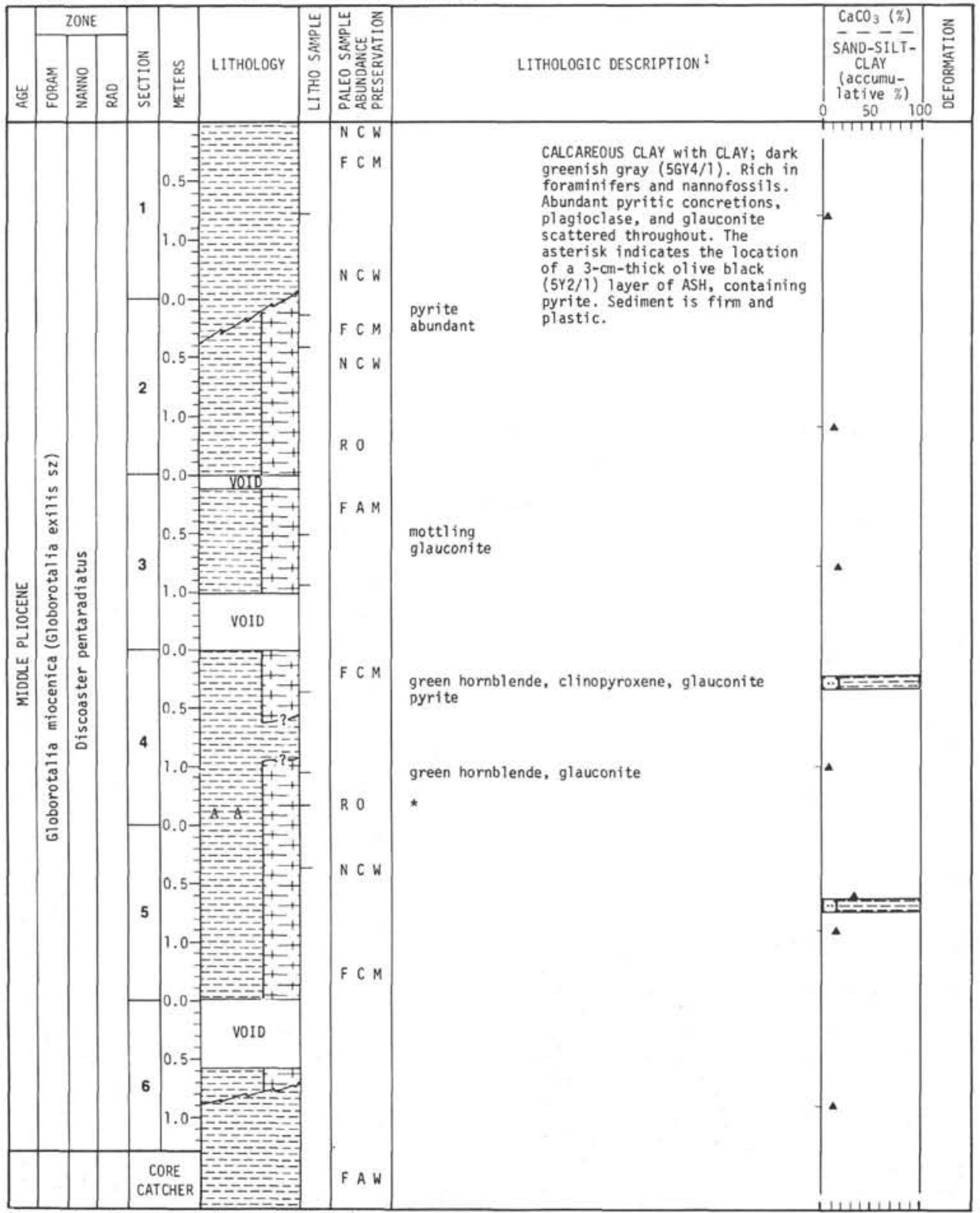

CALCAREOUS CLAY with CLAY; dark greenish gray (5GY4/1). Rich in foraminifers and nannofossils. Abundant pyritic concretions, plagioclase, and glauconite scattered throughout. The asterisk indicates the location of a 3-cm-thick olive black (5Y2/1) layer of ASH, containing pyrite. Sediment is firm and plastic.

pyrite abundant

mottling glauconite

green hornblende, clinopyroxene, glauconite pyrite

green hornblende, glauconite

*

¹For explanation of symbols, see Chapter 1

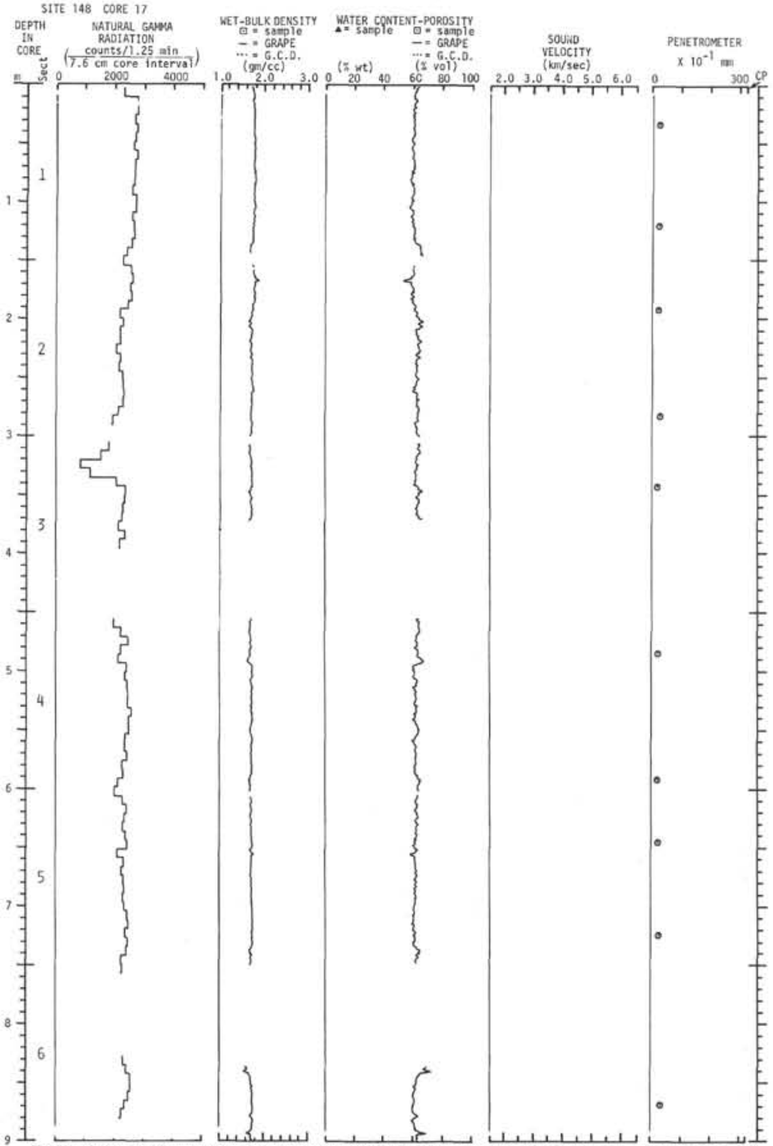

The "0" of the natural gamma data is equal to the atmospheric background count (gamma count when equipment was empty) of 1373. This background was subtracted from the data.

SITE 148 HOLE CORE 18 CORED INTERVAL (m) 156-165

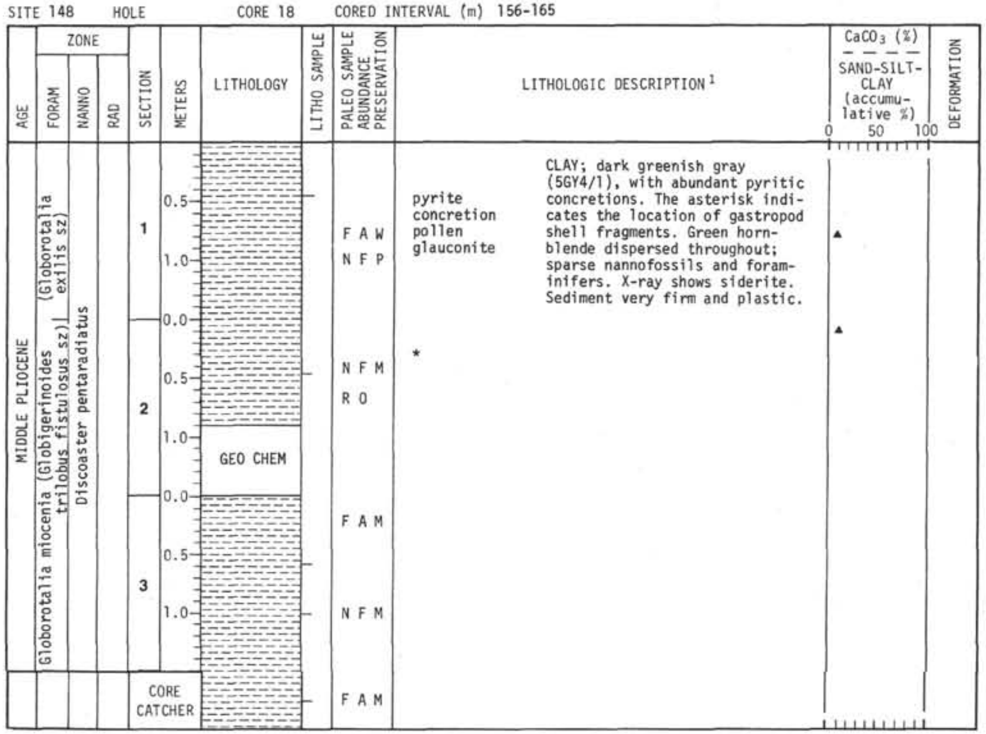

SECTION	PALEO SAMPLE ABUNDANCE PRESERVATION	
1	F A W N F P	pyrite concretion pollen glauconite
2	N F M R O	*
3	F A M N F M	
CORE CATCHER	F A M	

CLAY; dark greenish gray (5GY4/1), with abundant pyritic concretions. The asterisk indicates the location of gastropod shell fragments. Green hornblende dispersed throughout; sparse nannofossils and foraminifers. X-ray shows siderite. Sediment very firm and plastic.

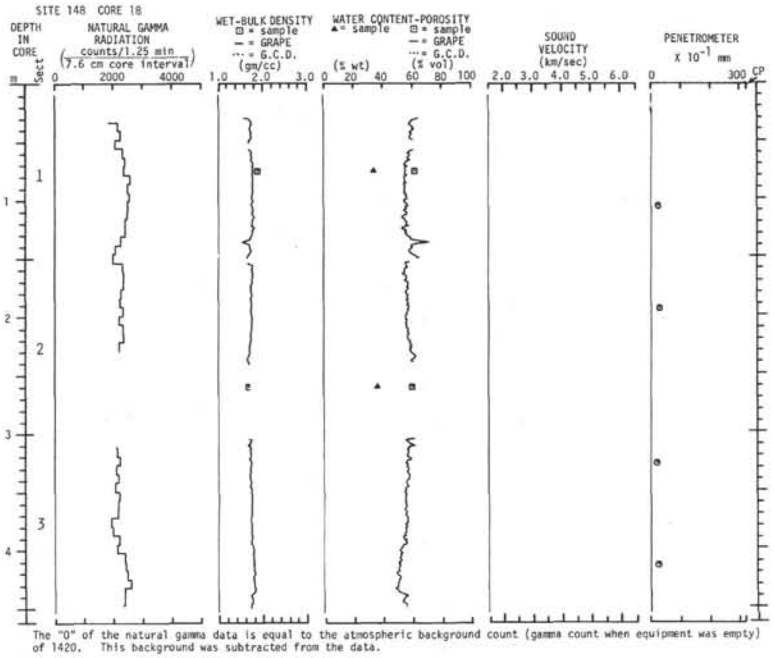

The "0" of the natural gamma data is equal to the atmospheric background count (gamma count when equipment was empty) of 1420. This background was subtracted from the data.

SITE 148 HOLE CORE 19 CORED INTERVAL (m) 165-175

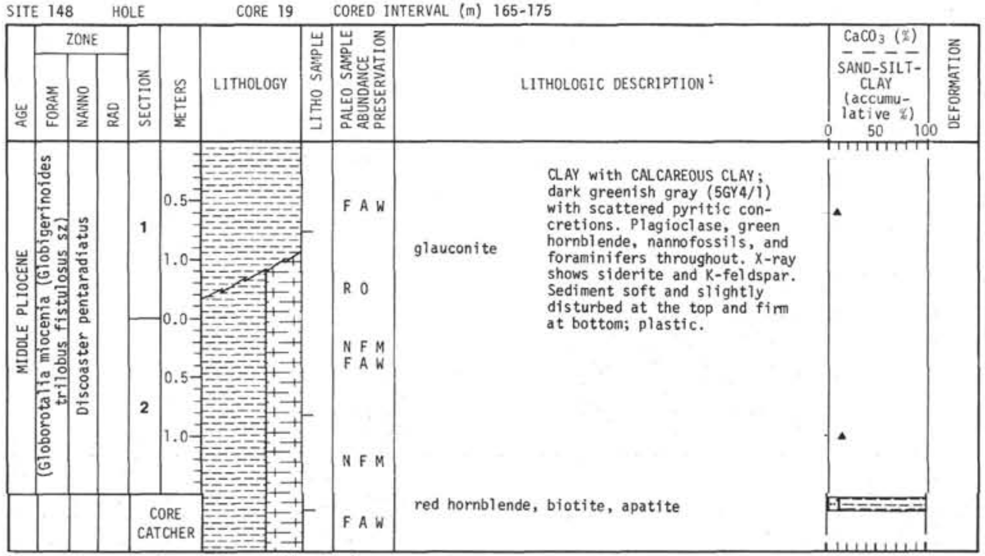

SECTION	PALEO SAMPLE ABUNDANCE PRESERVATION	
1	F A W R O	glauconite
2	N F M F A W N F M	
CORE CATCHER	F A W	red hornblende, biotite, apatite

CLAY with CALCAREOUS CLAY; dark greenish gray (5GY4/1) with scattered pyritic concretions. Plagioclase, green hornblende, nannofossils, and foraminifers throughout. X-ray shows siderite and K-feldspar. Sediment soft and slightly disturbed at the top and firm at bottom; plastic.

---

¹For explanation of symbols, see Chapter 1

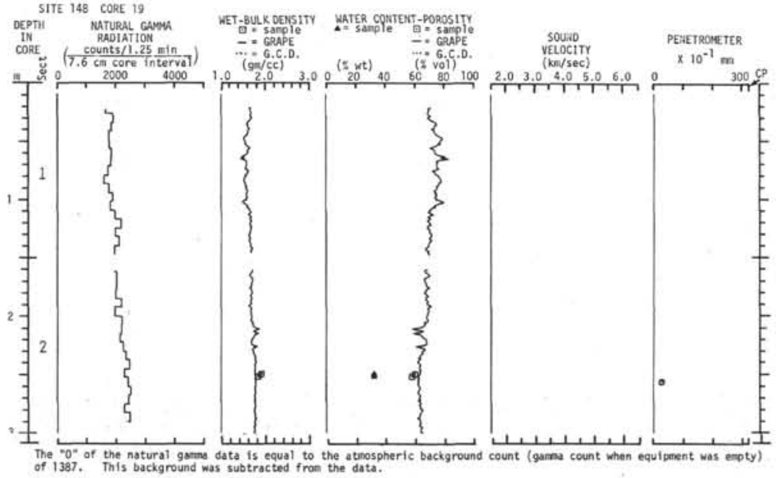

The "0" of the natural gamma data is equal to the atmospheric background count (gamma count when equipment was empty) of 1387. This background was subtracted from the data.

SITE 148 HOLE CORE 20 CORED INTERVAL (m) 175-184

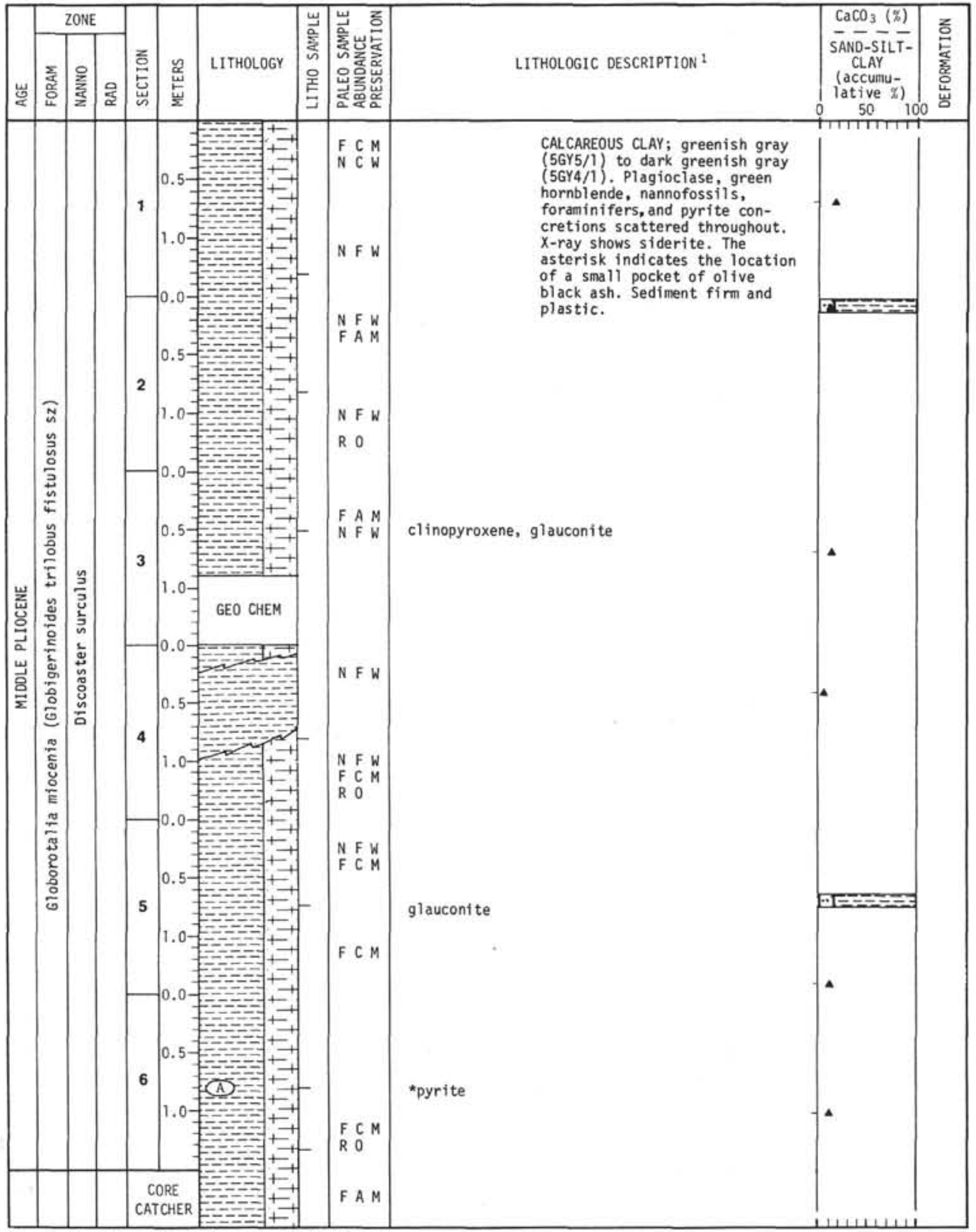

CALCAREOUS CLAY; greenish gray (5GY5/1) to dark greenish gray (5GY4/1). Plagioclase, green hornblende, nannofossils, foraminifers, and pyrite concretions scattered throughout. X-ray shows siderite. The asterisk indicates the location of a small pocket of olive black ash. Sediment firm and plastic.

clinopyroxene, glauconite

glauconite

*pyrite

¹For explanation of symbols, see Chapter 1

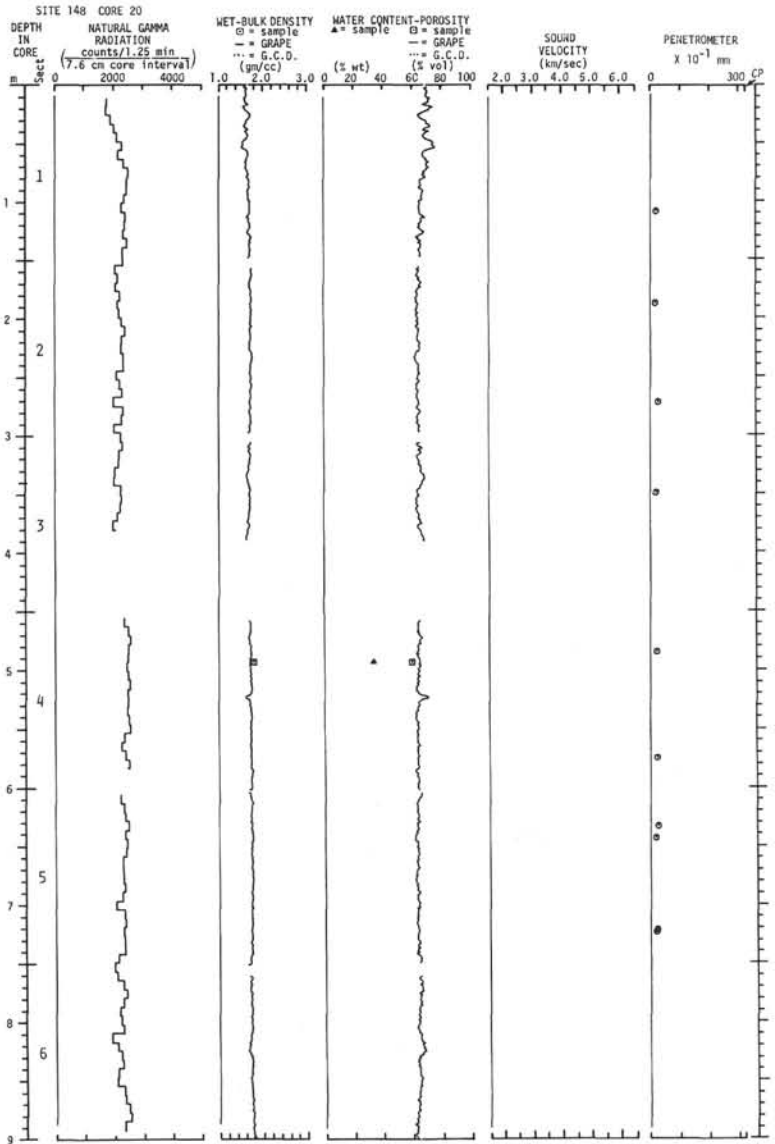

The "0" of the natural gamma data is equal to the atmospheric background count (gamma count when equipment was empty) of 1387. This background was subtracted from the data.

SITE 148 HOLE CORE 21 CORED INTERVAL (m) 184-193

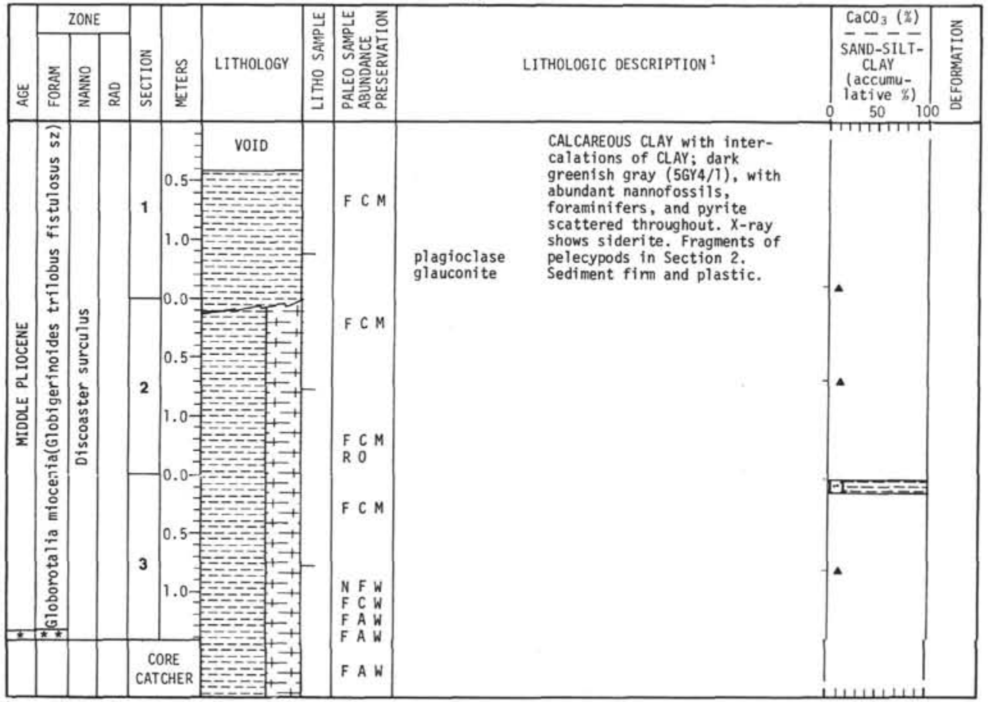

plagioclase
glauconite

CALCAREOUS CLAY with intercalations of CLAY; dark greenish gray (5GY4/1), with abundant nannofossils, foraminifers, and pyrite scattered throughout. X-ray shows siderite. Fragments of pelecypods in Section 2. Sediment firm and plastic.

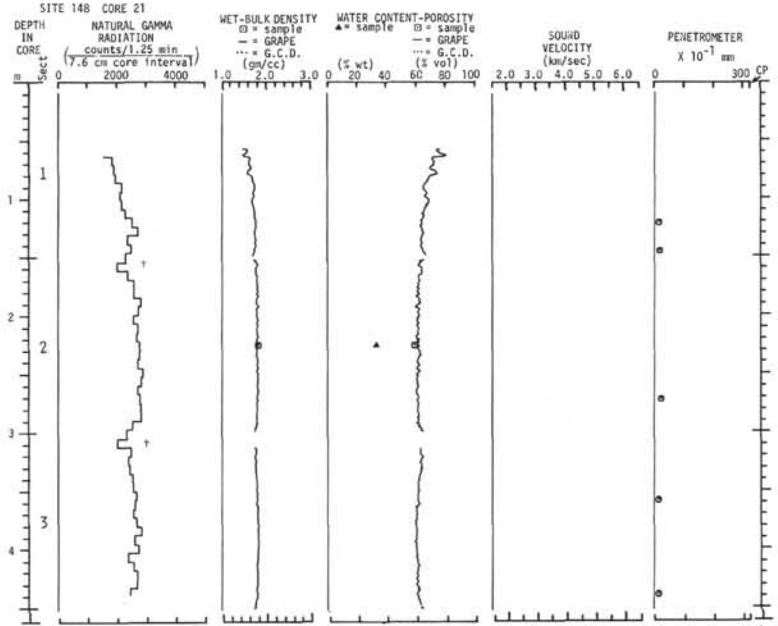

The "0" of the natural gamma data is equal to the atmospheric background count (gamma count when equipment was empty) of 1389. This background was subtracted from the data.

---

¹For explanation of symbols, see Chapter 1

* EARLY PLIOCENE

** Globorotalia margaritae(Globorotalia m. evoluta sz)

SITE 148 HOLE CORE 22 CORED INTERVAL (m) 193-203

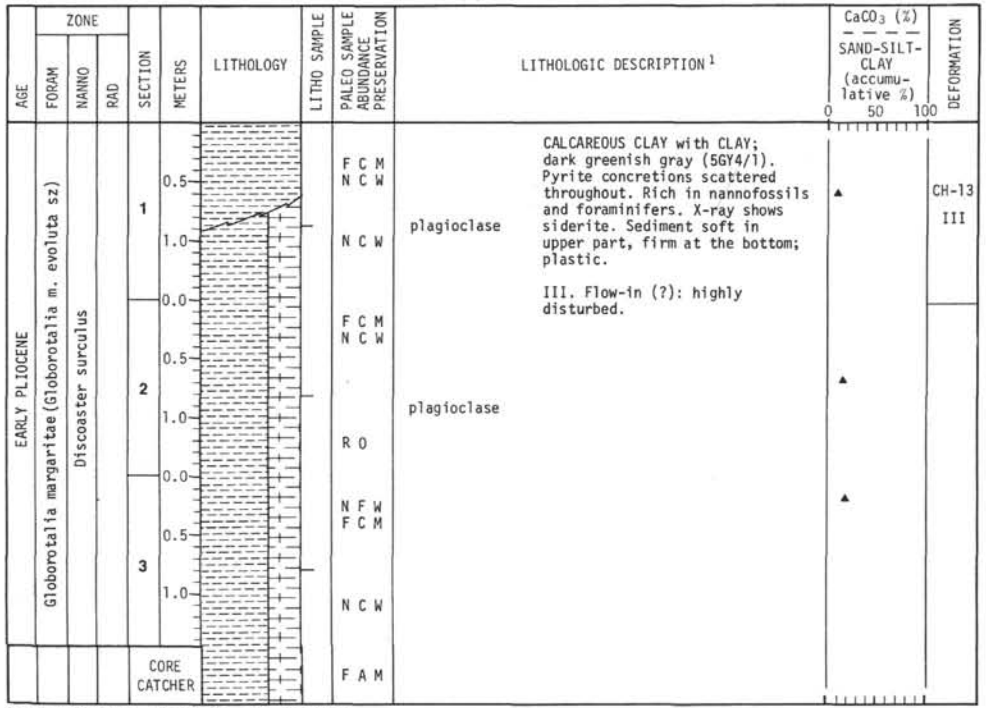

CALCAREOUS CLAY with CLAY; dark greenish gray (5GY4/1). Pyrite concretions scattered throughout. Rich in nannofossils and foraminifers. X-ray shows siderite. Sediment soft in upper part, firm at the bottom; plastic.

III. Flow-in (?): highly disturbed.

¹For explanation of symbols, see Chapter 1

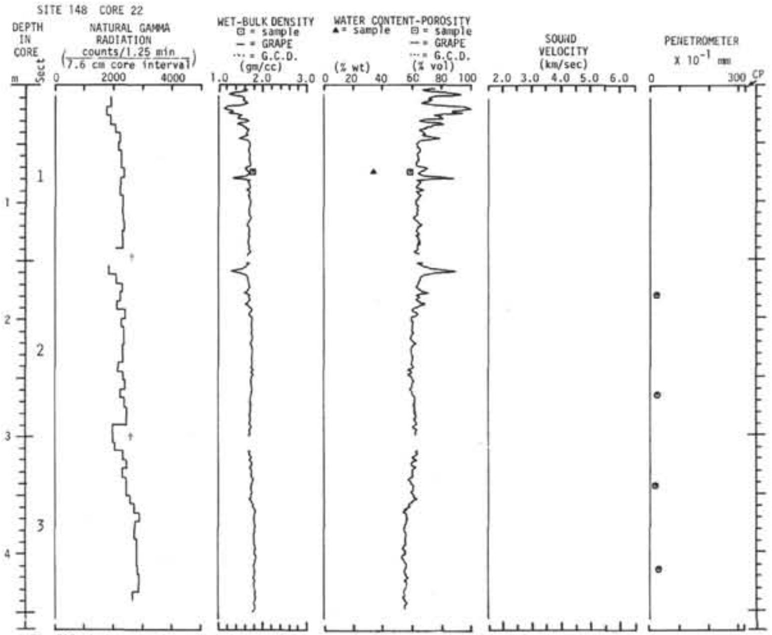

The "0" of the natural gamma data is equal to the atmospheric background count (gamma count when equipment was empty) of 1389. This background was subtracted from the data.

SITE 148 HOLE CORE 23 CORED INTERVAL (m) 203-212

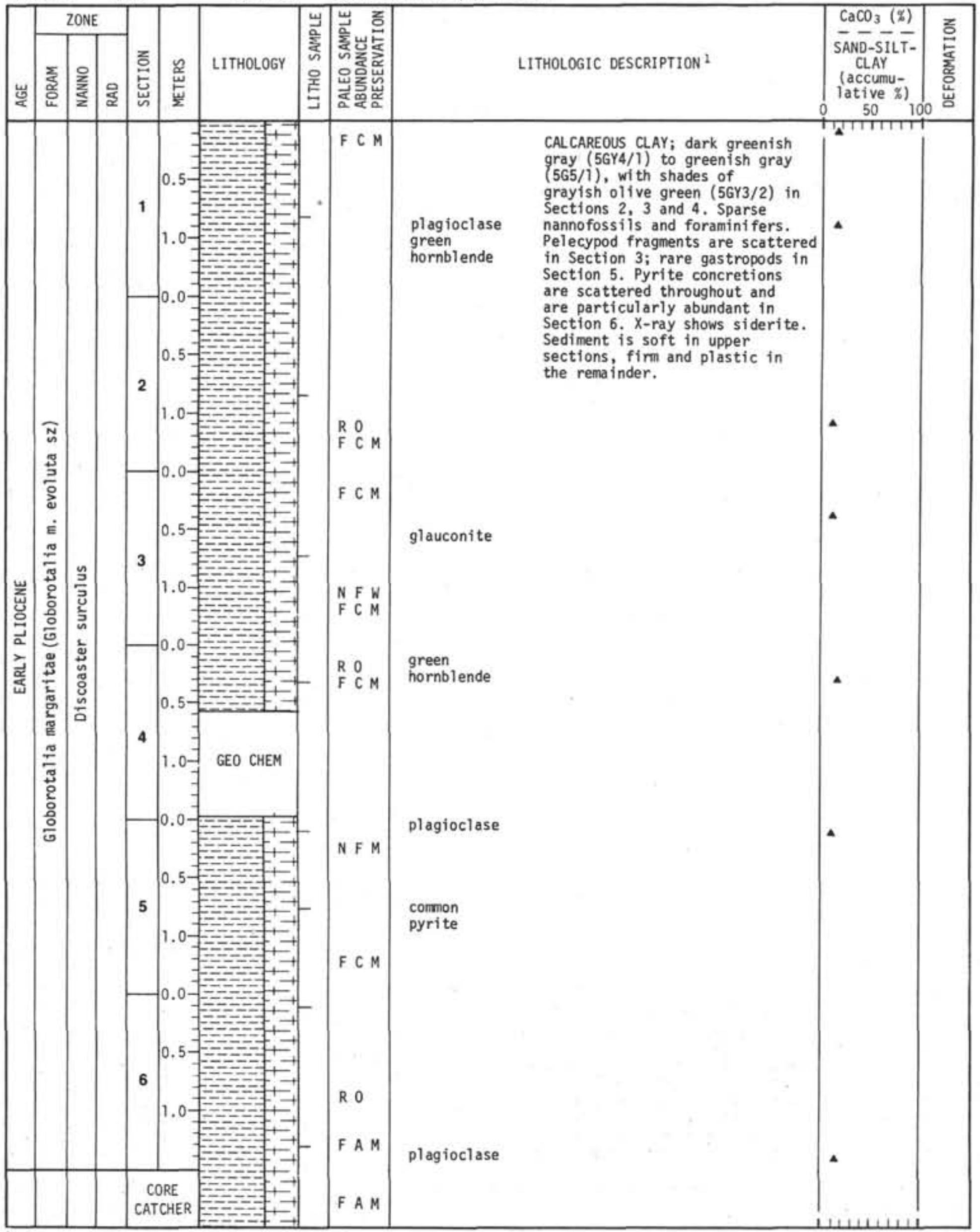

CALCAREOUS CLAY; dark greenish gray (5GY4/1) to greenish gray (5G5/1), with shades of grayish olive green (5GY3/2) in Sections 2, 3 and 4. Sparse nannofossils and foraminifers. Pelecypod fragments are scattered in Section 3; rare gastropods in Section 5. Pyrite concretions are scattered throughout and are particularly abundant in Section 6. X-ray shows siderite. Sediment is soft in upper sections, firm and plastic in the remainder.

¹For explanation of symbols, see Chapter 1

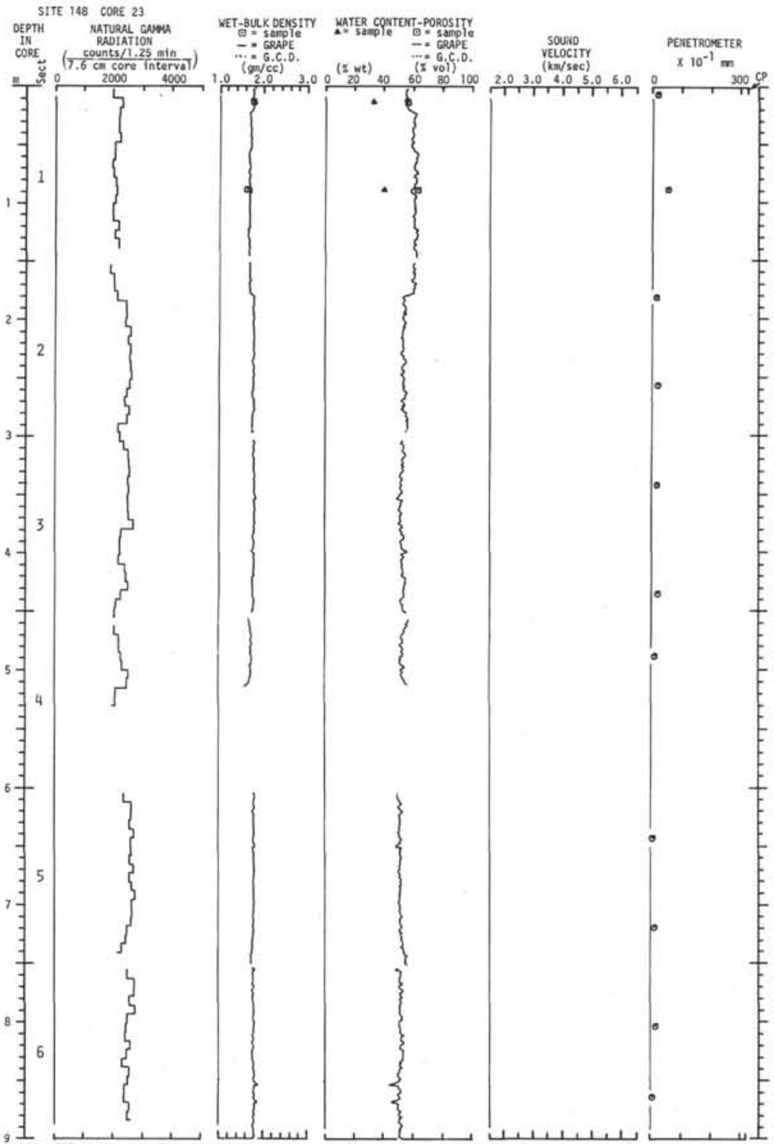

The "0" of the natural gamma data is equal to the atmospheric background count (gamma count when equipment was empty) of 1380. This background was subtracted from the data.

SITE 148 HOLE CORE 24 CORED INTERVAL (m) 212-221

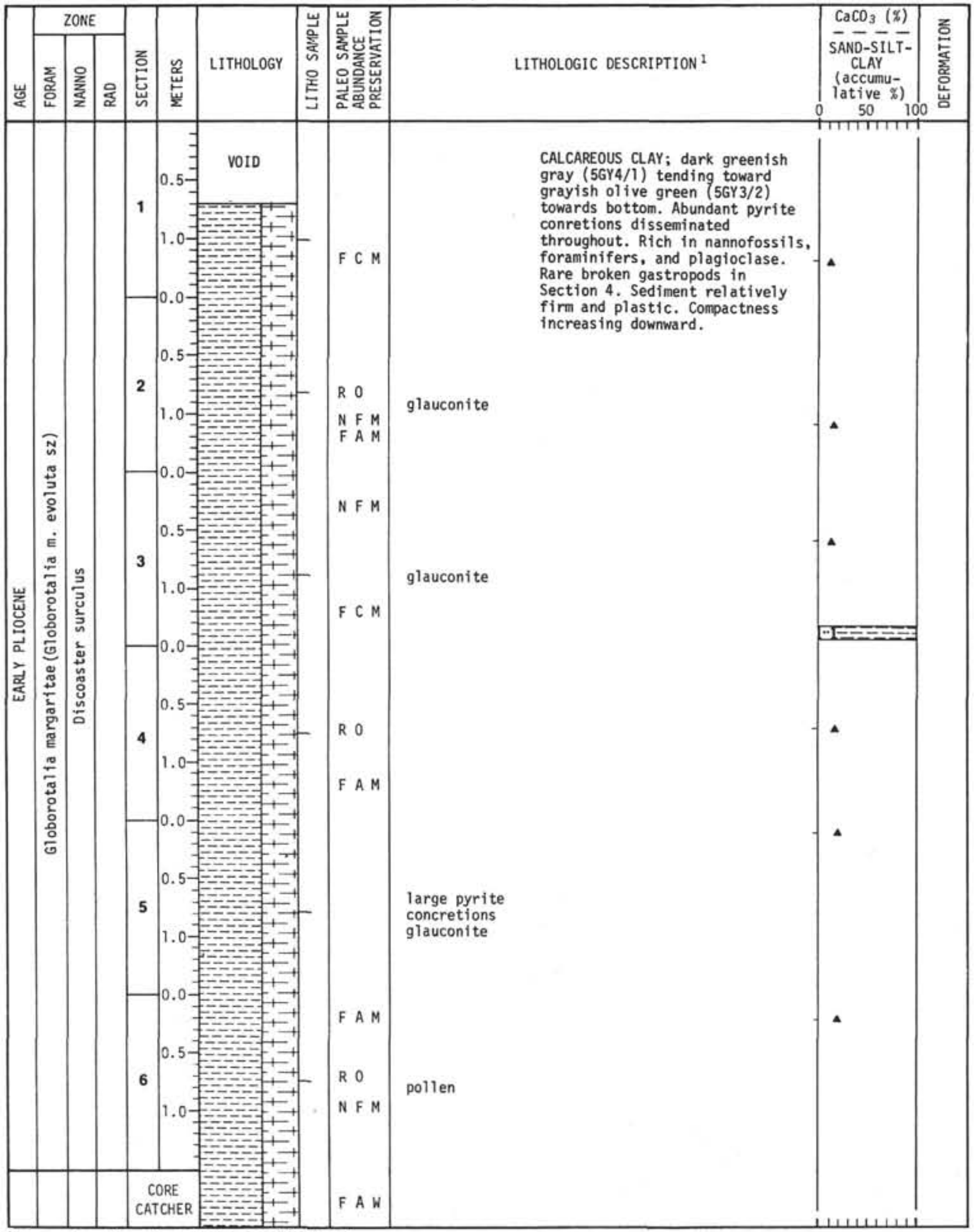

CALCAREOUS CLAY; dark greenish gray (5GY4/1) tending toward grayish olive green (5GY3/2) towards bottom. Abundant pyrite conretions disseminated throughout. Rich in nannofossils, foraminifers, and plagioclase. Rare broken gastropods in Section 4. Sediment relatively firm and plastic. Compactness increasing downward.

---

¹For explanation of symbols, see Chapter 1

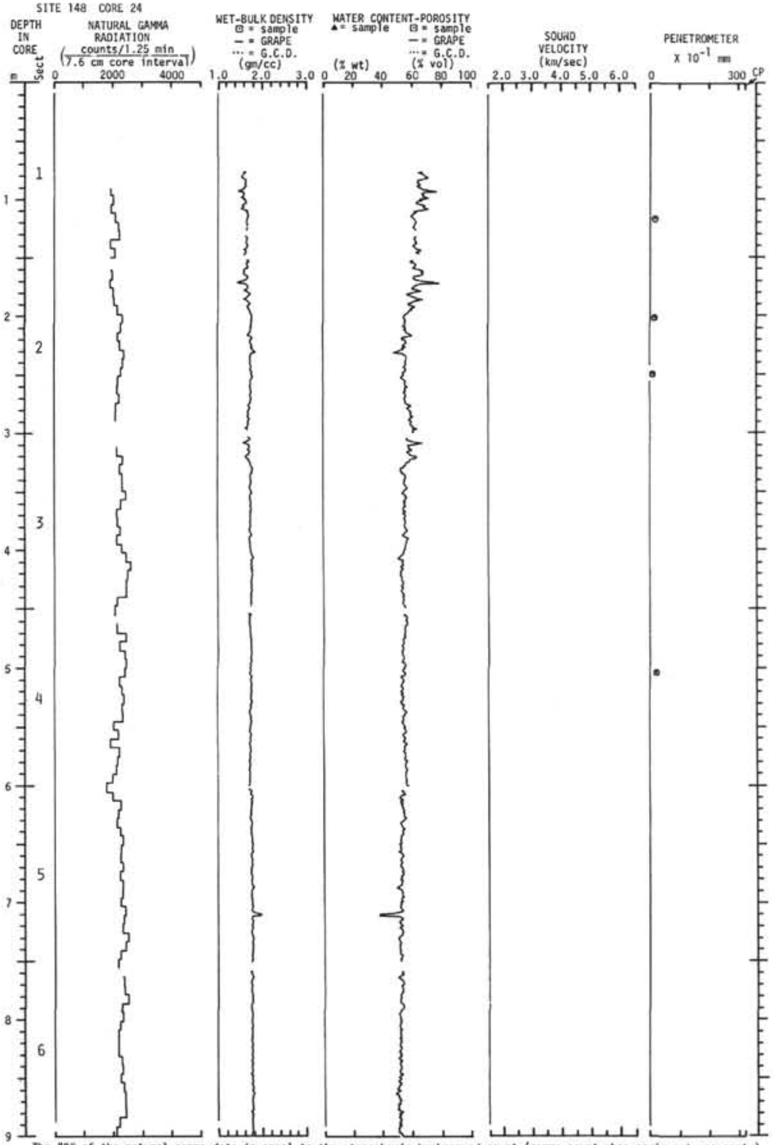

The "0" of the natural gamma data is equal to the atmospheric background count (gamma count when equipment was empty) of 1345. This background was subtracted from the data.

SITE 148 HOLE CORE 25 CORED INTERVAL (m) 221-230

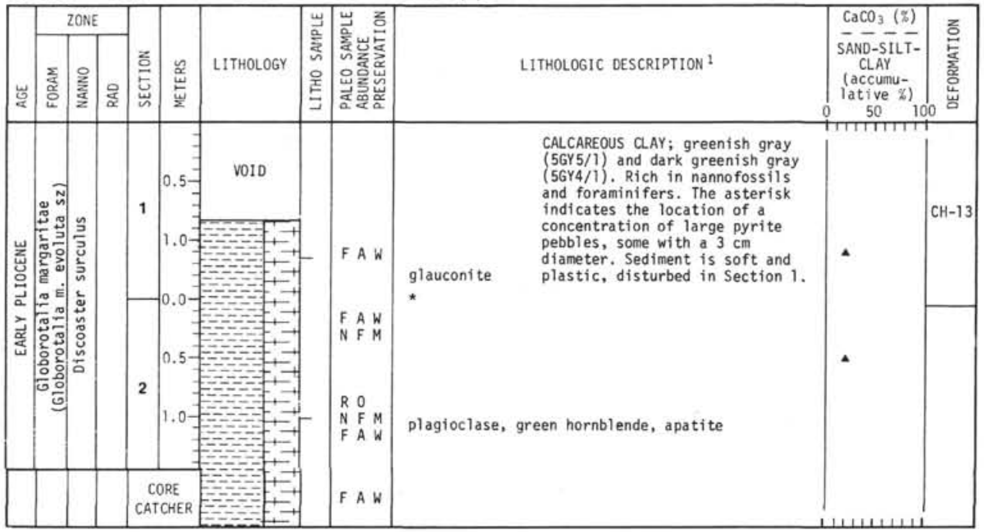

CALCAREOUS CLAY; greenish gray (5GY5/1) and dark greenish gray (5GY4/1). Rich in nannofossils and foraminifers. The asterisk indicates the location of a concentration of large pyrite pebbles, some with a 3 cm diameter. Sediment is soft and plastic, disturbed in Section 1.

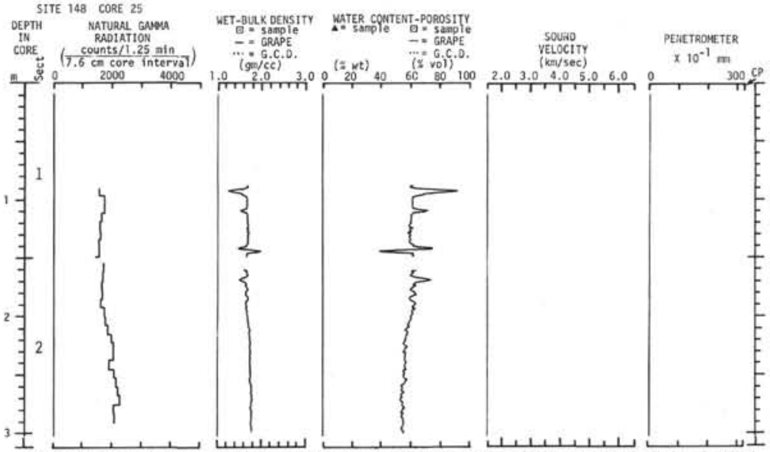

The "0" of the natural gamma data is equal to the atmospheric background count (gamma count when equipment was empty) of 1397. This background was subtracted from the data.

SITE 148 HOLE CORE 26 CORED INTERVAL (m) 230-240

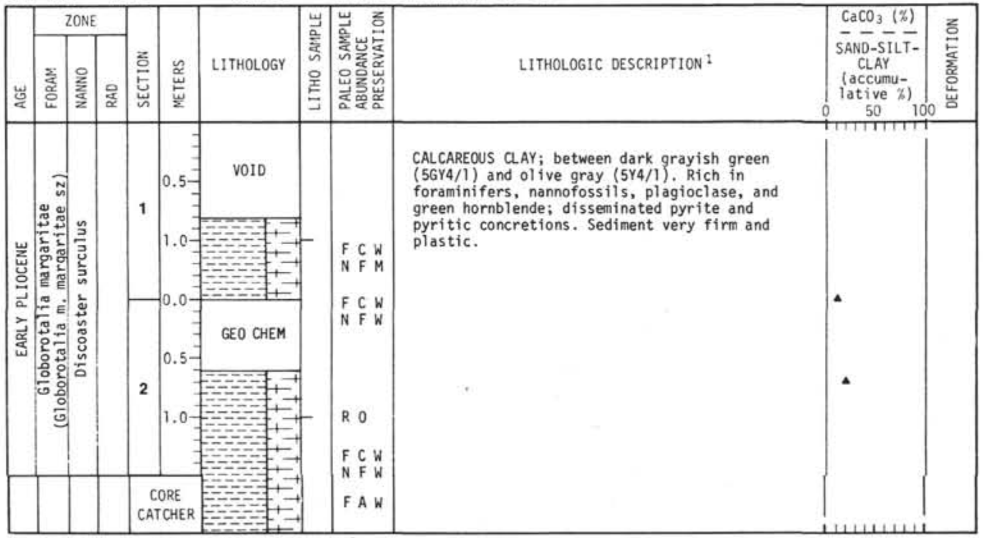

CALCAREOUS CLAY; between dark grayish green (5GY4/1) and olive gray (5Y4/1). Rich in foraminifers, nannofossils, plagioclase, and green hornblende; disseminated pyrite and pyritic concretions. Sediment very firm and plastic.

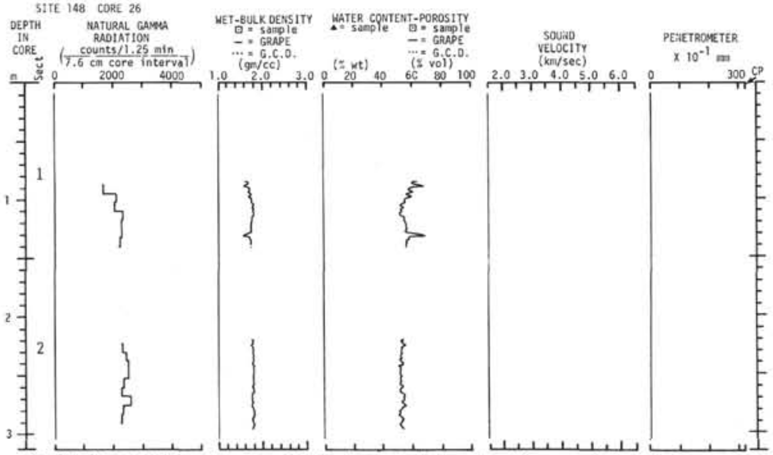

The "0" of the natural gamma data is equal to the atmospheric background count (gamma count when equipment was empty) of 1397. This background was subtracted from the data.

[1] For explanation of symbols, see Chapter 1

SITE 148 HOLE CORE 27 CORED INTERVAL (m) 240-249

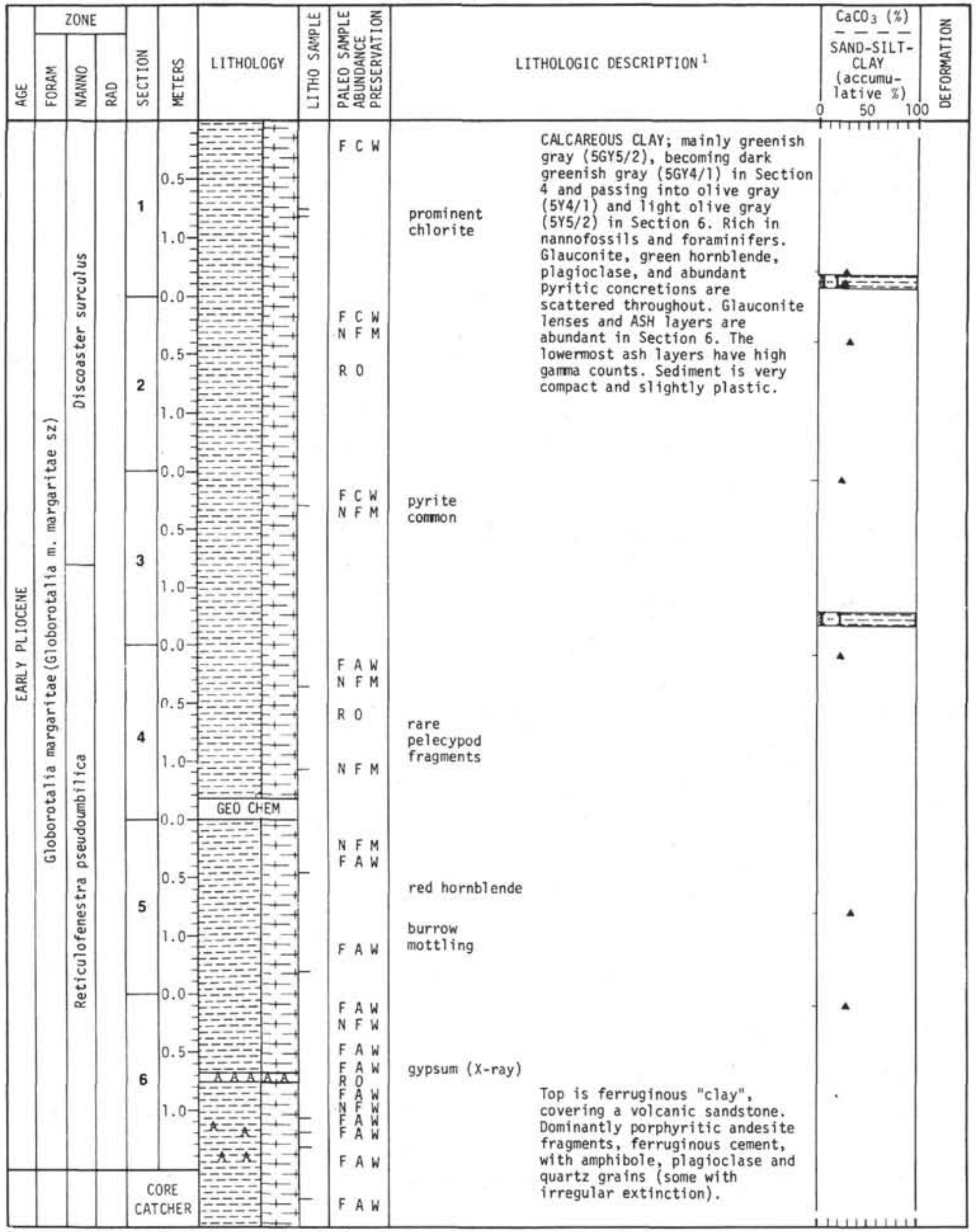

CALCAREOUS CLAY; mainly greenish gray (5GY5/2), becoming dark greenish gray (5GY4/1) in Section 4 and passing into olive gray (5Y4/1) and light olive gray (5Y5/2) in Section 6. Rich in nannofossils and foraminifers. Glauconite, green hornblende, plagioclase, and abundant pyritic concretions are scattered throughout. Glauconite lenses and ASH layers are abundant in Section 6. The lowermost ash layers have high gamma counts. Sediment is very compact and slightly plastic.

Top is ferruginous "clay", covering a volcanic sandstone. Dominantly porphyritic andesite fragments, ferruginous cement, with amphibole, plagioclase and quartz grains (some with irregular extinction).

---

[1] For explanation of symbols, see Chapter 1

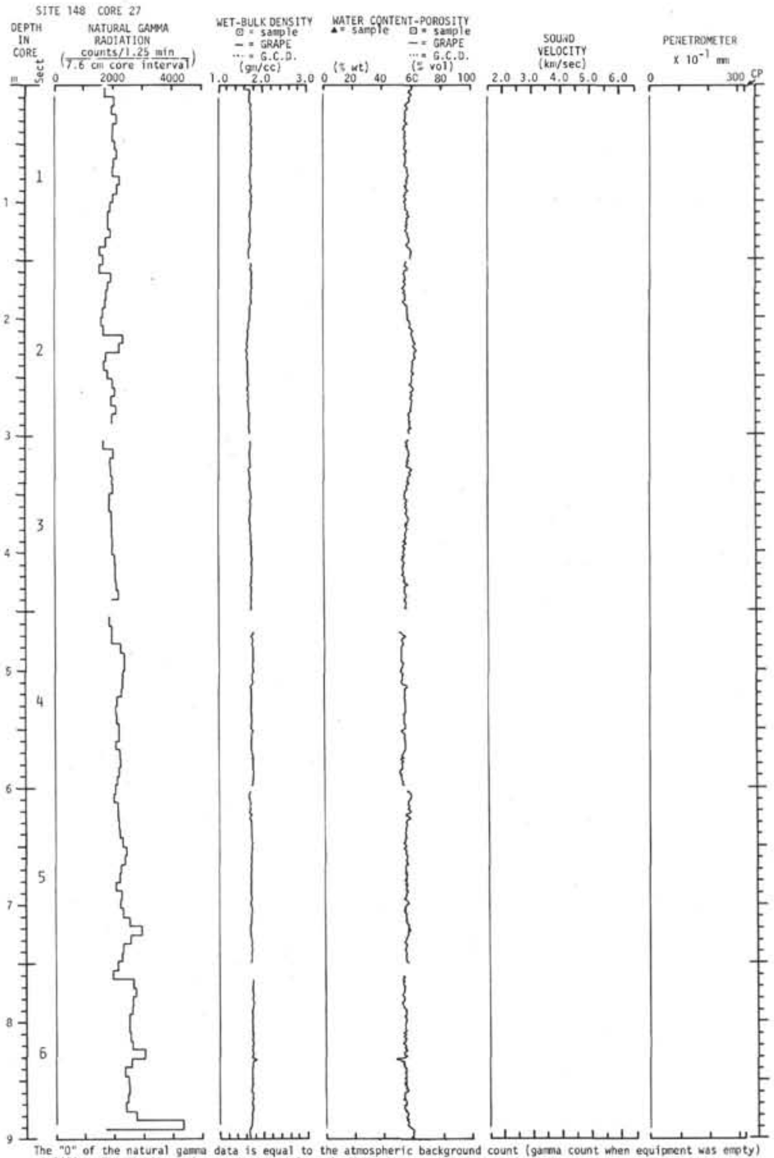

The "0" of the natural gamma data is equal to the atmospheric background count (gamma count when equipment was empty) of 1404. This background was subtracted from the data.

SITE 148 HOLE CORE 28 CORED INTERVAL (m) 249-258

AGE	ZONE FORAM	ZONE NANNO	ZONE RAD	SECTION	METERS	LITHOLOGY	LITHO SAMPLE	PALEO SAMPLE ABUNDANCE PRESERVATION	LITHOLOGIC DESCRIPTION[1]	CaCO3 (%) SAND-SILT-CLAY (accumulative %) 0 50 100	DEFORMATION
	Heterogeneous fauna (PALEOCENE - MIOCENE)	reworked CRETACEOUS		1	0.5 1.0	VOID 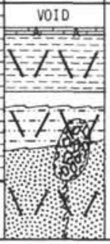		F R M R F M N R P N R P f	LIMESTONE fragments mixed with ASH. The limestone is very pale grayish orange (10YR8/4) and contains foraminifers. The ash ranges from very pale gray (N7) to greenish gray (5GY6/1) and rusty. CLAYSTONE; friable, dusky yellow (5Y6/4) to light olive gray (5Y6/2), very firm, disturbed throughout, rust streaks and volcanic.		CH-13 V
				CORE CATCHER				f	SILTY SANDSTONE; friable, intermixed with CLAY, volcanic in origin, rusty veins cutting through the fragments. Breccia cemented by the rusty veins. Some layers are graded. V. Drilling breccia: dark clay injected into fractures, fragmentation.		

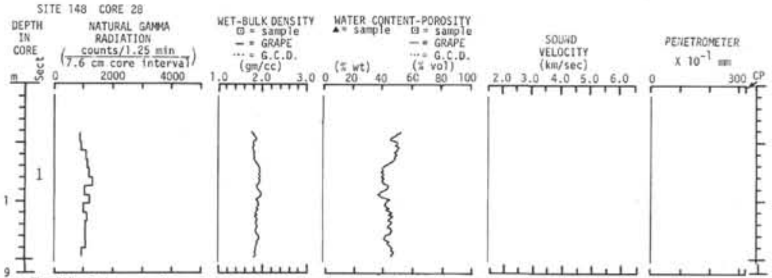

The "0" of the natural gamma data is equal to the atmospheric background count (gamma count when equipment was empty) of 1404. This background was subtracted from the data.

SITE 148 HOLE CORE 29 CORED INTERVAL (m) 258-260

AGE	ZONE FORAM	ZONE NANNO	ZONE RAD	SECTION	METERS	LITHOLOGY	LITHO SAMPLE	PALEO SAMPLE ABUNDANCE PRESERVATION	LITHOLOGIC DESCRIPTION[1]	CaCO3 (%) SAND-SILT-CLAY (accumulative %) 0 50 100	DEFORMATION
	Heterogeneous fauna (PALEOCENE-MIOCENE)	reworked CRETACEOUS		1	0.5 1.0	VOID 		R F M f f R F M N R P f	plagioclase glauconite CLAYSTONE; friable, light olive brown (5Y4/6) to moderate olive brown (5Y4/4). Compacted; rusted streaks and blotches. Slightly disturbed. SAND, SILT and CLAY; interbedded layers, olive black (5Y2/1) to grayish black (N2), slightly calcareous in lower 30 cm. Brecciation similar to that in Core 28. Some layers display graded bedding. Abundant volcanic debris, mainly feldspar and rock fragments.		
				CORE CATCHER				f	green hornblende, apatite, clinopyroxene, K-feldspar, quartz, plagioclase, green hornblende		

[1] For explanation of symbols, see Chapter 1

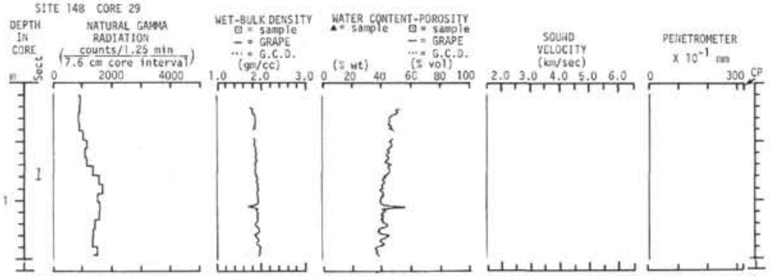

The "0" of the natural gamma data is equal to the atmospheric background count (gamma count when equipment was empty) of 1404. This background was subtracted from the data.

SITE 148 HOLE CORE 30 CORED INTERVAL (m) 260-267

AGE	ZONE FORAM	 NANNO	 RAD	SECTION	METERS	LITHOLOGY	LITHO SAMPLE	PALEO SAMPLE ABUNDANCE PRESERVATION	LITHOLOGIC DESCRIPTION[1]	CaCO3 (%) SAND-SILT-CLAY (accumulative %) 0 50 100	DEFORMATION
				CORE CATCHER					NO RECOVERY Core catcher only, not described.		

SITE 148 HOLE CORE 31 CORED INTERVAL (m) 267-272

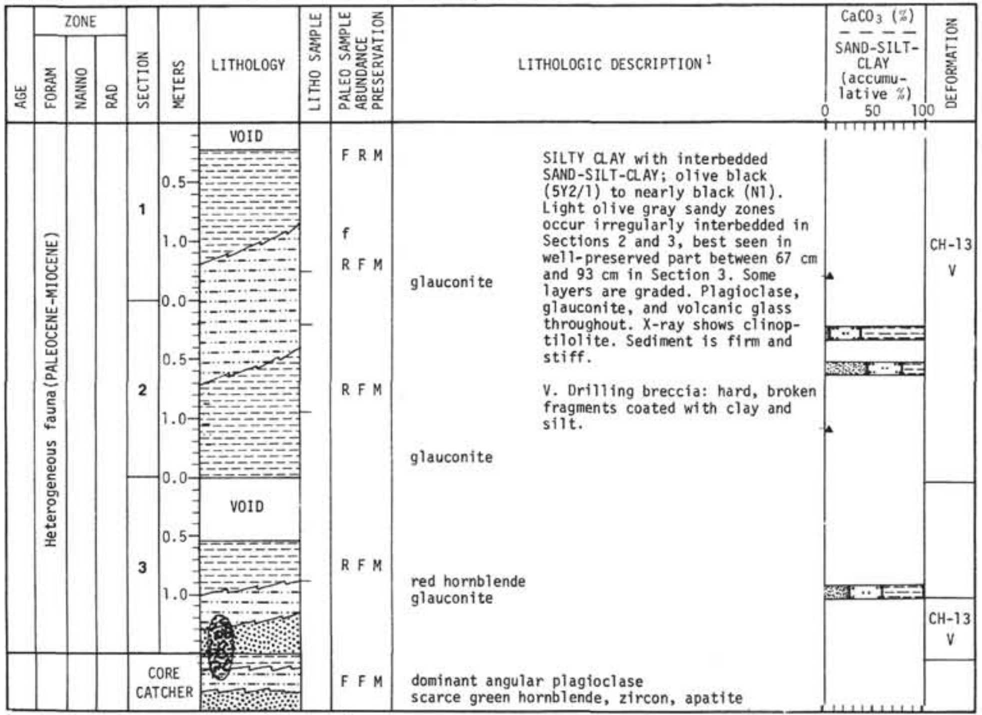

AGE	ZONE FORAM	 NANNO	 RAD	SECTION	METERS	LITHOLOGY	LITHO SAMPLE	PALEO SAMPLE ABUNDANCE PRESERVATION	LITHOLOGIC DESCRIPTION[1]		CaCO3 (%) SAND-SILT-CLAY (accumulative %) 0 50 100	DEFORMATION
	Heterogeneous fauna (PALEOCENE-MIOCENE)			1	0.5 1.0	VOID		F R M f R F M	glauconite	SILTY CLAY with interbedded SAND-SILT-CLAY; olive black (5Y2/1) to nearly black (N1). Light olive gray sandy zones occur irregularly interbedded in Sections 2 and 3, best seen in well-preserved part between 67 cm and 93 cm in Section 3. Some layers are graded. Plagioclase, glauconite, and volcanic glass throughout. X-ray shows clinoptilolite. Sediment is firm and stiff.		CH-13 V
				2	0.0 0.5 1.0			R F M	glauconite	V. Drilling breccia: hard, broken fragments coated with clay and silt.		
				3	0.0 0.5 1.0	VOID		R F M	red hornblende glauconite			CH-13 V
				CORE CATCHER				F F M	dominant angular plagioclase scarce green hornblende, zircon, apatite			

[1] For explanation of symbols, see Chapter 1

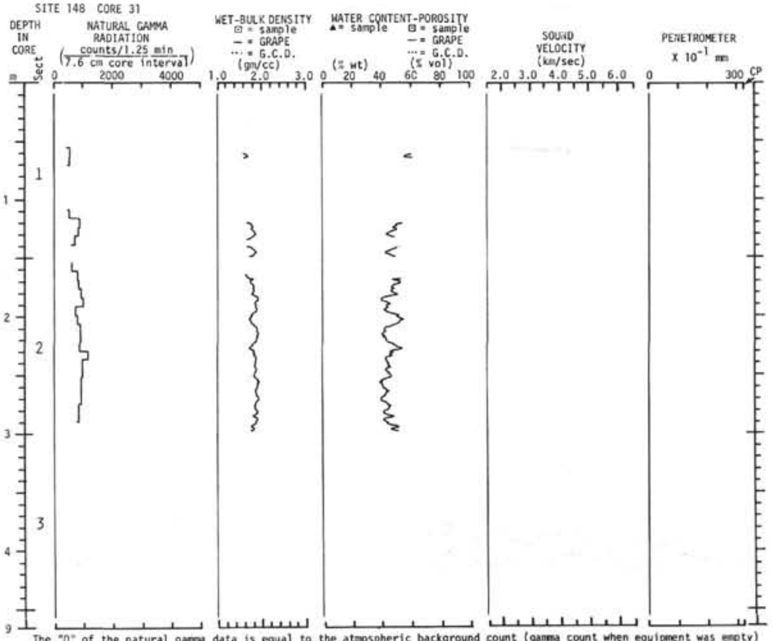

The "0" of the natural gamma data is equal to the atmospheric background count (gamma count when equipment was empty) of 1397. This background was subtracted from the data.

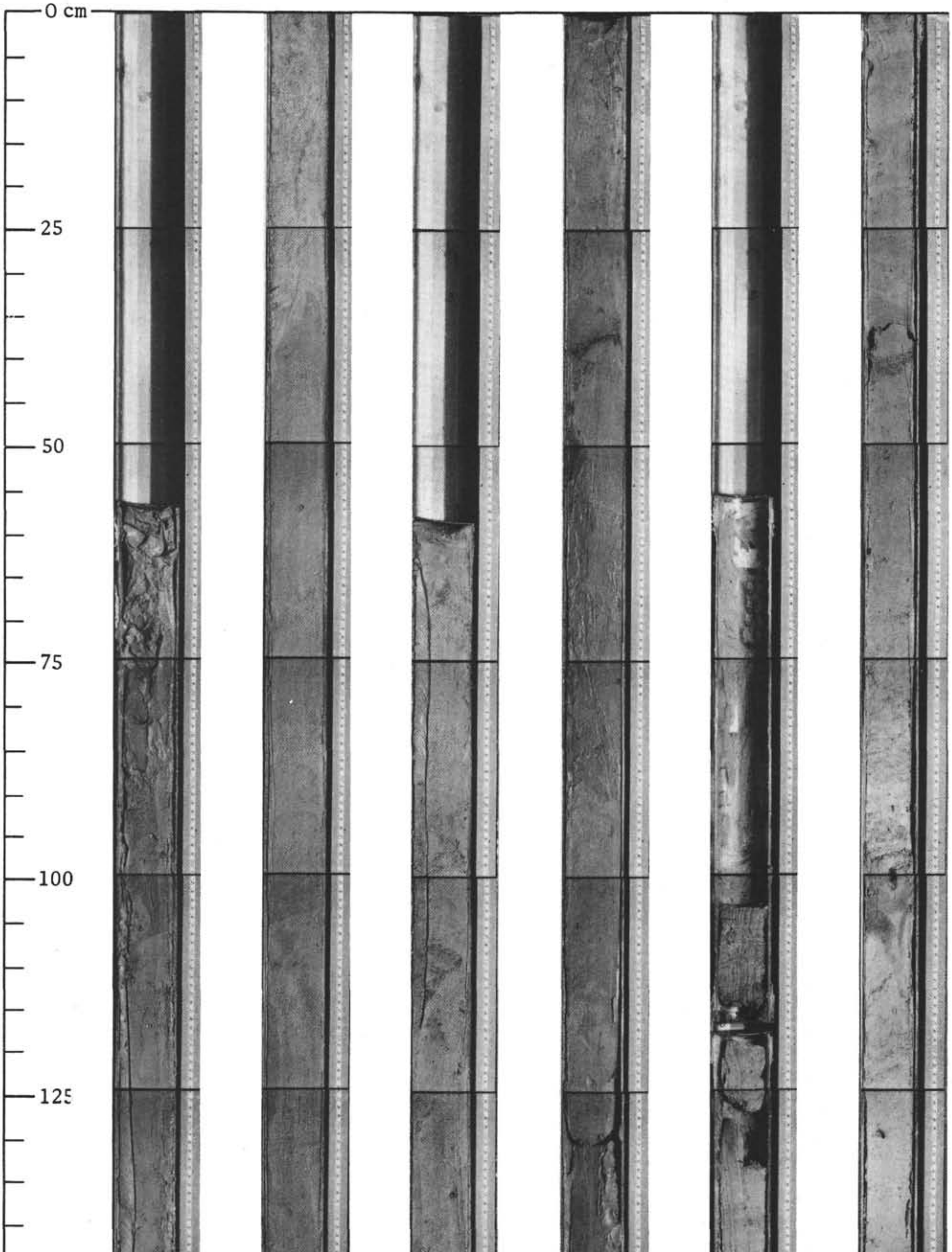
0 cm
25
50
75
100
125
150
148-1-2
148-1-3
148-1-4
148-1-5
148-2-1
148-2-2

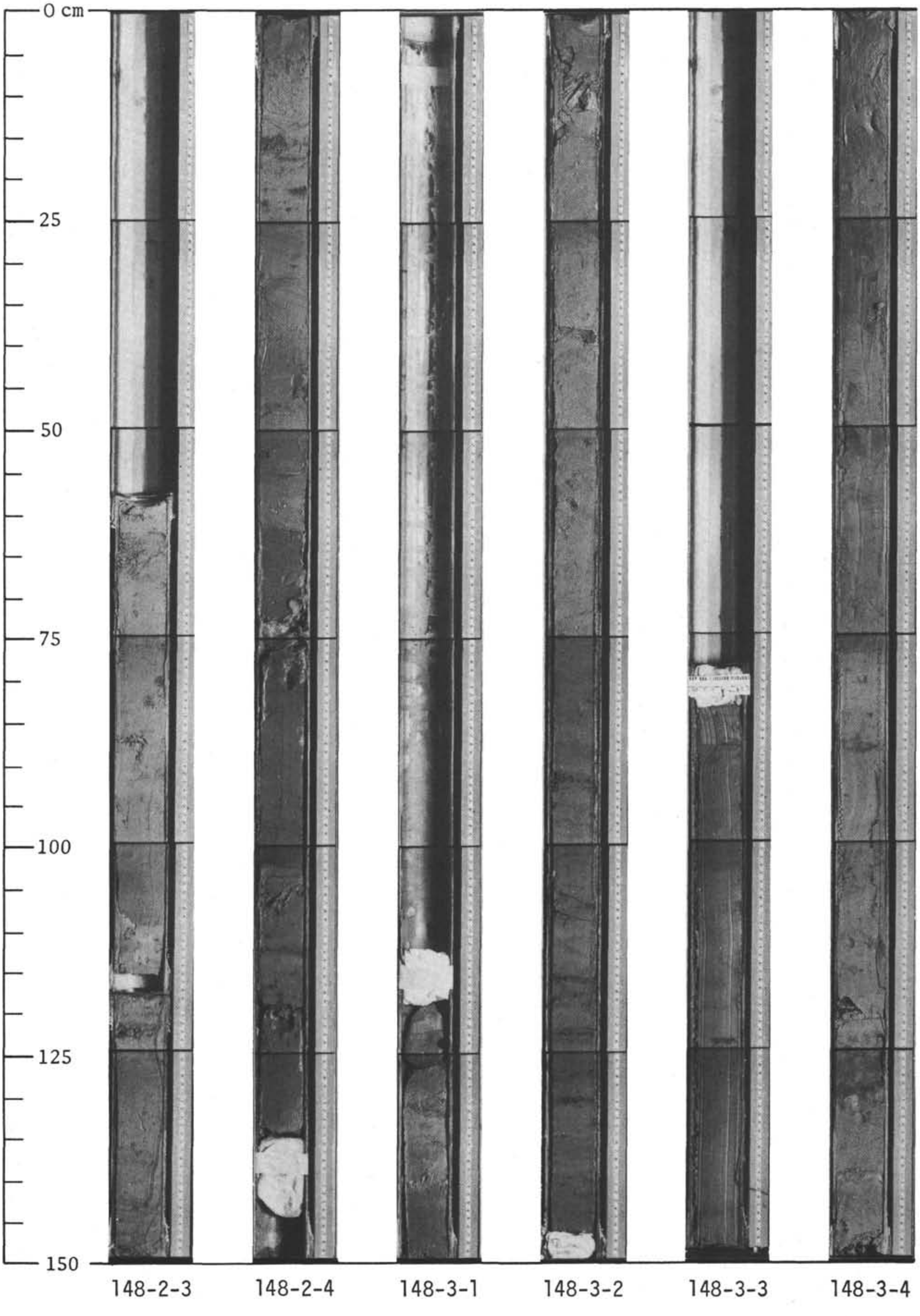
0 cm
25
50
75
100
125
150
148-2-3
148-2-4
148-3-1
148-3-2
148-3-3
148-3-4

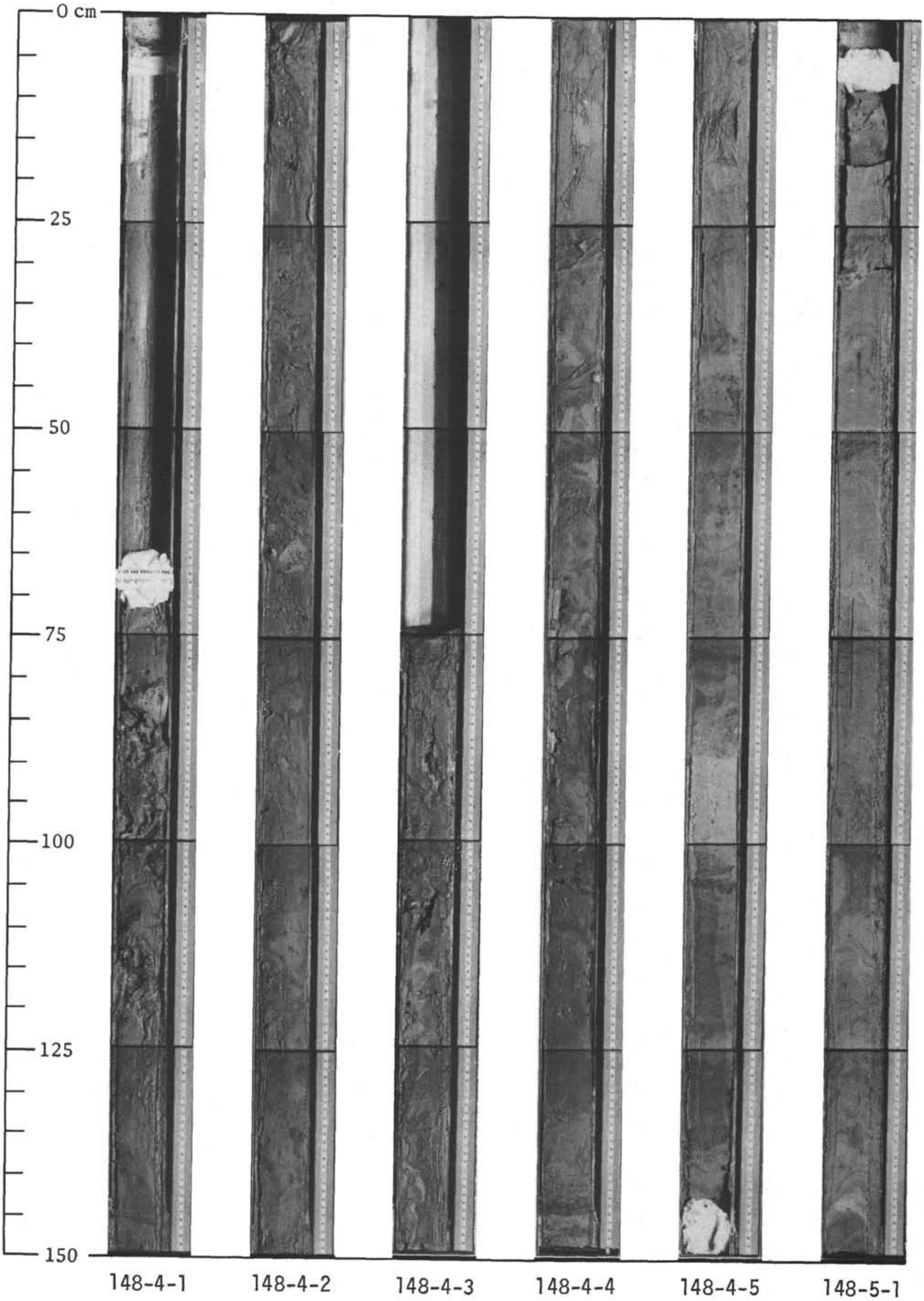
0 cm
25
50
75
100
125
150
148-4-1
148-4-2
148-4-3
148-4-4
148-4-5
148-5-1

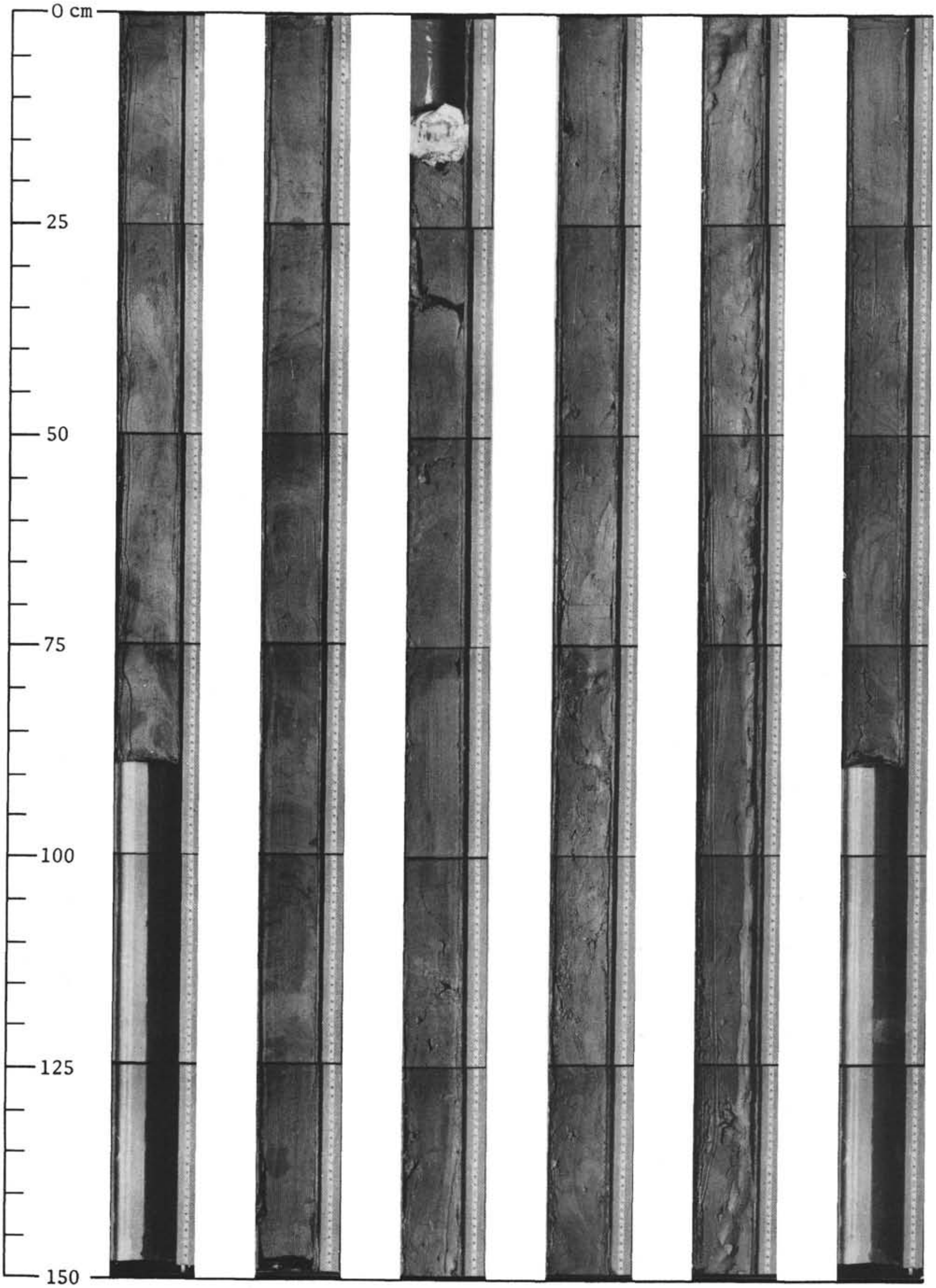
0 cm
25
50
75
100
125
150
148-5-2
148-5-3
148-6-1
148-6-2
148-6-3
148-6-4

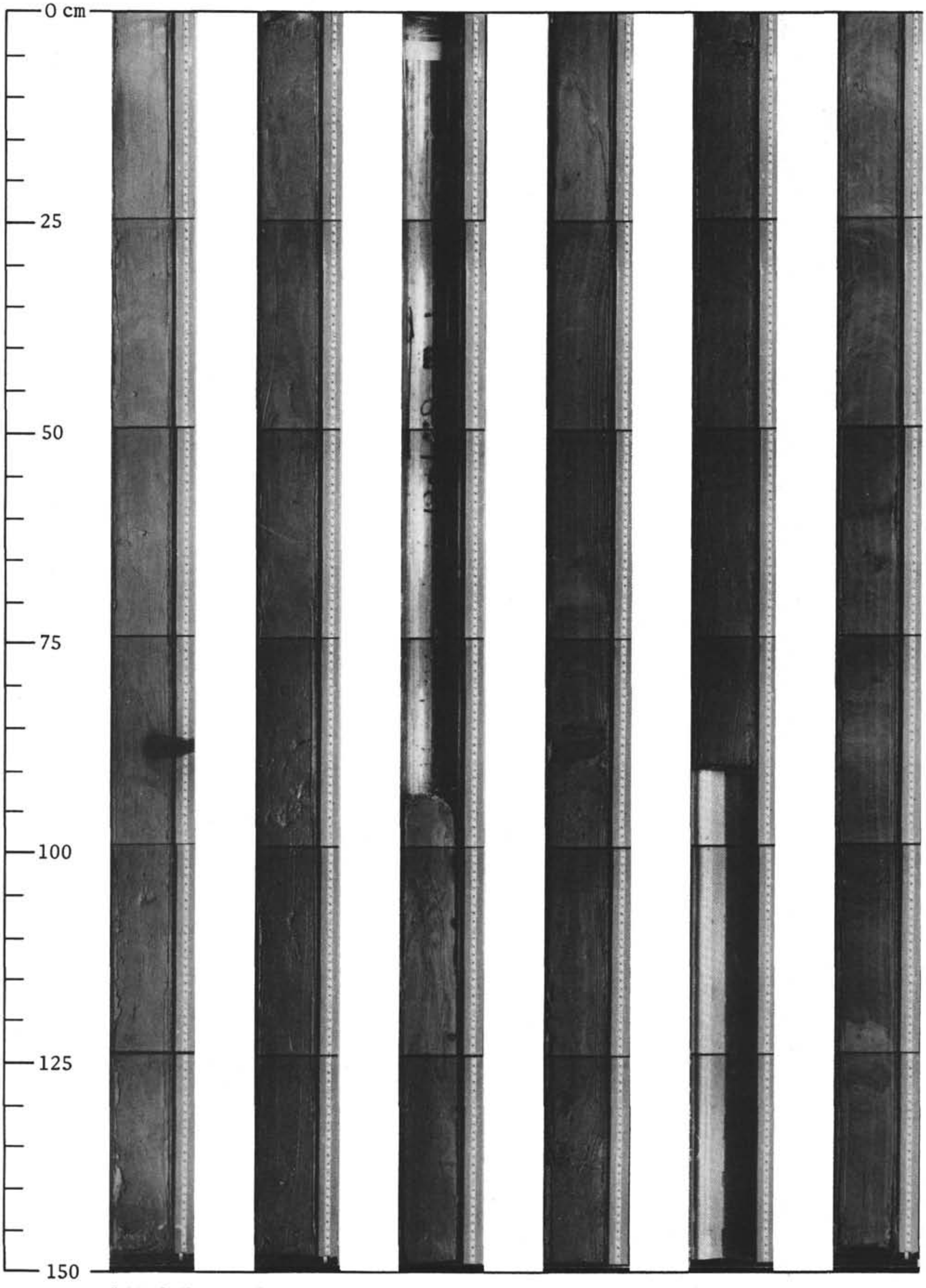
0 cm
25
50
75
100
125
150
148-6-5
148-6-6
148-7-1
148-7-2
148-7-3
148-7-4

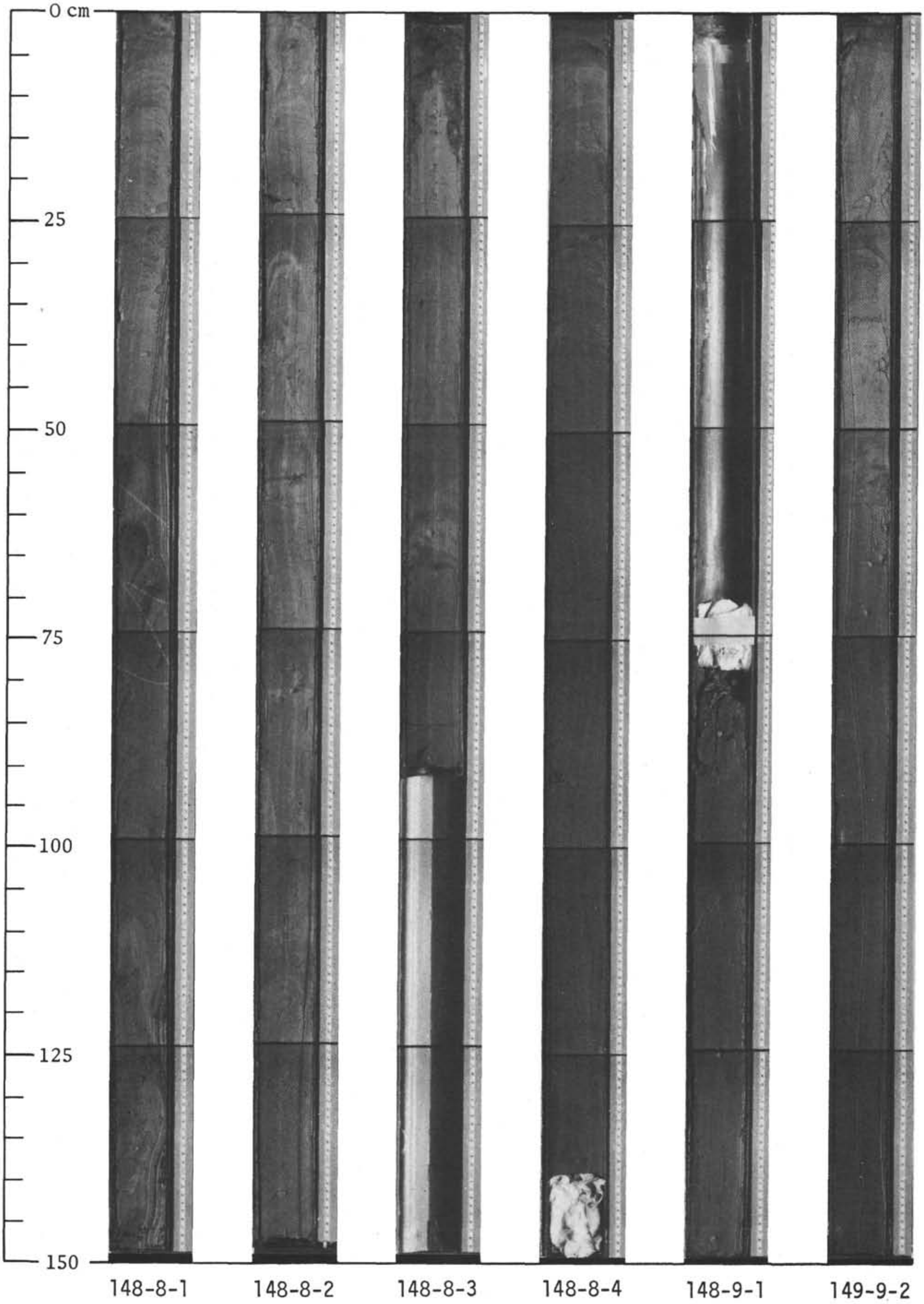
0 cm
25
50
75
100
125
150
148-8-1
148-8-2
148-8-3
148-8-4
148-9-1
149-9-2

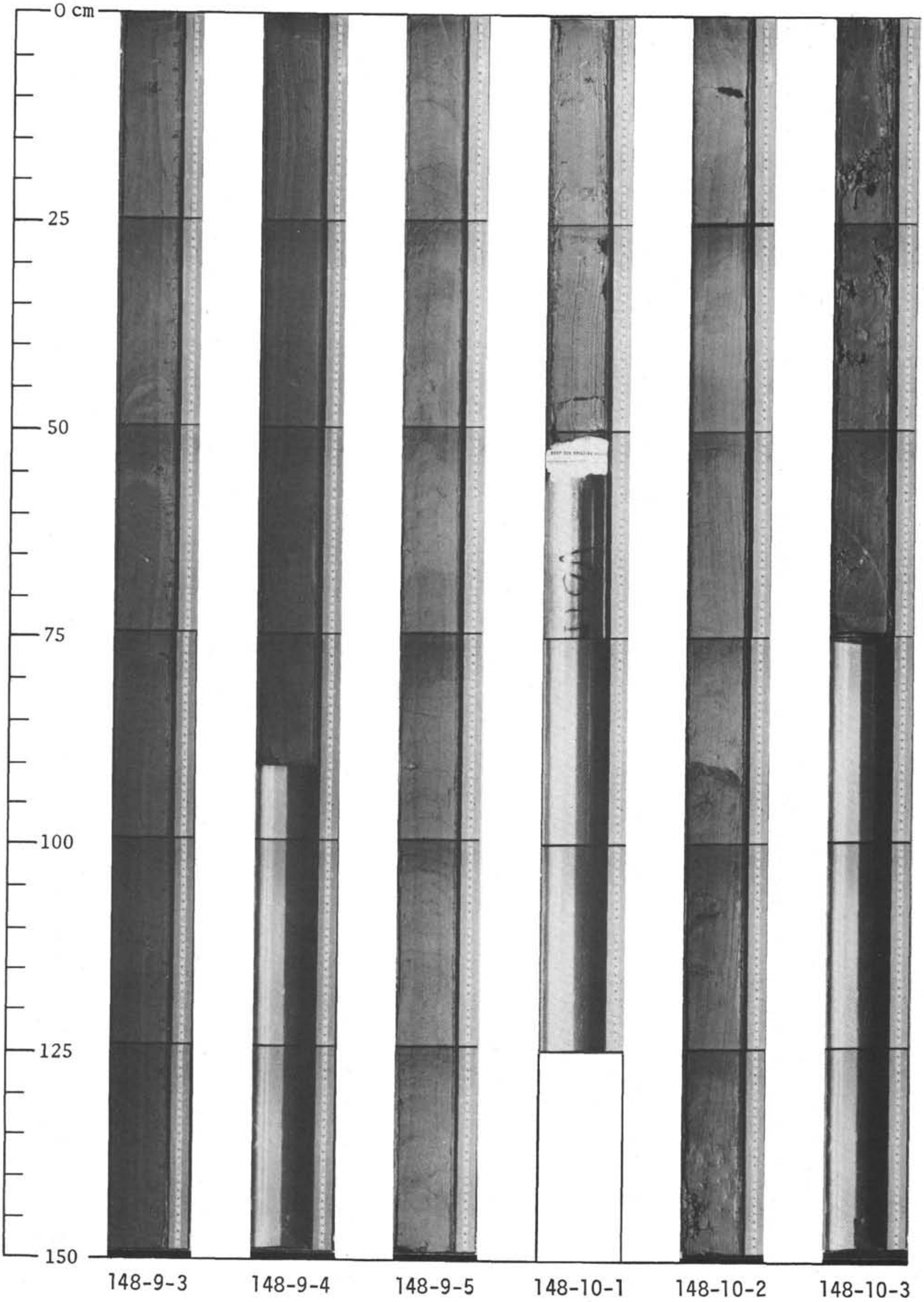
0 cm
25
50
75
100
125
150
148-9-3
148-9-4
148-9-5
148-10-1
148-10-2
148-10-3

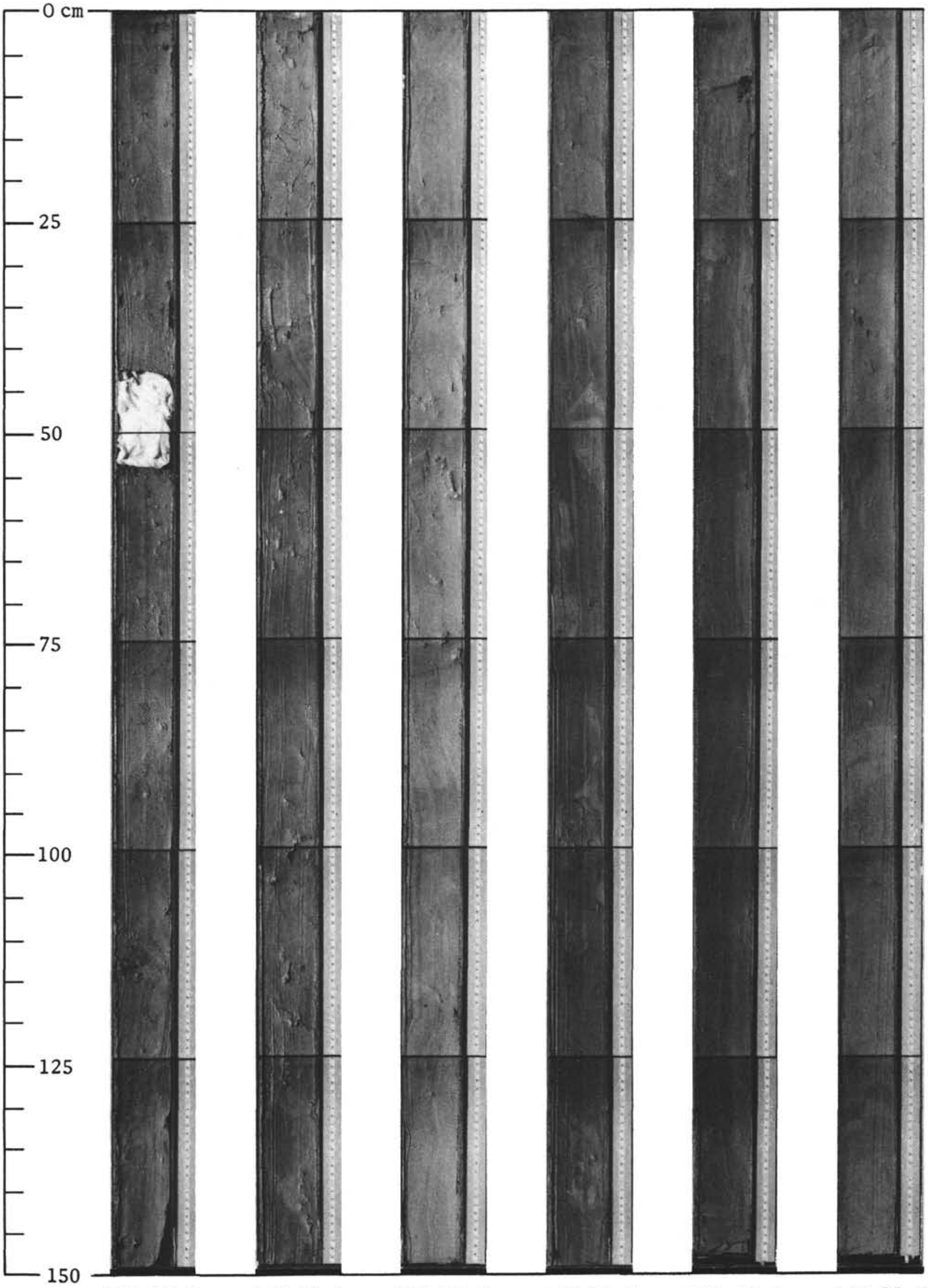

0 cm
25
50
75
100
125
150
148-10-4
148-11-1
148-11-2
148-11-3
148-11-4
148-11-5

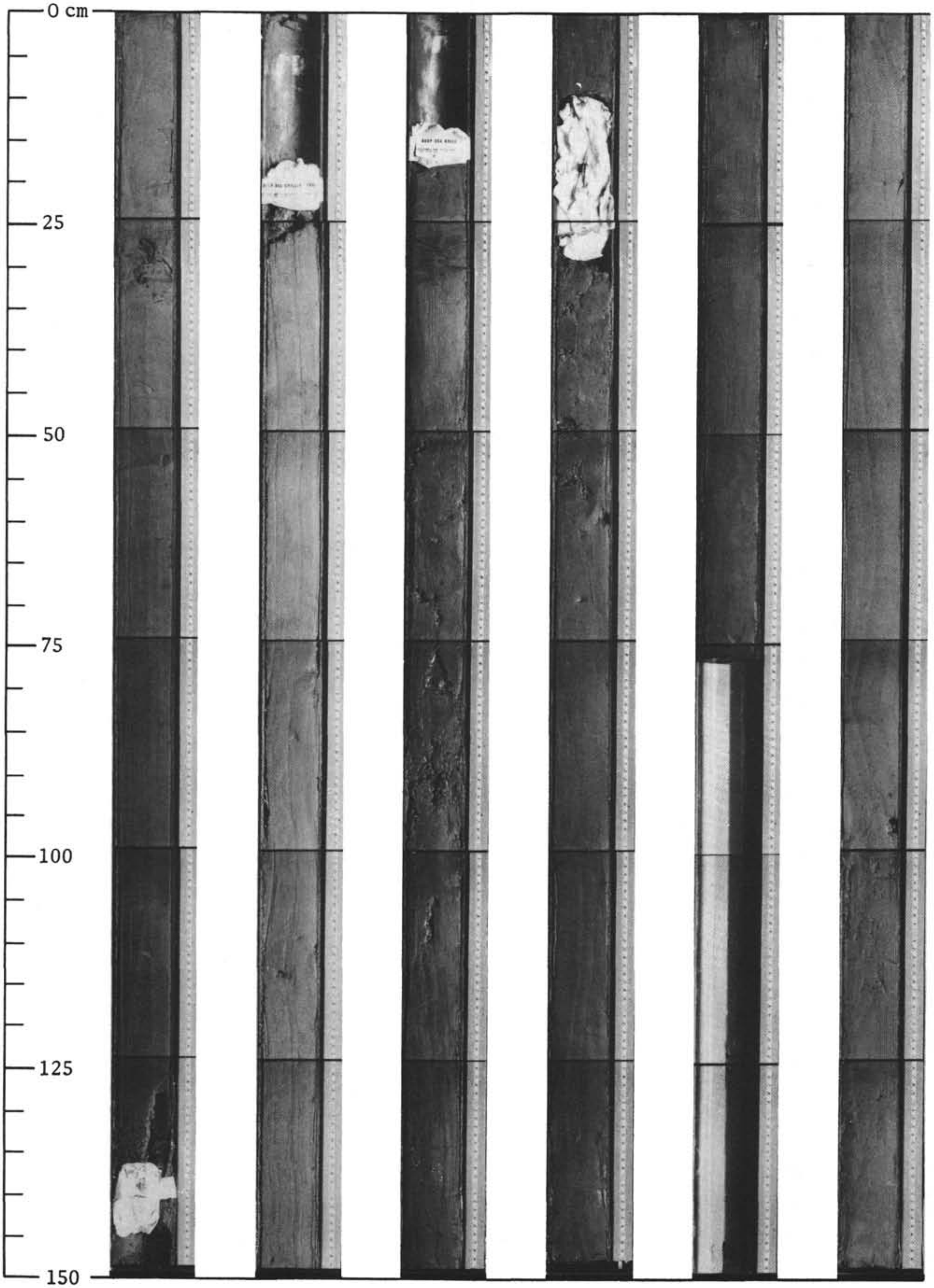

148-11-6 148-12-1 148-12-2 148-12-3 148-12-4 148-12-5

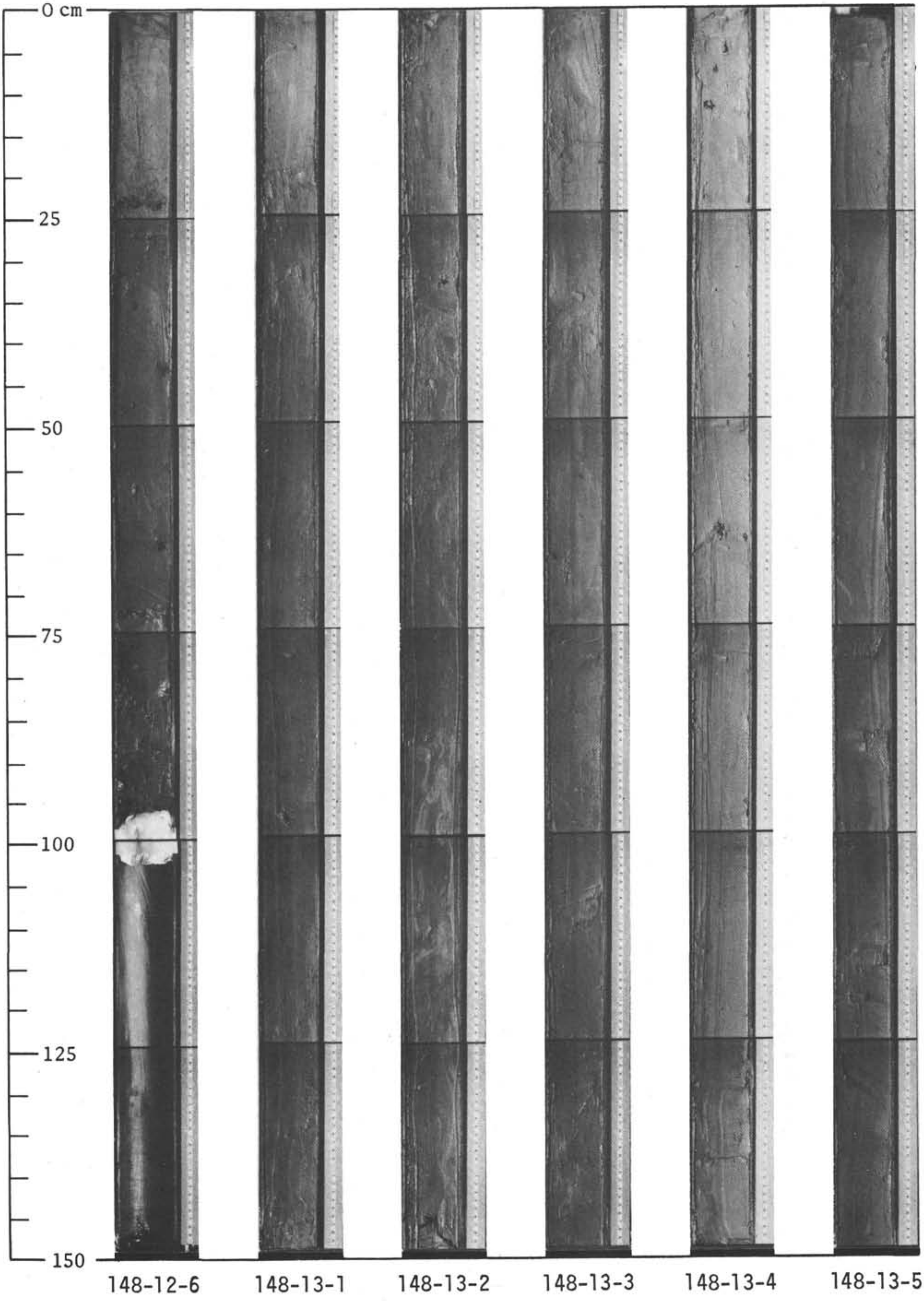
0 cm
25
50
75
100
125
150
148-12-6
148-13-1
148-13-2
148-13-3
148-13-4
148-13-5

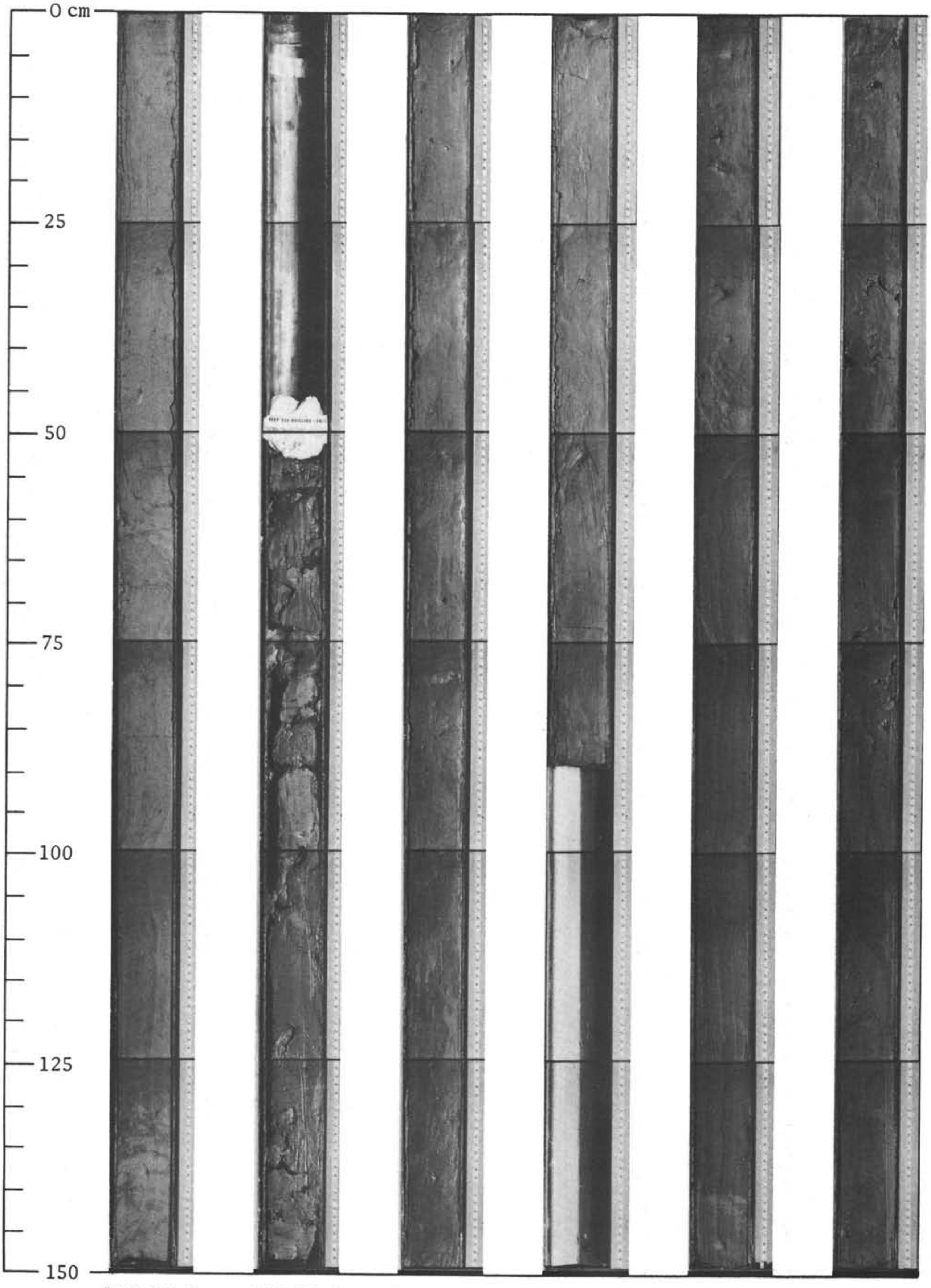
0 cm
25
50
75
100
125
150
148-13-6
148-14-1
148-14-2
148-14-3
148-14-4
148-15-1

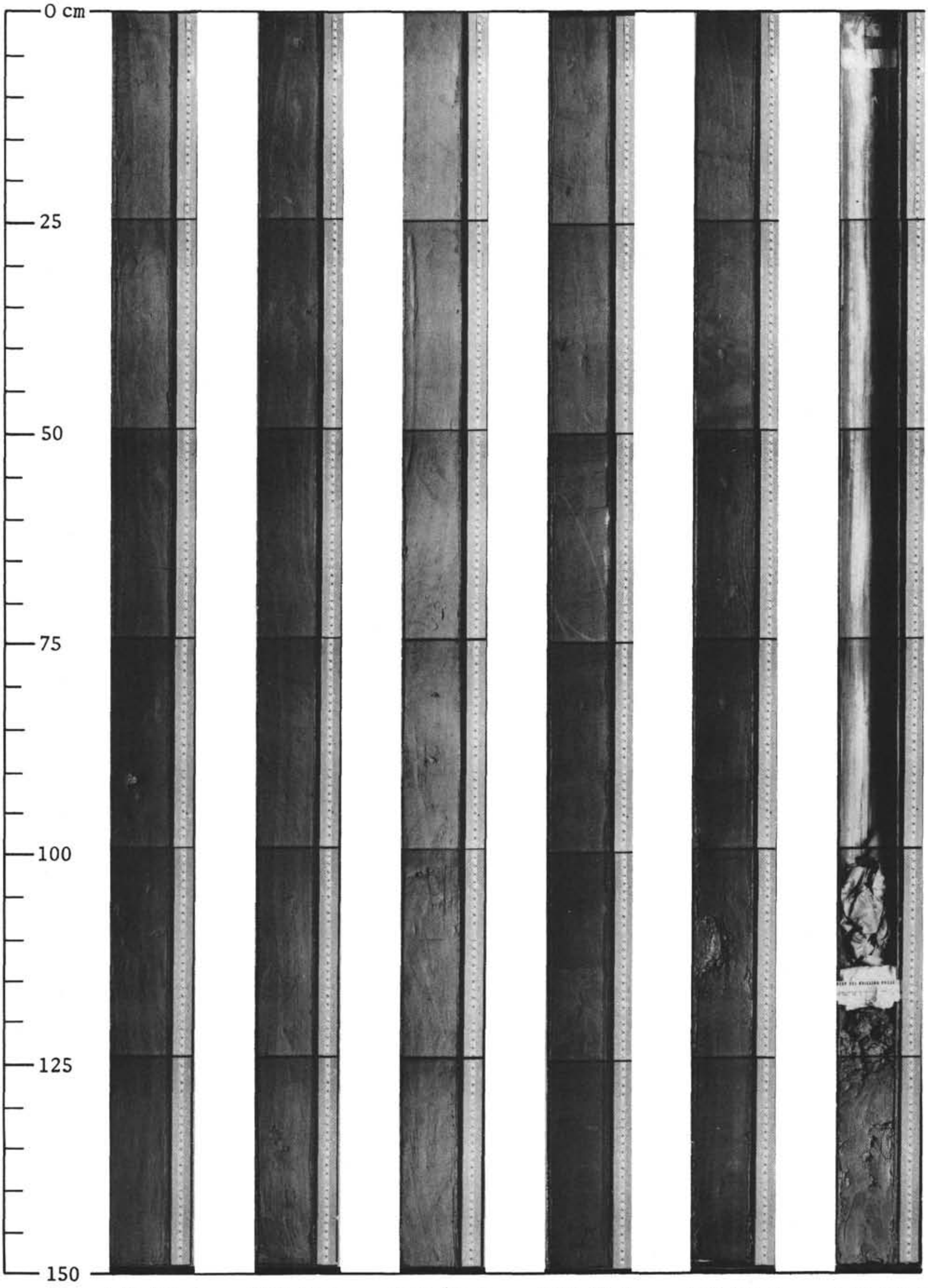
0 cm
25
50
75
100
125
150
148-15-2
148-15-3
148-15-4
148-15-5
148-15-6
148-16-1

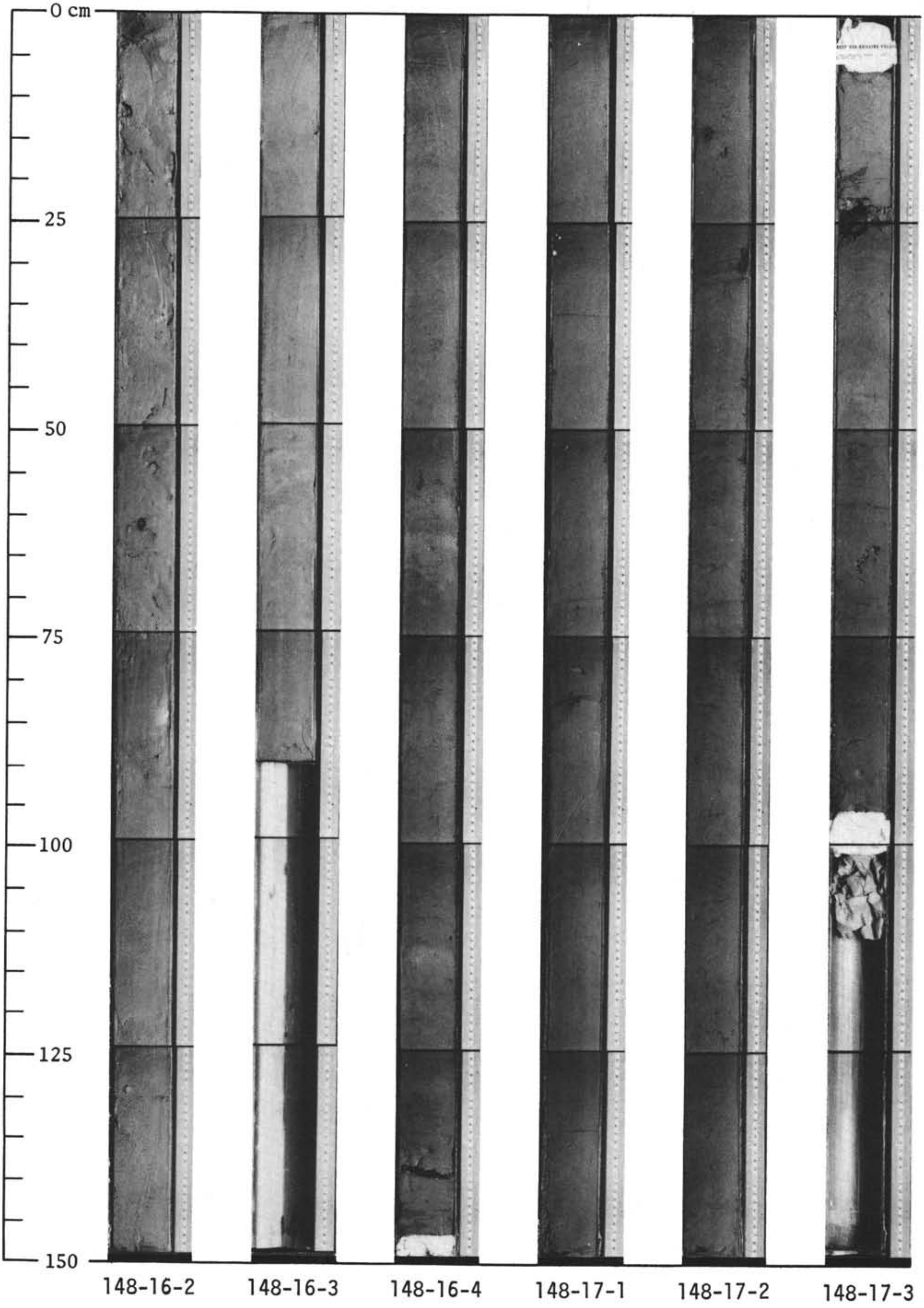
0 cm
25
50
75
100
125
150
148-16-2
148-16-3
148-16-4
148-17-1
148-17-2
148-17-3

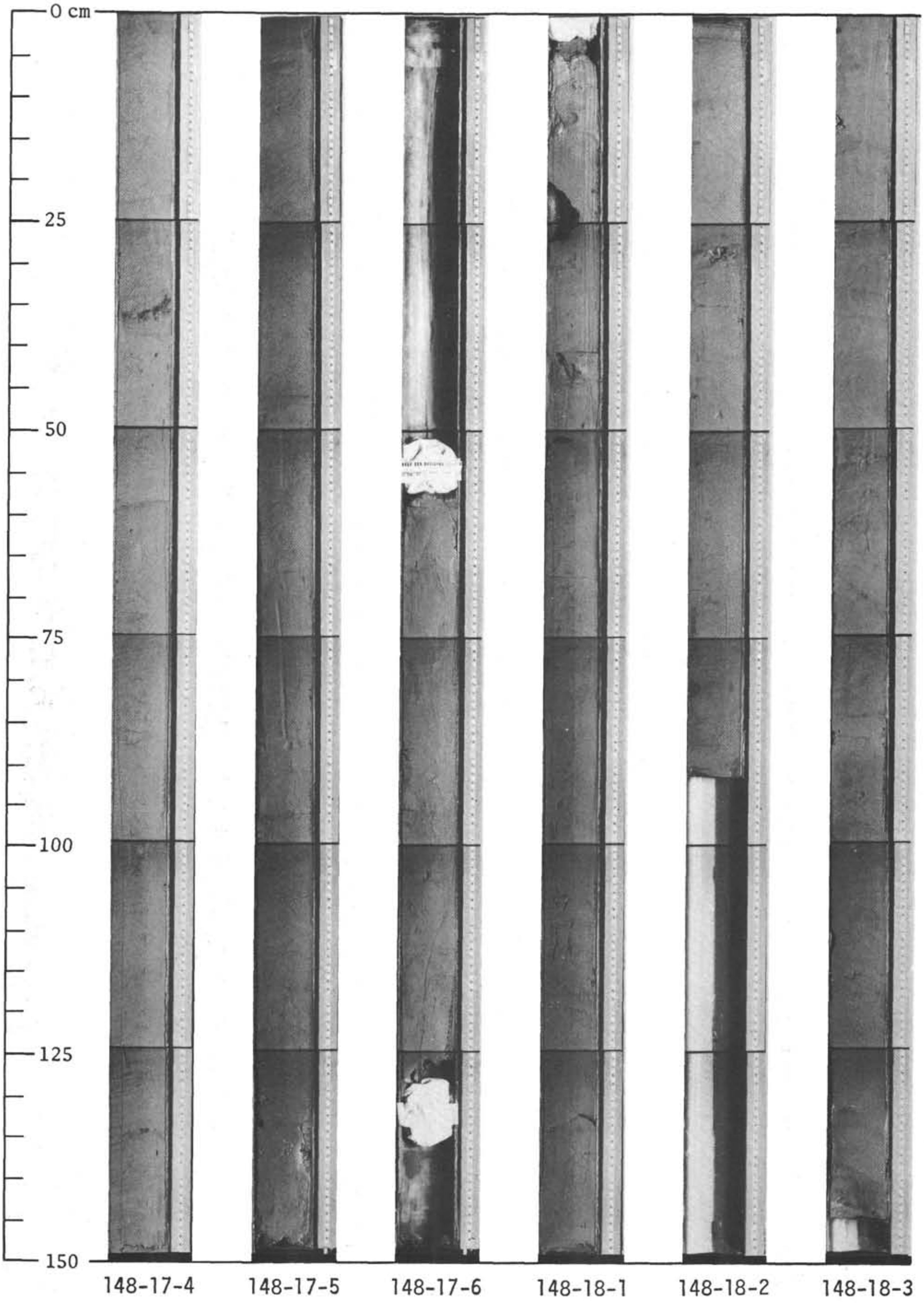
0 cm
25
50
75
100
125
150
148-17-4
148-17-5
148-17-6
148-18-1
148-18-2
148-18-3

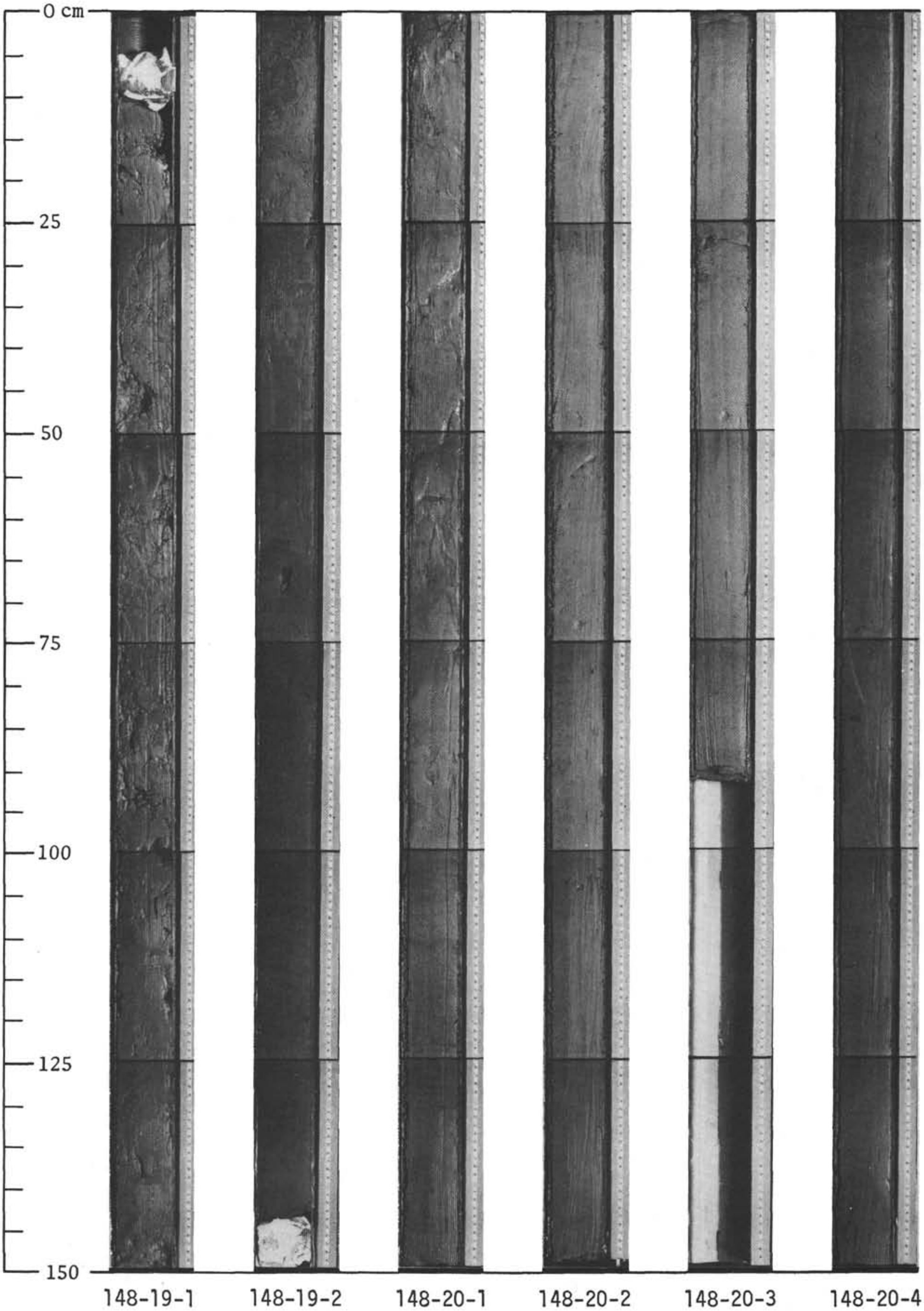
0 cm
25
50
75
100
125
150
148-19-1
148-19-2
148-20-1
148-20-2
148-20-3
148-20-4

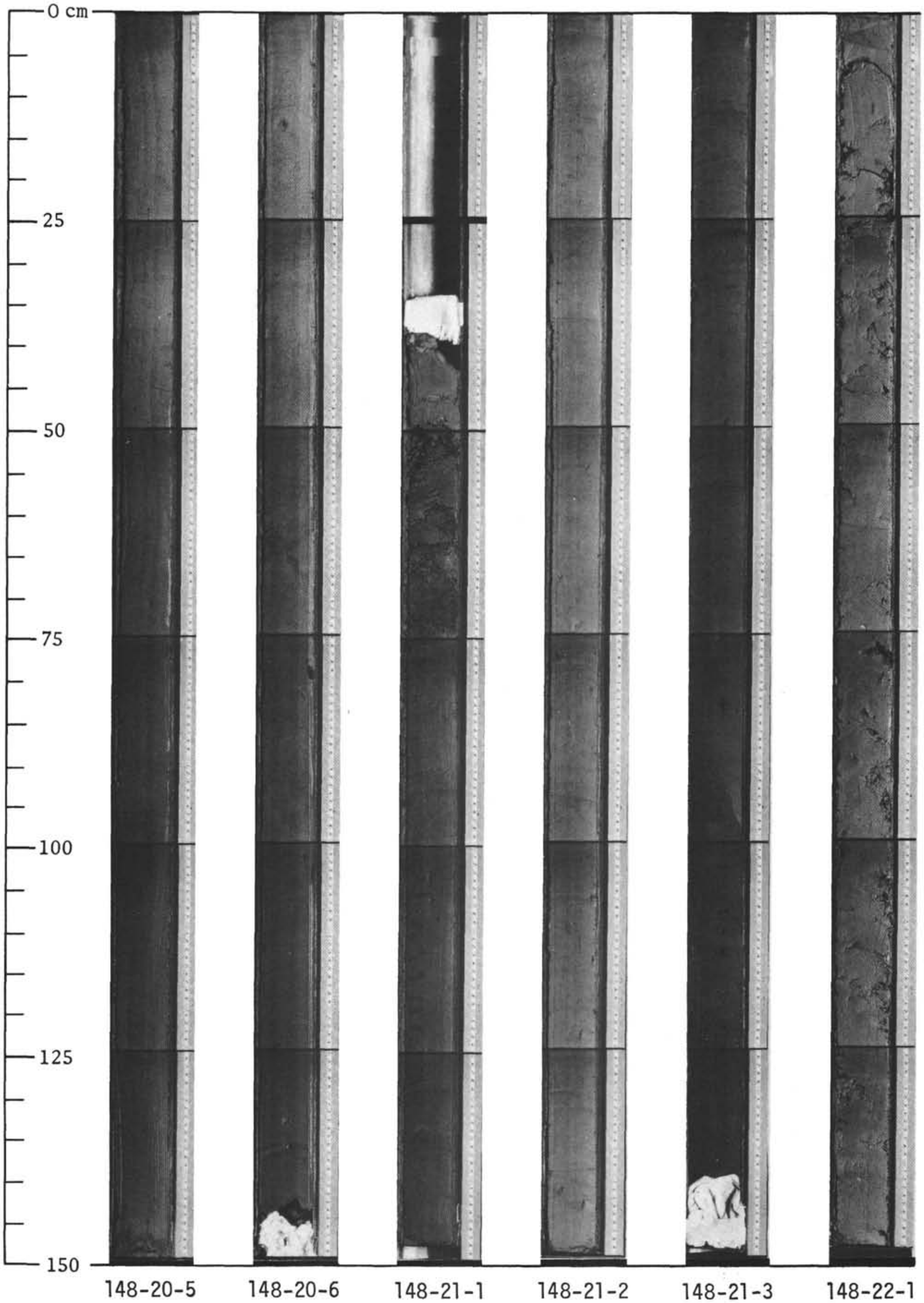
0 cm
25
50
75
100
125
150
148-20-5
148-20-6
148-21-1
148-21-2
148-21-3
148-22-1

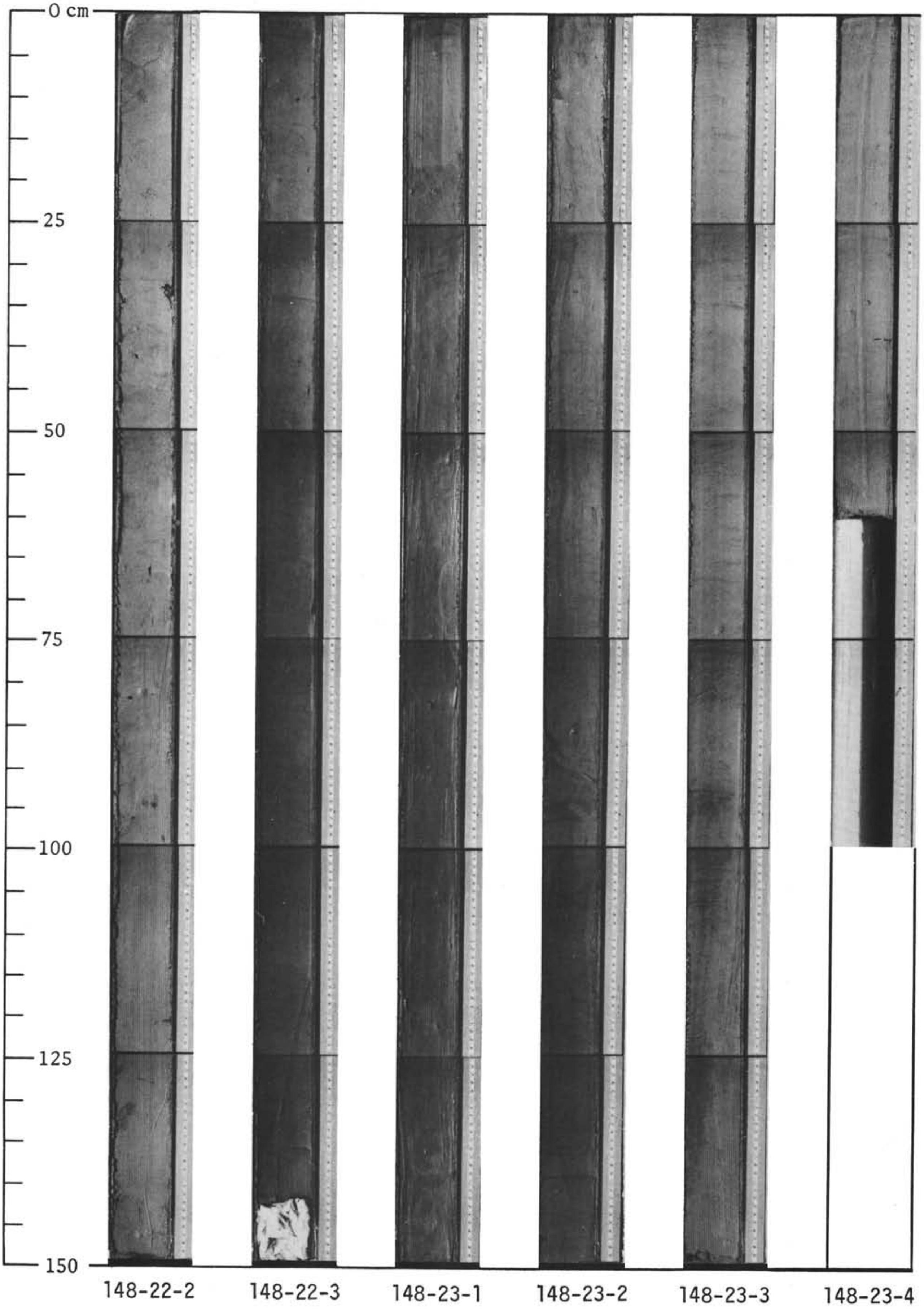
0 cm
25
50
75
100
125
150
148-22-2
148-22-3
148-23-1
148-23-2
148-23-3
148-23-4

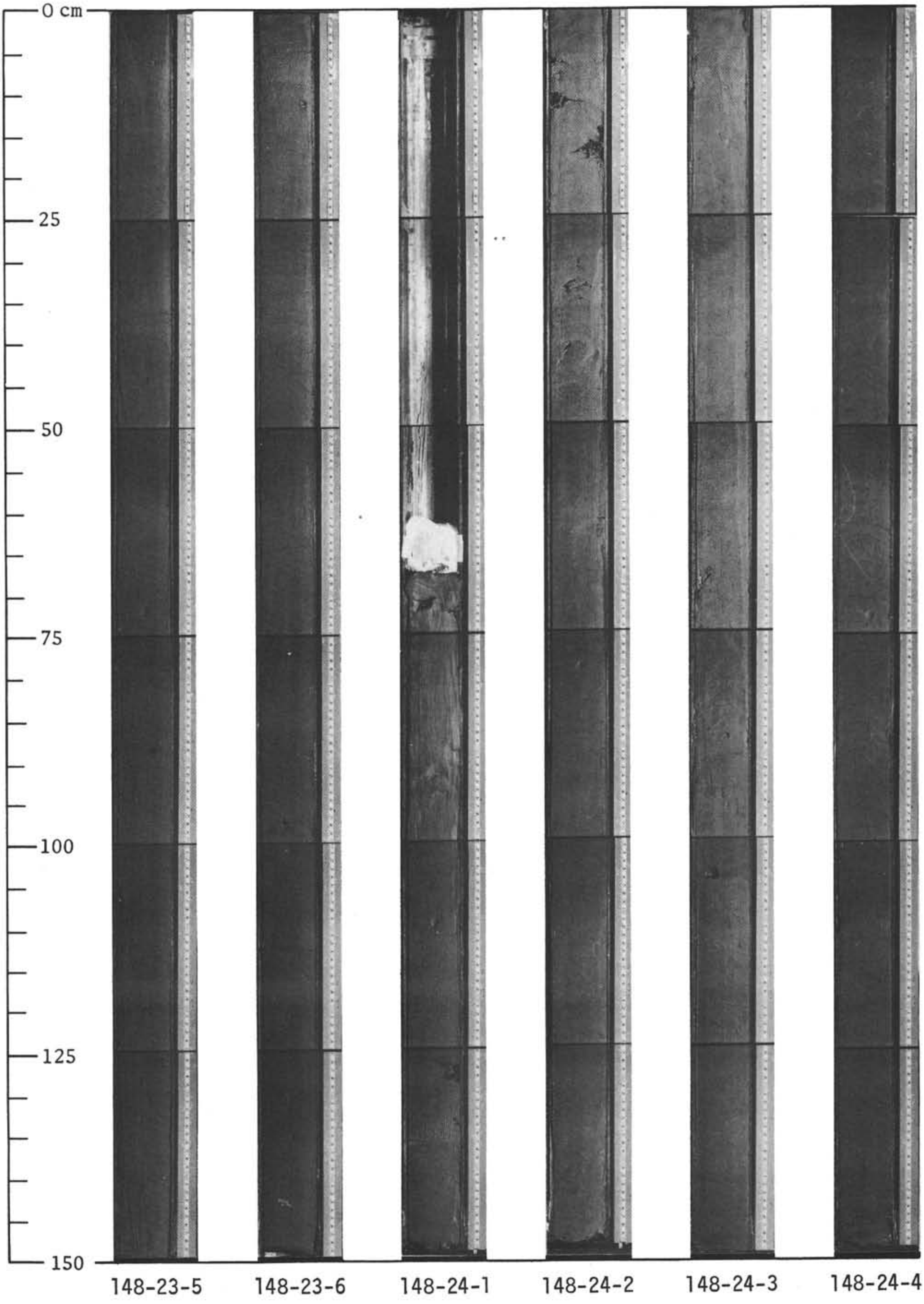
0 cm
25
50
75
100
125
150
148-23-5
148-23-6
148-24-1
148-24-2
148-24-3
148-24-4

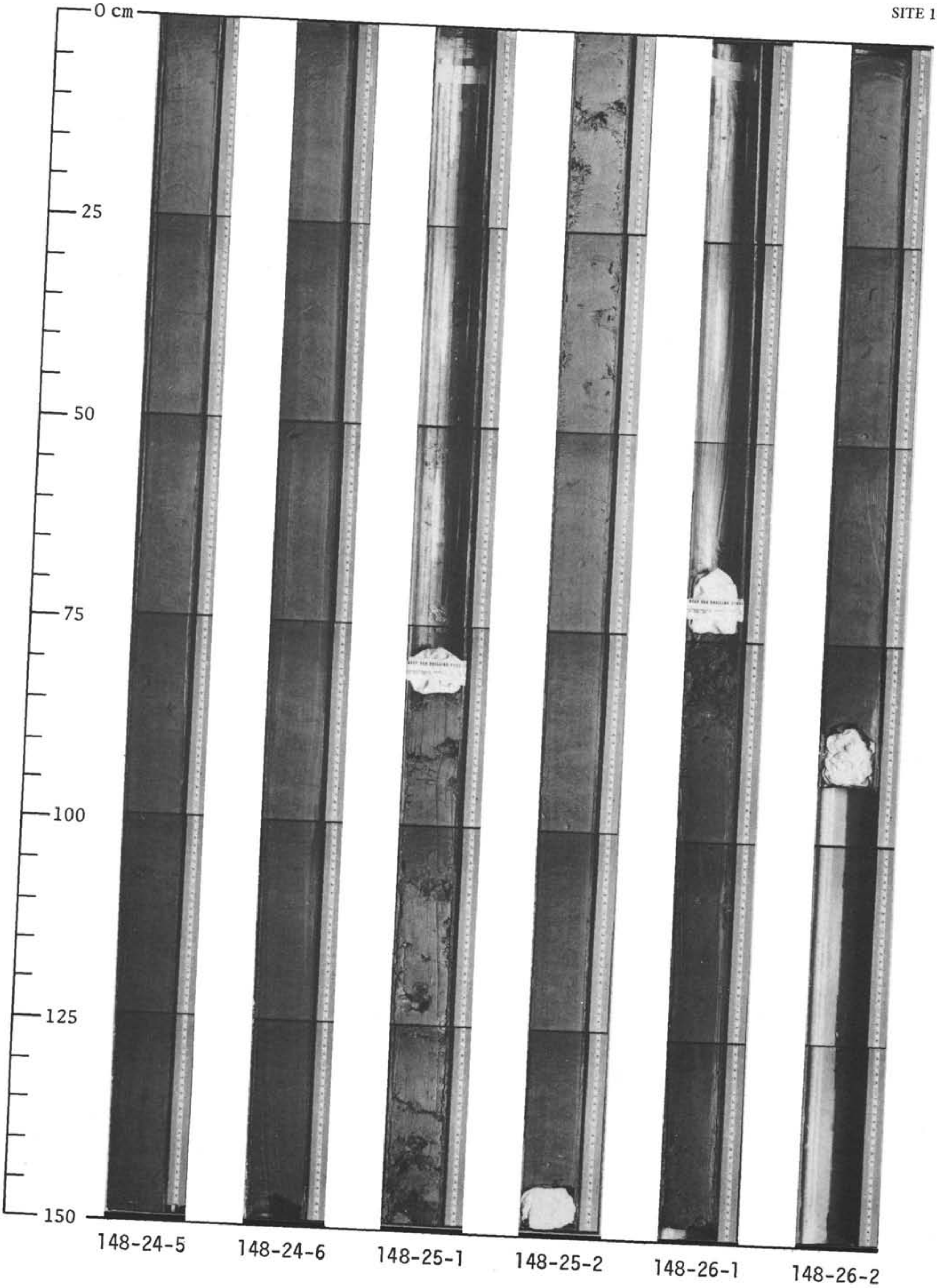
0 cm
25
50
75
100
125
150
148-24-5
148-24-6
148-25-1
148-25-2
148-26-1
148-26-2

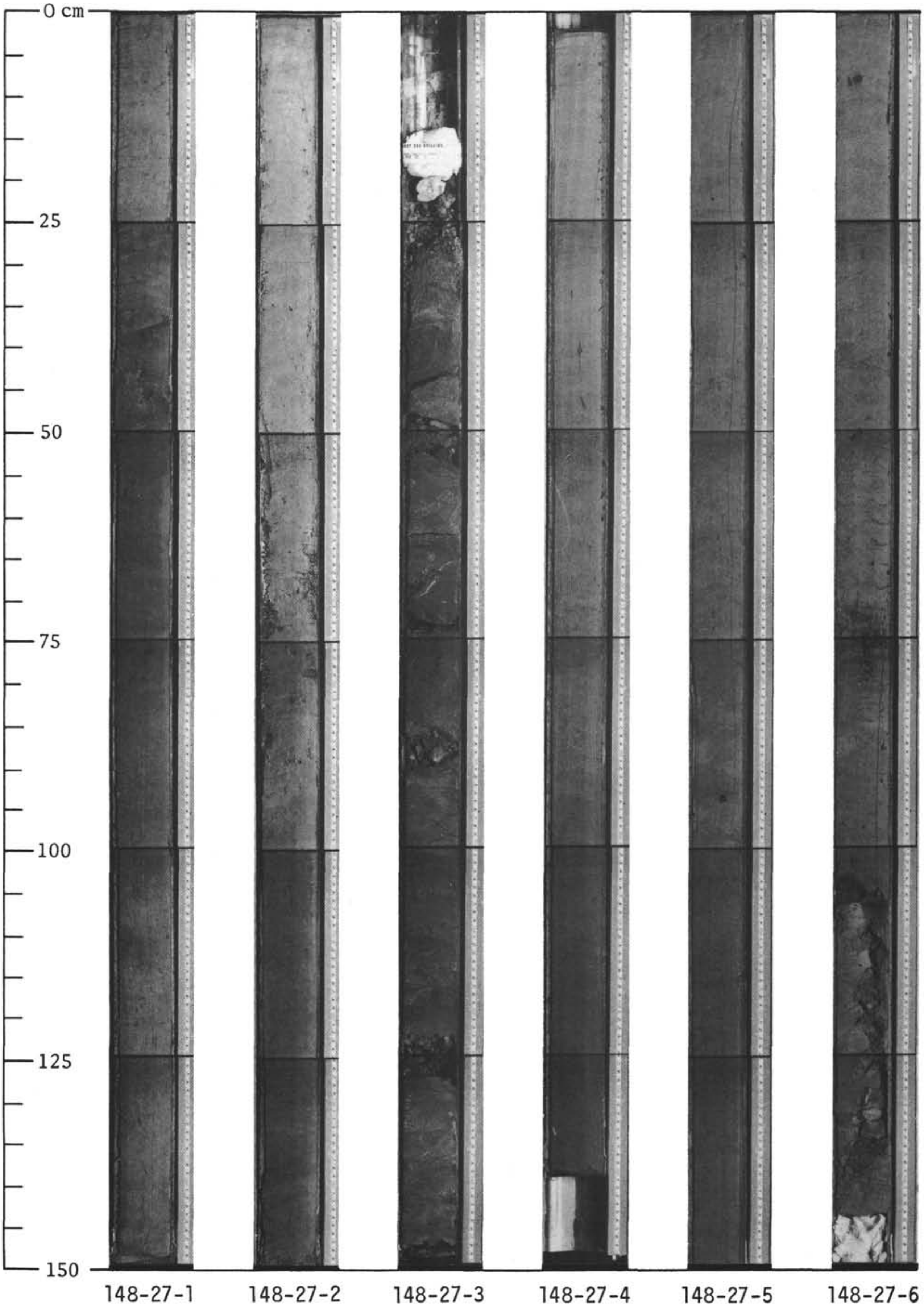
0 cm
25
50
75
100
125
150
148-27-1
148-27-2
148-27-3
148-27-4
148-27-5
148-27-6

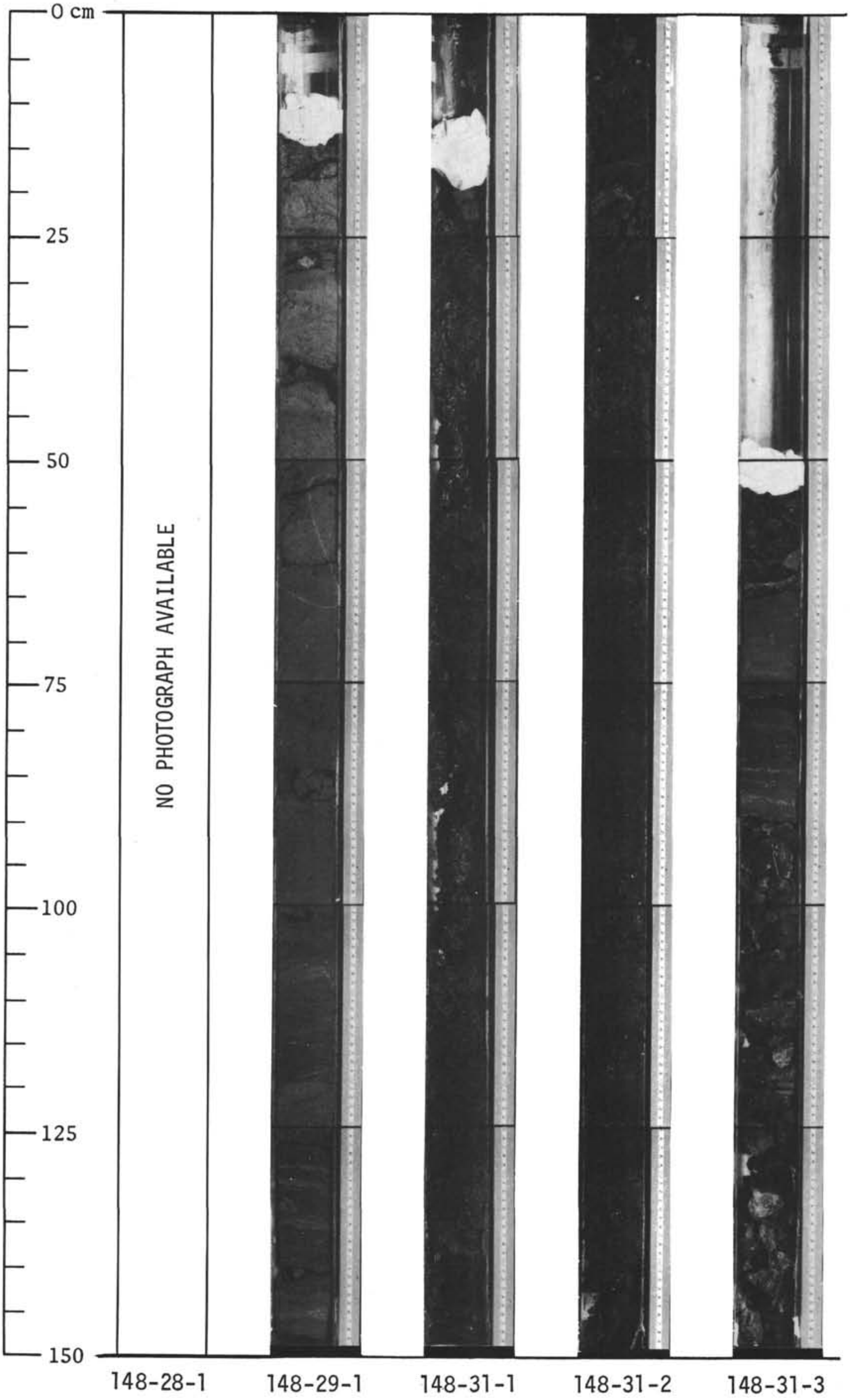
0 cm
25
50
75
100
125
150
NO PHOTOGRAPH AVAILABLE
148-28-1
148-29-1
148-31-1
148-31-2
148-31-3